GEORGIA INSTITUTE OF TECHNOLOGY
OFFICE OF RESEARCH ADMINISTRATION

RESEARCH PROJECT INITIATION

Date: April 18, 1973

Project Title: Research Initiation - High Capacity Information Storage Systems Using Lasers

Project No: E-21-626

Principal Investigator Dr. T. K. Gaylord

Sponsor: National Science Foundation

Agreement Period: From April 1, 1973 Until March 31, 1975*
* 3 month budget period plus 6 months for submission of required reports, etc.

Type Agreement:
Grant GK-37453

Amount: $17,000 - NSF Funds (E-21-626)
4,498 - GIT Contrb. (E-21-319)
$21,498 - Total

Reports Required:

Annual Letter Technical; Final Report

Sponsor Contact Person (s):

Administrative Matters
Mr. Wilbur W. Bolton, Jr.
Grants Officer
NSF
Washington, D. C. 20550

Technical Matters
Dr. M. S. Ghausi
Electrical Sciences & Analysis Section
Division of Engineering
NSF
Washington, D. C. 20550
Phone: (202) 632-5881

Assigned to: School of Electrical Engineering

COPIES TO:

Principal Investigator	Library
School Director	Rich Electronic Computer Center
Dean of the College	Photographic Laboratory
Director, Research Administration	Project File
Director, Financial Affairs (2)	
Security-Reports-Property Office	
Patent Coordinator	Other

RA-3 (6-71)

GEORGIA INSTITUTE OF TECHNOLOGY

OFFICE OF RESEARCH ADMINISTRATION

RESEARCH PROJECT TERMINATION

Date: 3 September 1975

Project Title: Research Initiation - High Capacity Information Storage Systems Using Lasers

Project No: E-21-626

Principal Investigator: Dr. T. K. Gaylord

Sponsor: National Science Foundation

Effective Termination Date: March 31, 1975

Clearance of Accounting Charges: March 31, 1975

Grant/Contract Closeout Actions Remaining: Final Fiscal Report

Assigned to School of Electrical Engineering

COPIES TO:

- Principal Investigator
- School Director
- Dean of the College
- Director of Research Administration
- Office of Financial Affairs (2)
- Security - Reports - Property Office ✓
- Patent and Inventions Coordinator
- Library, Technical Reports Section
- Computer Sciences
- Photographic Laboratory
- Terminated Project File No. _____
- Other _____

Journal of
APPLIED PHYSICS

Volume 44 October 1973 Number 10

Angular selectivity of lithium niobate volume holograms

T. K. Gaylord

School of Electrical Engineering, Georgia Institute of Technology, Atlanta, Georgia 30332

F. K. Tittel

Electrical Engineering Department, Rice University, Houston, Texas 77001

pp. 4771–4773

a publication of the American Institute of Physics

Angular selectivity of lithium niobate volume holograms

T. K. Gaylord

School of Electrical Engineering, Georgia Institute of Technology, Atlanta, Georgia 30332

F. K. Tittel

Electrical Engineering Department, Rice University, Houston, Texas 77001
(Received 29 May 1973)

The angular selectivities for the reconstruction of volume-phase holograms in doped and nominally pure $LiNbO_3$ crystals have been measured. The half-power angular widths for reading were found for the cases studied to be in agreement with theoretically predicted values.

It has been demonstrated that $LiNbO_3$ can be used as a recording material for volume-phase holograms.[1] These holograms are produced directly (without processing) by the interference of laser beams of the appropriate wavelength intersecting in the crystal. The volume nature of this holographic storage is especially interesting since it indicates the possibility of very-high-capacity information storage. Volume (thick) holograms exhibit a number of properties in addition to those possessed by two-dimensional (thin) holograms. Among these properties is angular selectivity—the need for the reference beam to illuminate the hologram at a precise angle in order to achieve reconstruction. Illumination outside of a narrow angular corridor produces a rapidly decreasing intensity of the reconstructed data.

A standard two-beam holographic configuration was used and plane-wave holograms were written. These holograms were reproductions of the original interference pattern, which has the geometry of a series of vertical planes, with an intensity variation perpendicular to the planes of $I(z) = 2I_0 \sin^2(\pi z/L)$, where I_0 is the intensity of each writing beam and L is the resultant grating spacing ($L = \lambda/2 \sin\phi_{Bragg}$).

Two poled single-domain $LiNbO_3$ crystals were used, one doped with 0.05 mole% iron and one nominally pure sample. The crystals were oriented as shown in Fig. 1 with their b-face surfaces perpendicular to the bisector of the writing beams and with the c axis in the plane of the writing beams. A frequency-doubled Nd:YAG laser (5300 Å) and an argon-ion laser operating at 5145 Å were used in these experiments to write the holograms.

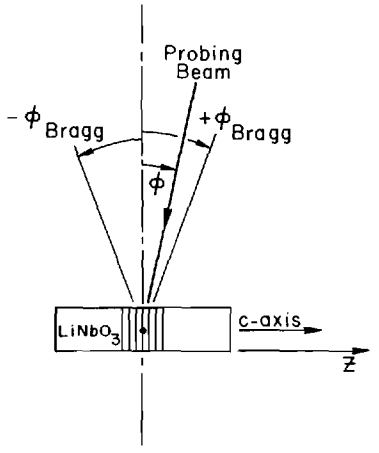

FIG. 1. Geometry of the writing and measuring configuration.

A HeNe laser (6328 Å) aligned to its corresponding Bragg angle was used to monitor the diffraction efficiency and to measure the angular selectivity. The polarization of the two writing beams was in the plane of these beams, while the polarization of the HeNe monitoring beam was perpendicular to the plane of incidence.

To measure the angular selectivity for reconstruction, the single HeNe probing beam was allowed to illuminate the hologram and the diffracted power was monitored. Then, by rotating the incident beam with respect to the crystal (varying the angle ϕ shown in Fig. 1), the variations in diffraction efficiency were measured. For the iron-doped $LiNbO_3$ crystal the measured angular selectivity is shown in Fig. 2.

Assuming that the sinusoidal interference pattern, $I(z)$, produced by the intersection of the two writing beams produces a sinusoidal variation in the index of refraction, then the diffraction efficiency of the volume grating hologram is given by[2] $\eta_0 = \sin^2(\pi\Delta n t/\lambda \cos\phi_{Bragg})$, where η_0 is the on-Bragg-angle diffraction efficiency, Δn is the peak value of the sinusoidal grating of index of refraction, and t is the length of the interaction region (thickness of the crystal for these cases). During the writing process Δn increases and a peak in the diffraction efficiency (predicted to be 100%) occurs when Δn reaches a value of $(\lambda \cos\phi_{Bragg})/2t$. A further increase in Δn causes the diffraction efficiency to decrease until a Δn of $(\lambda \cos\phi_{Bragg})/t$ is reached at which

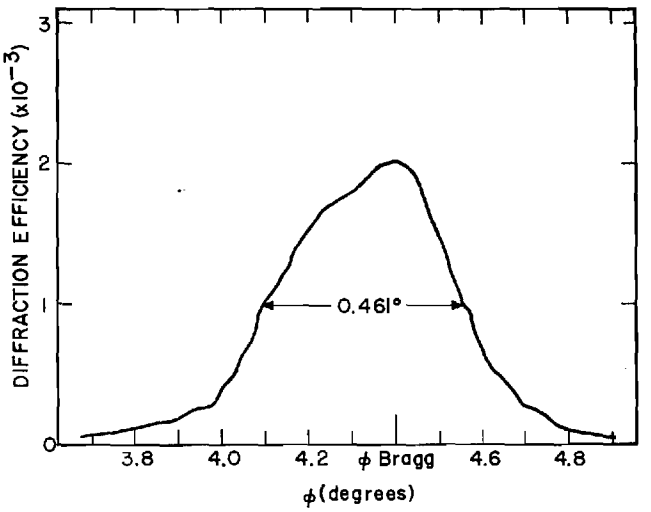

FIG. 2. Angular selectivity for reading of a hologram recorded in a 1-mm-thick iron-doped $LiNbO_3$ crystal using a writing wavelength of 5300 Å and a probing wavelength of 6328 Å.

where the angle of refraction $(\phi_{Bragg})_i = \sin^{-1}\{[1/n(\lambda, P)] \sin\phi_{Bragg}\}$. The HeNe probing beam ($\lambda = 6328$ Å) was polarized perpendicular to the c axis of the crystal (ordinary ray) and thus $n(\lambda, P) = 2.288$ for $LiNbO_3$. For the 1-mm-thick iron-doped $LiNbO_3$ sample, the measured half-power full angular width from Fig. 2 is seen to be $0.461° \pm 0.004°$. For the conditions of this experiment ($\phi_{Bragg} = 4.4°$, $\lambda = 5300$ Å, and $\eta_0 = 2.0\times10^{-3}$) the calculated value from (2) is $0.402°$. For the 5-mm-thick nominally pure $LiNbO_3$ crystal, the half-power angular width was measured to be $0.080° \pm 0.004°$ as compared to the calculated value from (2) for that experiment ($\phi_{Bragg} = 4.35°$, $\lambda = 5145$ Å, and $\eta_0 = 1.1\times10^{-4}$) of $0.0789°$. The deviations between the theoretical and experimental values were 14 and 1.6%, respectively. The agreement between theoretical and experimental values may be taken as an indication that the presence of divergence in the writing beams (writing beam divergence $= 0.143°$ for the 5300-Å beams and $0.035°$ for the 5145-Å beams) does not have an appreciable effect on the resultant angular selectivity for reading. The presence of optical absorption has previously been shown to have very little effect on the angular selectivity of dielectric transmission holograms.[2]

In summary, the angular selectivity for the reconstruction of $LiNbO_3$ volume holograms has been measured and found to be in agreement with theoretical predictions. This information is of particular interest for high-capacity information storage applications since it indicates (1) a practical limit on the angular packing density of multiple holograms stored at a single location and (2) the required beam positioning accuracy to perform the process of reading.

*Work supported by the National Science Foundation.

[1]F. S. Chen, J. T. LaMacchia, and D. B. Fraser, Appl. Phys. Lett. **13,** 223 (1968).
[2]H. Kogelnik, Bell Syst. Tech. J. **48,** 2909 (1969).
[3]J. J. Amodei, W. Phillips, and D. L. Staebler, Appl. Opt. **11,** 390 (1972).
[4]A. Ishida, O. Mikami, S. Miyazawa, and M. Sumi, Appl. Phys. Lett. **21,** 192 (1972).
[5]The angular selectivity expression [Eq. (1)] has previously appeared in the literature without the index of refraction factor (Refs. 1 and 6) and without the $A(\eta_0)$ factor (Refs. 1 and 7).
[6]T. K. Gaylord, T. A. Rabson, and F. K. Tittel, Appl. Phys. Lett. **20,** 47 (1972).
[7]R. L. Townsend and J. T. LaMacchia, J. Appl. Phys. **41,** 5188 (1970).

GEORGIA INSTITUTE OF TECHNOLOGY
ATLANTA, GEORGIA 30332

SCHOOL OF
ELECTRICAL ENGINEERING

March 18, 1974

Dr. M. S. Ghausi
Engineering Division
National Science Foundation
Washington, D. C. 20550

Dear Dr. Ghausi:

Re: Annual Technical Letter for Grant No. GK-37453

Please accept this correspondence as the Annual Technical Letter for the above research grant. Other information related to this grant includes the following:

Name of Institution: School of Electrical Engineering
Georgia Institute of Technology
Name of Principal Investigator: Thomas K. Gaylord
Starting Date: April 1, 1973
Completion Date: September 30, 1974
Type of Grant: Research Initiation Grant
Grant Title: High Capacity Information Storage Systems Using Lasers

This research grant has produced and is producing many important results related to optical memories. Since the inception of this program, I have been very fortunate to attract two outstanding Ph.D. students to join me in this work. In addition, a second faculty member has started to work with me in this research. Through these joint efforts, we are gaining momentum rapidly.

To date, we have finished two papers and three copies of each of these are enclosed. We are, however, expecting considerably more results to send you by the completion date of this grant. We feel that we are just now becoming organized and productive.

We would be delighted to have you stop by should you get to Atlanta. I believe this would be a very informative method for you to learn what we are doing and sense the enthusiasm that exists related to this research.

Please let me know if any further information is needed for me to fulfill the requirements of the Annual Technical Letter. Thank you.

Sincerely,

Tom Gaylord

Thomas K. Gaylord
Assistant Professor

TKG:bpm

Enclosures: 3 copies of "Angular Selectivity of Lithium Niobate Volume Holograms," J. Appl. Phys. 44, 4771 (1973).
3 copies of "Laser Scattering Induced Holograms in Lithium Niobate," (submitted to Appl. Opitcs).

Grant GK–37453

HIGH CAPACITY INFORMATION STORAGE USING LASERS

T.K. Gaylord
School of Electrical Engineering
Georgia Institute of Technology
Atlanta, Georgia 30332

FINAL REPORT FOR PERIOD 1 APRIL 1973 TO 31 MARCH 1975

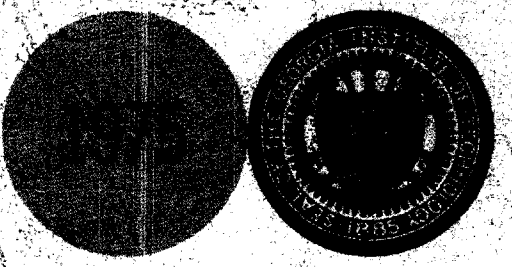

March 1975

Performed for

National Science Foundation
Engineering Division
Electrical Sciences and Analysis Section
Washington, D.C. 20550

SCHOOL OF ELECTRICAL ENGINEERING
Georgia Institute of Technology
Atlanta, Georgia 30332

FINAL REPORT

PROJECT NO. E-21-626

HIGH CAPACITY INFORMATION STORAGE USING LASERS

by

T. K. Gaylord

RESEARCH GRANT GK-37453

1 April 1973 to 31 March 1975

Performed for

NATIONAL SCIENCE FOUNDATION
Engineering Division
Electrical Sciences and Analysis Section
Washington, D.C. 20550

TABLE OF CONTENTS

LIST OF FIGURES

I. ABSTRACT

A program of study of high capacity information storage in electro-optic crystals was undertaken. This study focused on the problems associated with very high capacity storage (through multiple hologram superposition) and the use of lithium niobate as the recording medium.

A number of important problem areas were identified and significant experimental and theoretical results were obtained in the study of these areas. The areas included: 1) the angular selectivity of the stored holograms; 2) interference effects due to the crystal surfaces; 3) beam divergence effects; 4) material recording sensitivity; 5) scattered light from material inhomogeneities; 6) prediction of read-out parameters of volume holograms; 7) multiple hologram superposition; and 8) optical memory system considerations. Numerous significant results were obtained in the investigation of these areas. Five technical journal articles were published based on these new results.

Single hologram and multiple hologram recording experiments were performed using the experimental configuration shown in Fig. 1. Holograms were analyzed experimentally at wavelengths of 488.0nm, 514.5nm, and 632.8nm. Many important practical considerations were identified in addition to the published results. These practical findings are also included in this report.

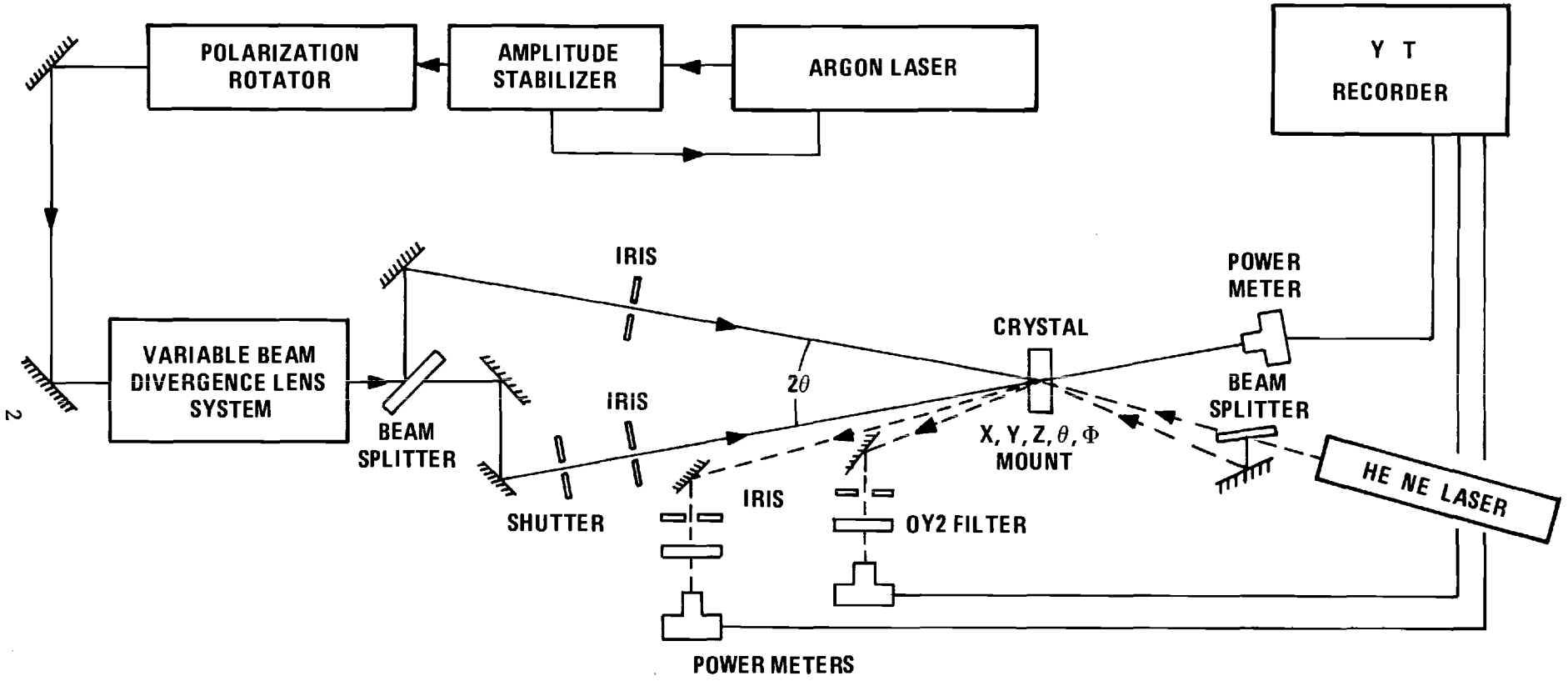

FIGURE 1. EXPERIMENTAL CONFIGURATION FOR MEASURING THE OPTICAL HOLOGRAPHIC STORAGE PROPERTIES OF FERROELECTRIC CRYSTALS.

II. POTENTIAL ENGINEERING APPLICATIONS

The need for large-capacity rapid-access information storage has greatly exceeded the capability of present day memory systems. In addition, this need is growing very rapidly. Thus the gap between needed memory systems and existing memories has only increased. A number of high capacity storage schemes are currently available but these all have very slow access times. Likewise, very fast rapid access memories are presently available but their storage capacity is very small. An inherent trade-off seems to exist between storage capacity and access time. The optical memory, on the other hand, has been recognized as an extremely promising approach for simultaneously achieving both very high storage capacity and rapid random access [1].

The need for mass storage may be divided into several categories. Perhaps the least demanding of these categories is archival storage or record access. In this category very large amounts of data need to be stored in a central memory and occasionally accessed. Examples in this category include libraries, insurance data, medical data, seismic data, criminal data, tax information, patent records, national defense data, telephone numbers, stock market information, computer software packages, postal data, credit data, large inventories, etc. Numerous governmental and private organizations, for example, currently have very large magnetic tape libraries containing over 200,000 reels of magnetic tape. This amount of information is both expensive to store and only very slowly accessible. This category of storage would thus be primarily read-only. Changing the data would occur only infrequently by computer standards.

The second category is the need for high data rate recording and temporary storage. An example in this category would be very high bit

rate optical communications systems. In optical communications the efficient use of turbulent channels will require very high capacity, very fast, reusable mass storage for recording during temporary interruptions of these channels. Another example in this category would be data recording during a fly-by space probe. In this situation a very large amount of data may be gathered during a brief period of time. If this information could be stored, it could later be transmitted at a low bit rate in order to minimize transmission errors in the data. Still another example of temporary storage would be in the use of large scale weather prediction programs.

A third category of need for high capacity storage is in computer memories. Present day computing systems utilize a complex hierarchy of storage devices. Some of the more important of these memories are magnetic tape, disks, drums, cores, and semiconductors. Modern computers use a combination of the large and slow along with the small and fast memories in a hierarchical structure in order to realize efficient computing. The optical memory, due to its very high capacity and fast random access, offers the potential of replacing a large portion of the existing memory hierarchy. This is probably the most obvious application of high capacity, rapid access optical memories.

A fourth category of need is in the development of new computer architectures. This represents a new area based largely on the multiport capability of optical memories [2]

III. ANGULAR SELECTIVITY

Because of the three-dimensional nature of the crystal, holograms recorded in lithium niobate are volume holograms. These holograms are produced directly (without processing) by the interference of laser beams of the appropriate wavelength intersecting in the crystal. The volume nature of this holographic storage is especially interesting since it indicates the possibility of very high capacity information storage.

Volume (thick) holograms exhibit a number of properties in addition to those possessed by two-dimensional (thin) holograms. Among these properties is angular selectivity—the need for the reference beam to illuminate the hologram at a precise angle in order to achieve reconstruction. Illumination outside of this angular corridor produces a rapidly decreasing intensity of the reconstructed data. To perform these diagnostic experiments plane wave holograms (caused by the interference of two plane waves) were used. Even though this is a special case, a general hologram may be constructed by the superposition of an infinite number of plane wave holograms. Reconstruction of a volume hologram [3] is possible (with half maximum diffracted power or greater) only over the range of wavelengths given by

$$\frac{\Delta\lambda}{\lambda} \simeq \cot\ \theta\ \frac{L}{t} \qquad (1)$$

and only over the range of angles given by

$$\Delta\theta \simeq A(\eta_o)n(\lambda,P)\ \frac{L}{t}\ , \qquad (2)$$

where $\Delta\lambda$ and $\Delta\theta$ are centered about the writing wavelength λ, and the writing angle, θ. The thickness of the hologram is given by t, L is the fringe

spacing of the fundamental grating ($L = \lambda/2\sin\theta$), $n(\lambda,P)$ is the appropriate index of refraction for the probing beam wavelength and polarization, and $A(\eta_b)$ is the angular selectivity coefficient (approximately equal to unity). These types of properties are in actuality just manifestations of the increased storage capacity of the volume storage medium.

The experimental configuration shown in Figure 1 was used to measure the angular selectivity and compare it with the theoretical value. Thicknesses from 1mm to 5mm were tested. Both iron-doped and nominally pure crystals of lithium niobate were used. The half-power angular widths were found to be in agreement with theoretically predicted values. These results show that the theoretical angular packing density of multiple holograms is achievable! This important finding was reported in Appl. Phys. Letters [4]. This publication gives experimental details as well as results and is reproduced here for completeness.

Additional experimental results have been obtained since Ref. 4 was published. These show a much more detailed comparison of theory and experiment for a broader range of reading angles. These data are shown in Figs. 2 and 3.

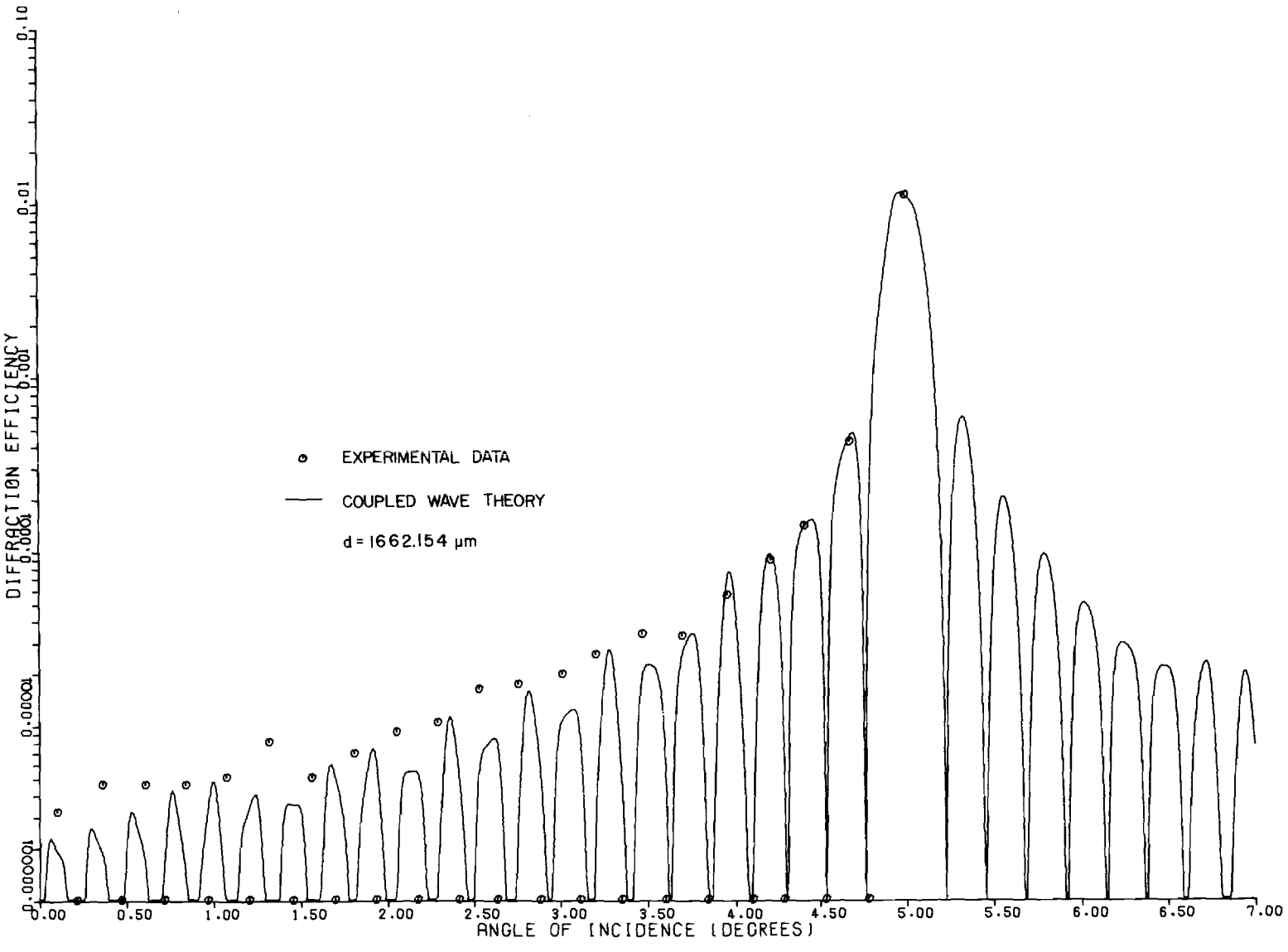

FIGURE 2. A COMPARISON OF ANGULAR SELECTIVITY EXPERIMENTAL DATA WITH RESULTS FROM THE COUPLED WAVE THEORY. The particular thickness chosen, d, yields the best fit close to the Bragg angle.

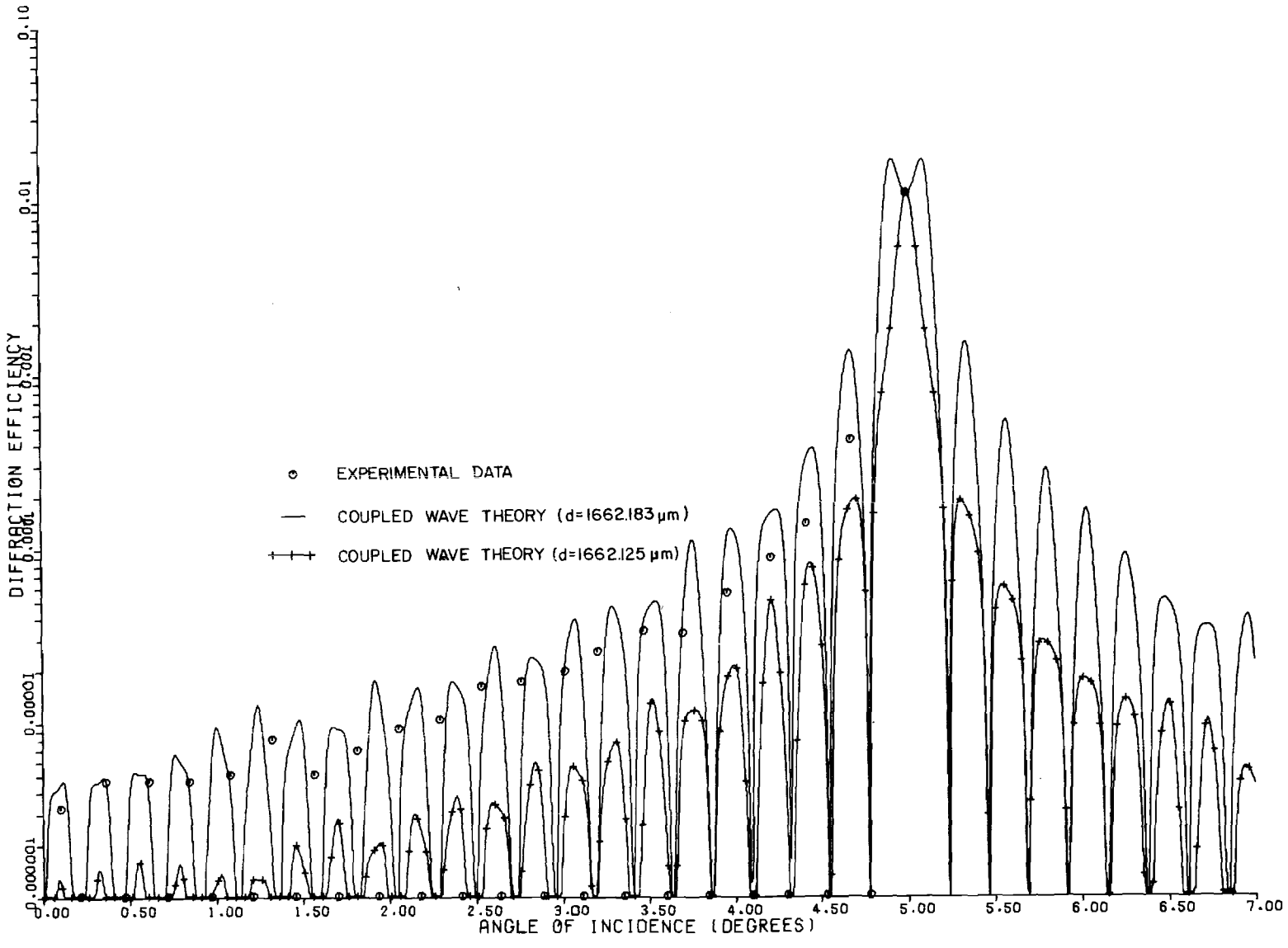

FIGURE 3. AMPLITUDE RANGE OF THEORETICAL ANGULAR SELECTIVITY DUE TO MINUTE THICKNESS VARIATIONS. The thickness used in producing the plain curve is that needed to obtain a minimum value of the transmittance factor on the Bragg angle ($\tau = 0.3$). The crossed curve corresponds to maximum transmittance ($\tau = 1.8$). The experimental data is seen to occur within these extremes.

Angular selectivity of lithium niobate volume holograms

T. K. Gaylord

School of Electrical Engineering, Georgia Institute of Technology, Atlanta, Georgia 30332

F. K. Tittel

Electrical Engineering Department, Rice University, Houston, Texas 77001
(Received 29 May 1973)

The angular selectivities for the reconstruction of volume-phase holograms in doped and nominally pure $LiNbO_3$ crystals have been measured. The half-power angular widths for reading were found for the cases studied to be in agreement with theoretically predicted values.

It has been demonstrated that $LiNbO_3$ can be used as a recording material for volume-phase holograms.[1] These holograms are produced directly (without processing) by the interference of laser beams of the appropriate wavelength intersecting in the crystal. The volume nature of this holographic storage is especially interesting since it indicates the possibility of very-high-capacity information storage. Volume (thick) holograms exhibit a number of properties in addition to those possessed by two-dimensional (thin) holograms. Among these properties is angular selectivity—the need for the reference beam to illuminate the hologram at a precise angle in order to achieve reconstruction. Illumination outside of a narrow angular corridor produces a rapidly decreasing intensity of the reconstructed data.

A standard two-beam holographic configuration was used and plane-wave holograms were written. These holograms were reproductions of the original interference pattern, which has the geometry of a series of vertical planes, with an intensity variation perpendicular to the planes of $I(z) = 2I_0 \sin^2(\pi z/L)$, where I_0 is the intensity of each writing beam and L is the resultant grating spacing ($L = \lambda/2 \sin\phi_{Bragg}$).

Two poled single-domain $LiNbO_3$ crystals were used, one doped with 0.05 mole% iron and one nominally pure sample. The crystals were oriented as shown in Fig. 1 with their b-face surfaces perpendicular to the bisector of the writing beams and with the c axis in the plane of the writing beams. A frequency-doubled Nd:YAG laser (5300 Å) and an argon-ion laser operating at 5145 Å were used in these experiments to write the holograms.

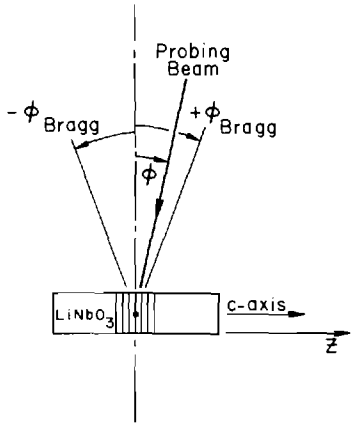

FIG. 1. Geometry of the writing and measuring configuration.

A HeNe laser (6328 Å) aligned to its corresponding Bragg angle was used to monitor the diffraction efficiency and to measure the angular selectivity. The polarization of the two writing beams was in the plane of these beams, while the polarization of the HeNe monitoring beam was perpendicular to the plane of incidence.

To measure the angular selectivity for reconstruction, the single HeNe probing beam was allowed to illuminate the hologram and the diffracted power was monitored. Then, by rotating the incident beam with respect to the crystal (varying the angle ϕ shown in Fig. 1), the variations in diffraction efficiency were measured. For the iron-doped $LiNbO_3$ crystal the measured angular selectivity is shown in Fig. 2.

Assuming that the sinusoidal interference pattern, $I(z)$, produced by the intersection of the two writing beams produces a sinusoidal variation in the index of refraction, then the diffraction efficiency of the volume grating hologram is given by[2] $\eta_0 = \sin^2(\pi\Delta n t/\lambda \cos\phi_{Bragg})$, where η_0 is the on-Bragg-angle diffraction efficiency, Δn is the peak value of the sinusoidal grating of index of refraction, and t is the length of the interaction region (thickness of the crystal for these cases). During the writing process Δn increases and a peak in the diffraction efficiency (predicted to be 100%) occurs when Δn reaches a value of $(\lambda \cos\phi_{Bragg})/2t$. A further increase in Δn causes the diffraction efficiency to decrease until a Δn of $(\lambda \cos\phi_{Bragg})/t$ is reached at which

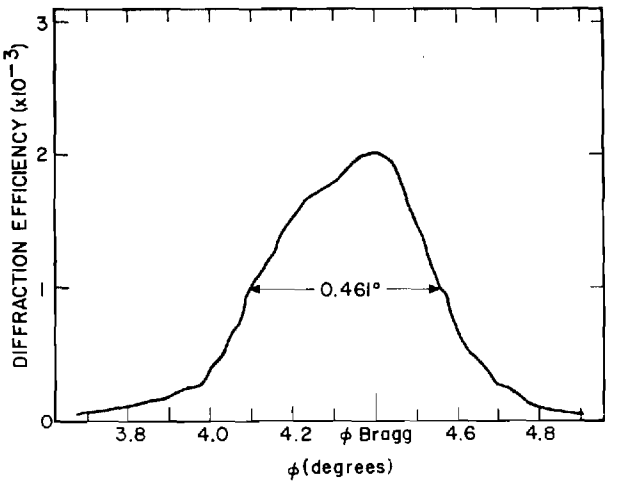

FIG. 2. Angular selectivity for reading of a hologram recorded in a 1-mm-thick iron-doped $LiNbO_3$ crystal using a writing wavelength of 5300 Å and a probing wavelength of 6328 Å.

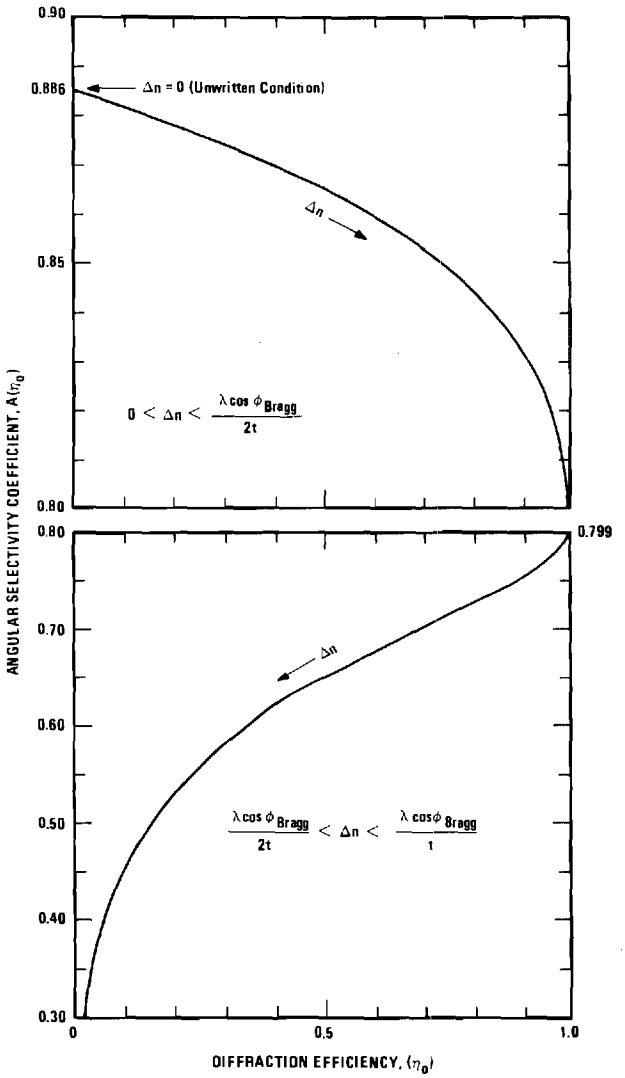

FIG. 3. The angular selectivity coefficient, $A(\eta_0)$, as a function of on-Bragg-angle diffraction efficiency, η_0.

time η_0 again begins to increase. This oscillatory behavior of the diffraction efficiency with exposure time has been experimentally observed.[3,4]

The theoretical angular selectivity for reading a volume hologram can be determined using the coupled-wave theory of Kogelnik.[2] For the full range of on-Bragg-angle diffraction efficiencies ($0 < \eta_0 < 1.00$), the half-power full angular width inside the crystal, $(\Delta\phi)_i$, can be determined by numerically solving Eqs. (42)–(45) in Ref. 2. The result is that $(\Delta\phi)_i = A(\eta_0)L/t$, where $A(\eta_0)$ is the angular selectivity coefficient. The half-power full angular width as measured from outside the crystal is thus

$$\Delta\phi \simeq A(\eta_0)n(\lambda, P)L/t \quad \text{rad},$$

where $n(\lambda, P)$ is the appropriate index of refraction for the probing beam wavelength and polarization. The angular selectivity coefficient, $A(\eta_0)$, as determined by the coupled-wave theory is evaluated in Fig. 3.[5] As the change in index of refraction varies from zero (unwritten condition) to $(\lambda\cos\phi_{\text{Bragg}})/2t$ this factor changes from 0.886 to 0.799. This initial range of Δn values includes the relatively low diffraction efficiencies which correspond to practical holographic storage of information. For Δn beyond $(\lambda\cos\phi_{\text{Bragg}})/2t$, the angular selectivity coefficient decreases rapidly as shown in Fig. 3. Thus the angular corridor for reading narrows considerably with further exposure. Simultaneously, the diffraction efficiency increases at larger angular deviations from the Bragg angle as shown in Fig. 4. As the change in index of refraction, Δn, increases, these side lobe positions increase in diffraction efficiency and decrease their angular separation, $\Delta\phi$, from the exact Bragg angle. These side lobes coalesce at the Bragg angle ($\Delta\phi = 0$) when Δn increases to $1.5(\lambda\cos\phi_{\text{Bragg}})/t$ at which time the next set of side lobes are increasing in diffraction efficiency and moving toward the Bragg angle. Obviously for Δn greater than about $0.75(\lambda\cos\phi_{\text{Bragg}})/t$ the conventional notion of angular selectivity becomes ambiguous due to the presence of these side lobes.

Equation (1) assumes small angles of incidence. For the geometry of the experiments reported here, only a 0.24% error is introduced into this equation by the small-angle approximation. The more nearly exact expression for the half-power full angular width for reading for any angle of incidence is

$$\Delta\phi \simeq \sin^{-1}\{n(\lambda, P)\sin[(\phi_{\text{Bragg}})_i + \tfrac{1}{2}(\Delta\phi)_i]\} - \sin^{-1}\{n(\lambda, P)\sin[(\phi_{\text{Bragg}})_i - \tfrac{1}{2}(\Delta\phi)_i]\}, \quad (2)$$

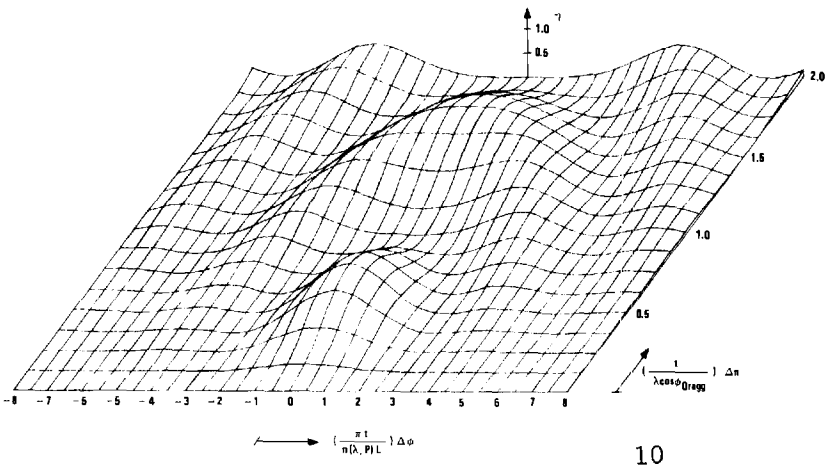

FIG. 4. Predicted variation of diffraction efficiency (η) with change in index of refraction (Δn) and angular deviation ($\Delta\phi$) from the exact Bragg angle.

where the angle of refraction $(\Phi_{Bragg})_i = \sin^{-1}\{[1/n(\lambda, P)] \sin\Phi_{Bragg}\}$. The HeNe probing beam ($\lambda = 6328$ Å) was polarized perpendicular to the c axis of the crystal (ordinary ray) and thus $n(\lambda, P) = 2.288$ for $LiNbO_3$. For a 1-mm-thick iron-doped $LiNbO_3$ sample, the measured half-power full angular width from Fig. 2 is seen to be $0.461 \pm 0.004°$. For the conditions of this experiment ($\Phi_{Bragg} = 4.4°$, $\lambda = 5300$ Å, and $\eta_0 = 2.0\times10^{-3}$) the calculated value from (2) is $0.402°$. For the 5-mm-thick nominally pure $LiNbO_3$ crystal, the half-power angular width was measured to be $0.080° \pm 0.004°$ as compared to the calculated value from (2) for that experiment ($\Phi_{Bragg} = 4.35°$, $\lambda = 5145$ Å, and $\eta_0 = 1.1\times10^{-4}$) of $0.0789°$. The deviations between the theoretical and experimental values were 14 and 1.6%, respectively. The agreement between theoretical and experimental values may be taken as an indication that the presence of divergence in the writing beams (writing beam divergence $= 0.143°$ for the 5300-Å beams and $0.035°$ for the 5145-Å beams) does not have an appreciable effect on the resultant angular selectivity for reading. The presence of optical absorption has previously been shown to have very little effect on the angular selectivity of dielectric transmission holograms.[2]

In summary, the angular selectivity for the reconstruction of $LiNbO_3$ volume holograms has been measured and found to be in agreement with theoretical predictions. This information is of particular interest for high-capacity information storage applications since it indicates (1) a practical limit on the angular packing density of multiple holograms stored at a single location and (2) the required beam positioning accuracy to perform the process of reading.

*Work supported by the National Science Foundation.

[1]F. S. Chen, J. T. LaMacchia, and D. B. Fraser, Appl. Phys. Lett. **13,** 223 (1968).
[2]H. Kogelnik, Bell Syst. Tech. J. **48,** 2909 (1969).
[3]J. J. Amodei, W. Phillips, and D. L. Staebler, Appl. Opt. **11,** 390 (1972).
[4]A. Ishida, O. Mikami, S. Miyazawa, and M. Sumi, Appl. Phys. Lett. **21,** 192 (1972).
[5]The angular selectivity expression [Eq. (1)] has previously appeared in the literature without the index of refraction factor (Refs. 1 and 6) and without the $A(\eta_0)$ factor (Refs. 1 and 7).
[6]T. K. Gaylord, T. A. Rabson, and F. K. Tittel, Appl. Phys. Lett. **20,** 47 (1972).
[7]R. L. Townsend and J. T. LaMacchia, J. Appl. Phys. **41,** 5188 (1970).

IV. SURFACE INTERFERENCE EFFECTS

Many analyses of hologram reconstruction do not account for boundary (surface) reflections. The diffraction efficiency results may be corrected to include boundary reflections by multiplying by a transmittance factor. This factor, τ, is developed by us in Ref. 5, a copy of which is included in this report. This factor is the same as the transmittance factor derived by Kogelnik and given as Eq. (8) in Ref. 6, but with νd in that equation replaced by the argument of the sine function in Eq. (27) in our paper [5].

From these results, we find that boundary reflections produced by the surfaces can considerably change the diffraction efficiency. The change can be an increase or a decrease depending on whether the transmittance factor is greater or less than unity. This effect has been studied by Cohen and Gordon [7]. For the grating parameters used here, τ is typically in the range 0.70 to 1.20. In practice, the boundary reflections can be eliminated by antireflection coatings on the surfaces of the gratings.

Calculated results showing the thickness dependence of τ for lithium niobate are shown in Fig. 4. The effect of τ as a function of reading angle is shown in Fig. 5.

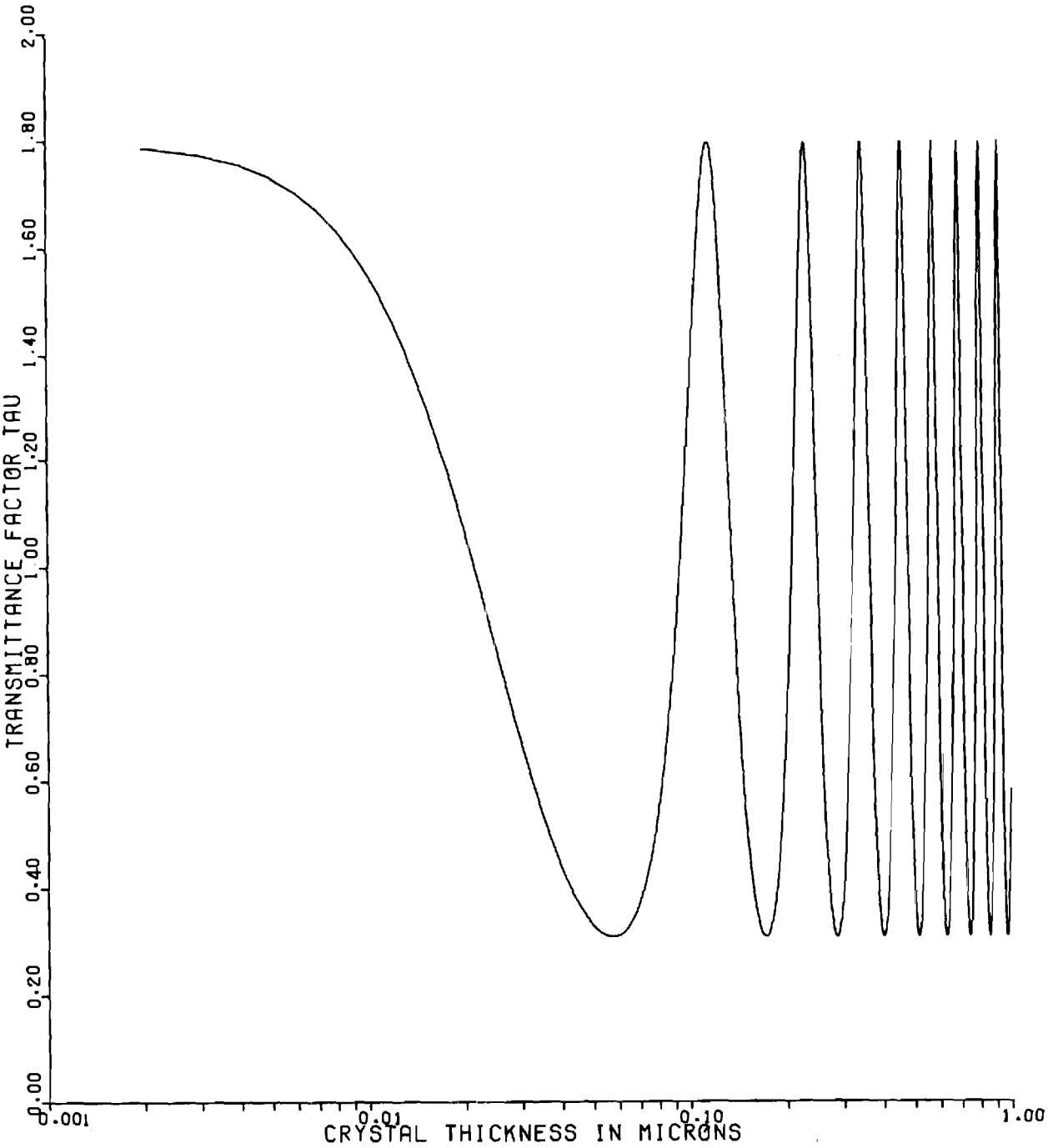

FIGURE 4. TRANSMITTANCE FACTOR, τ, AS A FUNCTION OF CRYSTAL THICKNESS.

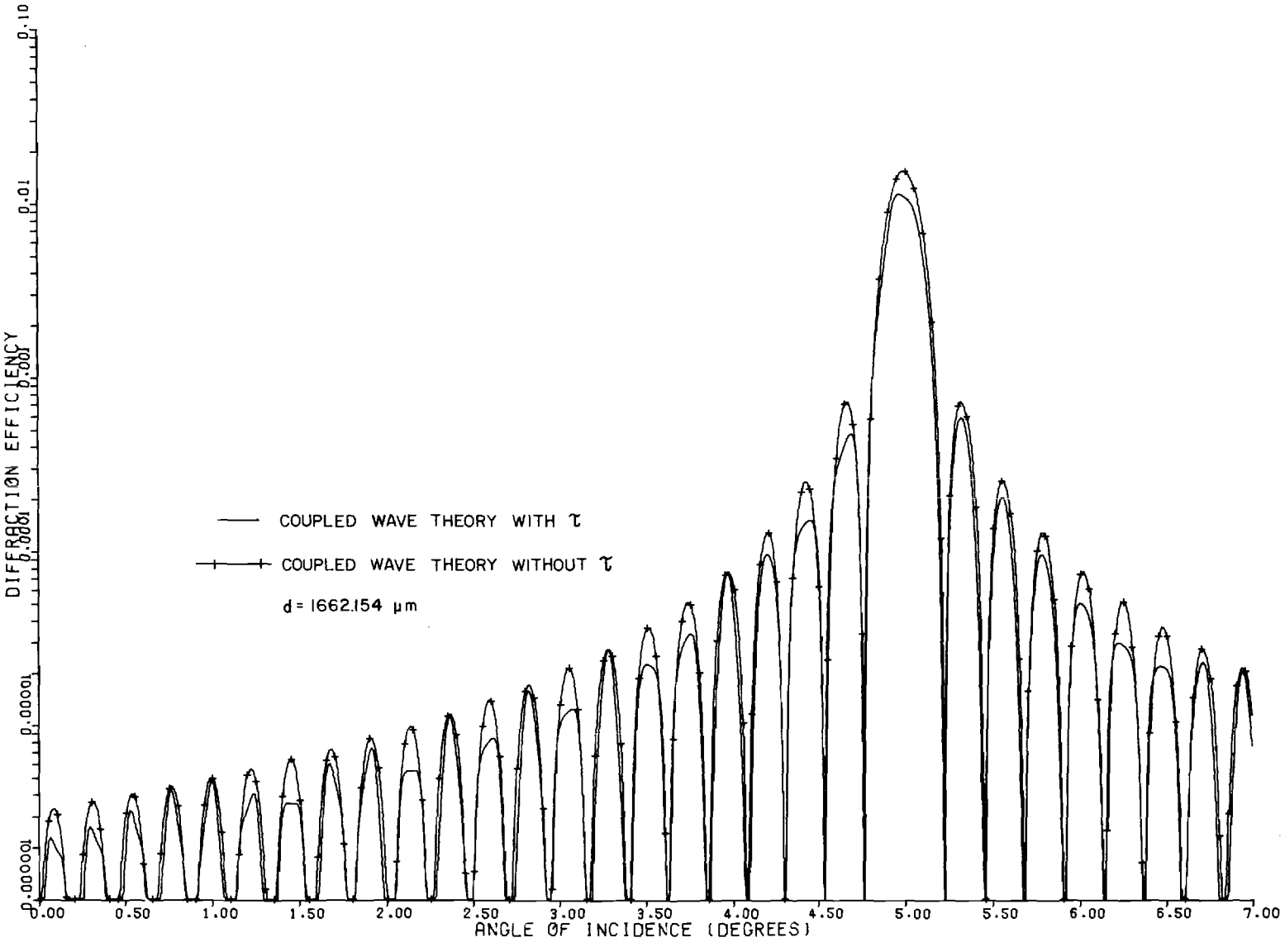

FIGURE 5. EFFECT OF THE TRANSMITTANCE FACTOR ON ANGULAR SELECTIVITY.

V. BEAM DIVERGENCE EFFECTS

The effect of writing beam divergence was studied. First, a hologram was written with a frequency doubled Nd:YAG laser (λ = 530nm) with a beam divergence of 0.143^{o}. Second, a hologram was written with an argon laser (λ = 514.5nm) with a beam divergence of 0.035^{o}. The angular selectivities of these holograms were then measured with a He-Ne laser. The half-power angular width in both cases was found to be within 10% of the theoretical value derived in our paper [4]. Thus, it was concluded that writing beam divergence has little effect on the final read-out process.

VI. RECORDING SENSITIVITY

Recording materials must possess a number of important characteristics to achieve the high storage capacities that have been predicted for optical memories. These requirements on the optical recording material include: 1. High sensitivity—It is desirable that only a small amount of optical energy per unit area be needed to record the hologram of a data page. Table 3 in Ref. 8 (reproduced later in this report) lists the necessary writing energy densities for a number of recording materials. For a practical system an energy density of about 0.1 millijoule/cm^2 or less will be needed. 2. Large diffraction efficiency—Diffraction efficiency is the fraction of the reading light (reference beam) that is diffracted into the reconstructed data beam. It must be possible to record a single hologram with a large diffraction efficiency, so that in practice many holograms may be recorded at a single location, each with an equal share of the total maximum diffraction efficiency. Therefore, it is desirable to have the maximum diffraction efficiency as close to 100% as possible. 3. Erasable and rewritable—For a rapid cycle read-write-erase memory system, it must be possible to continuously alter the stored data in the memory without encountering any degradation in the material characteristics. 4. Long lifetime of stored information—Stored data should persist for long periods of time before having to be refreshed. Ideally, storage should be permanent. 5. Non-volatile storage—Data should remain recorded in the memory in the absence of system power. 6. Nondestructive readout—It should be possible to perform an essentially unlimited number of read operations without degrading or altering the stored data. 7. Three dimensional storage—To achieve very high capacity storage, the information should be stored in thick (volume) holograms. Together with the requirement of high diffraction efficiency, this means that the hologram

should be a thick phase (nonabsorbing) hologram. 8. High resolution— The storage material obviously must be capable of recording the very fine (wavelength size) variations of the interference pattern produced by the intersection of the object and reference beams.

Considering all of the above material requirements, the photorefractive materials (optically induced changes in index of refraction) appear to be especially promising. These materials, often ferroelectric crystals such as lithium niobate and strontium barium niobate (SBN), have been considerably developed and improved. For example, in the first use of lithium niobate as a recording material in 1968 a writing energy density of approximately 100 joules/cm^2 was required [9]. Less than six years later, doped versions of lithium niobate have now been shown in this work to exhibit writing energy densities of 2 millijoules/cm^2! We have announced this improvement in sensitivity of almost 5 orders of magnitude in Applied Physics Letters [10]. This article is reproduced here for completeness. Fig. 6 depicts this recent jump in sensitivity with respect to other potential recording materials. In addition, recent work by von der Linde et al. [11] indicates that even higher sensitivities are possible in lithium niobate!

Material	Type of Material	Writing Energy Density (joules/cm^2)
$Bi_{12}Si\ O_{20}$	Ferroelectric–Photoconductive	1×10^{-5}
Malachite Green: Sucrose Benzoate	Thermoplastic	2×10^{-5}
Agfa 8E70	Photographic	2×10^{-5}
Kodak 649F	Photographic	7×10^{-5}
$Bi_4Ti_3O_{12}$–ZnSe	Ferroelectric–Photoconductive	1×10^{-3}
$LiNbO_3$:Fe	Photorefractive	2×10^{-3}
$Sr_{0.75}Ba_{0.25}Nb_2O_6$	Photorefractive	6×10^{-3}
Oichromated Gelatin	Photochemical	9×10^{-3}
Ca F_2: Ce	Photochrornic	1×10^{-2}
KCL:Na	Photochromic	1×10^{-2}
Mn Bi	Magnetooptic	3×10^{-2}
$Te_{88}Ge_7As_5$	Amorphous Semiconductor	5×10^{-2}
Gd I G	Magnetooptic	9×10^{-2}
Eu O	Magnetooptic	9×10^{-2}
Na F	Photochromic	9×10^{-2}
Co–P–Ni–Fe	Magnetooptic	1×10^{-1}
$SrTiO_3$:Ni:Mo	Photochromic	2×10^{-1}
Ba Ti O_3	Photorefractive	2×10^{-1}
Mn Al Ge	Magnetooptic	3×10^{-1}
$Te_{81}Ge_{15}Sb_2S_2$	Amorphous Semiconductor	5×10^{-1}
$LiNbO_3$:Fe	Photorefractive	8×10^{-1}
KBr	Photochromic	1
$Cu_2Hg\ I_4$	Thermoplastic	3
$BaNaNb_5O_{15}$	Photorefractive	5
$Bi_4Ti_3O_{12}$	Photorefractive	10
$Sr_{0.75}Ba_{0.25}Nb_2O_6$	Photorefractive	14
$LiNbO_3$	Photorefractive	100

Rice Univ.
Georgia Tech
1974

FIGURE 6. REQUIRED WRITING ENERGY DENSITY FOR VARIOUS OPTICAL RECORDING MATERIALS.

Volume holographic recording and storage in Fe-doped $LiNbO_3$ using optical pulses*

Pradeep Shah, T. A. Rabson, and F. K. Tittel
Department of Electrical Engineering, Rice University, Houston, Texas 77001

T. K. Gaylord
School of Electrical Engineering, Georgia Institute of Technology, Atlanta, Georgia 30332

(Received 4 June 1973)

Volume holographic recording and storage in Fe-doped $LiNbO_3$ using single 30–75-nsec duration optical pulses at 694.3 and 531 nm from Q-switched ruby and frequency-doubled Nd:glass lasers, respectively, is reported. The recording sensitivity for a pulsed writing source is found to be better than that estimated for a cw source. A sensitivity of 2 mJ/cm^2 at 476 nm and 2.5 mJ/cm^2 at 488 nm to record a hologram of 1% diffraction efficiency is the best sensitivity figure yet reported. The orders of magnitude of improvement in sensitivity is attributed to higher fractional concentration of Fe^{2+}.

Ferroelectric materials have recently become the subject of considerable interest on account of their potential use in optical storage and information processing. Such a ferroelectric storage medium must meet certain system requirements, which include high bit density storage capability, high sensitivity and speeds of recording, and high readout efficiency. In this work we discuss two of these parameters, speed and sensitivity of iron-doped $LiNbO_3$, which make it a most interesting storage medium in addition to strontium barium niobate (SBN). The results of the experiments conducted demonstrate the feasibility of volume holographic recording, storage, and retrieval of information by means of single optical pulses of nanosecond duration using the photoinduced index of refraction changes in lithium niobate. Here we report the best recording sensitivities yet published—an order-of-magnitude improvement over recent reported sensitivities of SBN[1] and almost two-orders-of-magnitude improvement in Fe-doped $LiNbO_3$.[2] These sensitivities are for the experiment conducted without any external electric field across the crystal. Further improvements in sensitivity are expected with external bias fields. Furthermore, our experiments indicate that the charge generation and transport processes occur with time constants considerably faster than 10^{-8} sec since no difficulty in recording and reconstructing was experienced using pulses from Q-switched lasers. The recording sensitivity for a pulsed source is slightly better than that estimated for a cw source.

Volume holograms in the form of interference fringes of two plane waves were recorded in two iron-doped $LiNbO_3$ crystals. Both these crystals were cut from the same boule grown by Crystal Technology, Inc. and contained 0.05 mole% concentration of iron. One of these crystals was annealed in pure oxygen atmosphere at 700 °C to increase the transmission in the shorter-wavelength region of the visible spectrum. The absorption spectra of both these crystals (1 mm thick) are shown in Fig. 1. In the same figure an absorption spectrum corrected for comparable crystal thickness from previously reported data[2] is plotted. The writing sources included single pulses from a Q-switched frequency-doubled Nd:glass laser capable of an output of 0.005 J at 531 nm with pulse duration of ~75 nsec, a ruby laser with 0.05 J energy at 694.3 nm with pulse duration of 30 nsec, and in addition a continuous wave argon laser using output at 476.5, 488, 496.5, and 514.5 nm and a He-Ne laser (632.8 nm). All these sources were made to operate in a single transverse mode. The recording of the hologram and the reconstruction was accomplished using an experimental set-up shown in schematic form in Fig. 2. The recording beam is split into a reference and an object beam of approximately equal intensity using a beam splitter and is lightly focused using a 125-cm-focal-length lens. These beams intersect in the storage medium at an angle of 12°. The writing beams are polarized perpendicular to the c axis of the crystal and the plane of the writing beams. The diffraction efficiency and the writing curve are measured using the reference beam with the object beam shuttered intermittently during the recording process and also by a He-Ne laser polarized parallel to the c axis of the $LiNbO_3$ crystal. The diffraction efficiency in the pulsed mode is measured by simultaneously monitoring the transmitted and diffracted reference beams. Optimum reconstruction is observed when the reading beam is polarized parallel to the c axis which is in agreement with the previously reported observations.[3] The recording sensitivity defined in terms of the total required exposure in J/cm^2 to construct a hologram with 1% diffraction efficiency[4] is plotted in Fig. 3 for various recording wavelengths available from the various pulsed and cw sources for both untreated and annealed crystals. The results and conclusions obtained from the experimental data are as follows:

(i) Volume holographic information recording, stor-

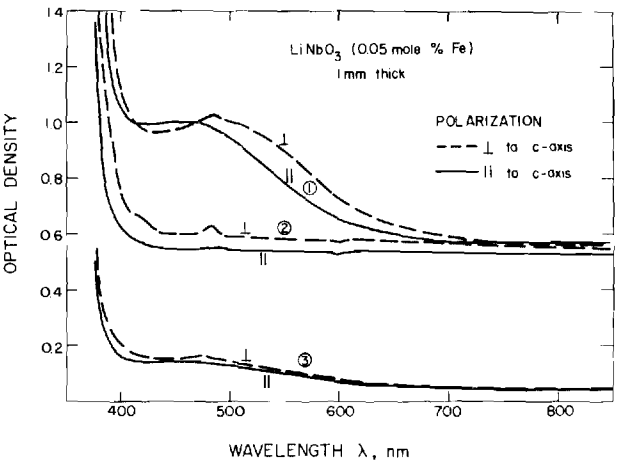

FIG. 1. Absorption spectra of 0.05 mole% iron-doped $LiNbO_3$ for (1) 1-mm-thick unannealed crystal and (2) 1-mm-thick annealed crystal. Curve (3) shows previously reported RCA spectral data corrected to a 1-mm-thick crystal for comparison.

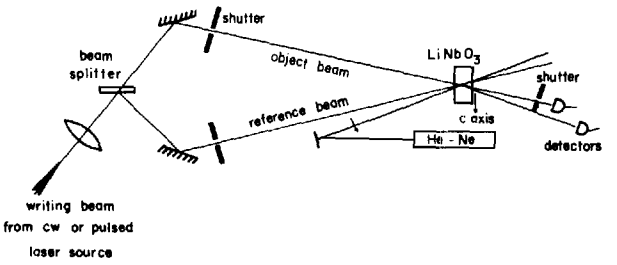

FIG. 2. Experimental arrangement for volume holographic storage. The writing beams used were from a cw argon laser (476.5, 488, 496.5, 514.5 nm), He-Ne laser (632.8 nm), and from a Q-switched frequency-doubled Nd:glass and ruby laser at 531 and 694.3 nm, respectively.

age, and retrieval has been accomplished in photorefractive crystals such as $LiNbO_3$ in times of 30 nsec, only limited by the duration of the optical source.

(ii) The recording sensitivities obtained for a pulsed writing source are slightly higher than the values estimated from sensitivity as a function of wavelength using cw sources at the other wavelengths.

(iii) The 1-mm-thick 0.05 mole% iron-doped $LiNbO_3$ crystal (not annealed) with a significant absorption band near the band edge had a recording sensitivity of 2.0 $mJ/cm^2/\%\eta$ at 476 nm and 2.5 $mJ/cm^2/\%\eta$ at 488 nm. These figures show that the crystal is at least 4 times more sensitive than the most sensitive strontium barium niobate crystal[1] and 60 times more sensitive than the previously reported most sensitive Fe-doped $LiNbO_3$.[2] In fact these sensitivities are even more significant if one considers the smaller interaction lengths of the crystal used in our experiments.

(iv) The storage with 10^{-8}-sec duration pulses indicates that the over-all time constant of recording process contributed by photoionization charge transport and retrapping is much shorter than the pulse duration times. Shorter pulses—such as picosecond duration—must be used to try to determine the dynamic response characteristics and ultimate speed limitations on the recording process.

(v) Increased sensitivity of the medium at longer wavelengths 632.8 nm and even at 694.3 nm is of considerable practical value since such storage material can be used with inexpensive low-power optical sources such as He-Ne lasers.

(vi) Comparison of the recording sensitivities and the absorption spectra of the two crystals cut from the same boule and heat treated after the growth conclusively indicates that the absorbing Fe^{+2} impurities play an important role in the recording sensitivity of the medium. The improvement in sensitivity for the unannealed crystal is by a factor of 100 over that of the annealed crystal characterized by the lower absorption. The unannealed crystal is also considerably more sensitive than the previously reported iron-doped $LiNbO_3$ of comparable doping concentration.[2] The improvement over the annealed crystal and the other reported

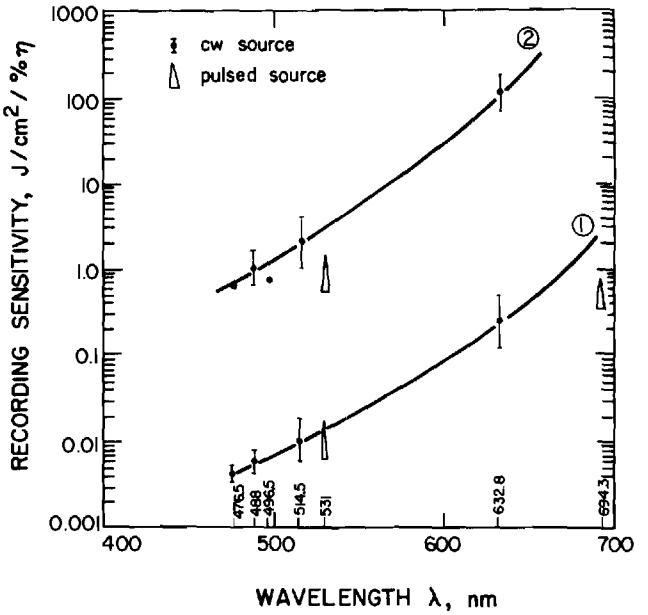

FIG. 3. Recording sensitivity measured in terms of energy required to write holograms capable of diffracting 1% of transmitted beam at 632.8 nm as a function of recording wavelength plotted for 0.05 mole% Fe-doped crystals; curve (1), 1-mm-thick unannealed and curve (2), 1-mm-thick but annealed. The required recording exposure (open triangles) for pulsed writing source is also plotted for these crystals.

results is significantly more than can be explained by only the increased absorption at writing wavelengths. Other processes in addition to photoionization, such as charge transport and retrapping, must play an additional role in determining the sensitivity. It is hypothesized that in addition to the above-mentioned effect the photoexcited carriers must be retrapped selectively to produce a space charge. This indicates that in addition to the absolute concentration of Fe^{+2} ions, the concentration of Fe^{+3} accepter ions and the relative concentration of the two ions must play a significant role in the improvement of the sensitivity. This point is also supported by the fact that the sensitivity data in Fig. 3. show that the ratio of the sensitivities of the two crystals seems relatively constant over the range of the studies.

*Work supported by the National Aeronautics and Space Administration.

[1] J. B. Thaxter and M. Kestigian, OSA Topical meeting on Optical Storage of Digital Data, Aspen, Colorado (unpublished).

[2] W. Phillips, J. J. Amodei, and D. L. Stabler, RCA Rev. 33, 94 (1972).

[3] F. S. Chen, J. T. La Macchia, and D. B. Frazer, Appl. Phys. Lett. 13, 223 (1968).

[4] The diffraction efficiency η is defined in terms of a fraction of transmitted light that is diffracted reconstructing the original information and is a function of interaction length L, change in index of refraction Δn, reading wavelength λ, and angle of incidence θ. All the diffraction efficiencies are either measured or corrected for a reading beam of wavelength $\lambda = 632.8$ nm using $\eta_\lambda = \sin^2(\pi \Delta n L/\lambda \cos\theta)$.

VII. SCATTERED LIGHT EFFECTS

Scattered light during hologram reconstruction has been recognized as a problem for high capacity storage in lithium niobate [12].

We have reported [13] the presence of cones of diffracted light upon illumination of previously laser-exposed crystals of lithium niobate. These diffraction cones are shown to result from the internally recorded interference pattern (hologram) resulting from the interference of the original incident laser beam with light scattered from material inhomogeneities. Diffraction cones are observed in iron-doped lithium niobate crystals that were exposed to a single laser beam and in crystals that were exposed to two superposed laser beams (i.e., during conventional holographic recording). In the two beam case, the diffraction cones are present in addition to the first order diffracted beam when the conventional two beam thick hologram is reconstructed. The diffracted cones produce the impression of scattered light during hologram reconstruction, an effect that has previously been reported in transition metal doped lithium niobate [12].

The diffraction cones, which have their apex in the exposed region of the crystal, are observed as rings (referred to as "scattering" rings, or diffraction rings) when a screen or a piece of film intersects the cone of light. Figure 1 in Reference 13 shows two typical diffraction ring patterns. For the single beam case, the observed results in lithium niobate are effectively the same as the experimental observations of Moran and Kaminow [14] for polymethyl methacrylate (PMMA), which had been exposed to ultraviolet laser light.

The presence of diffracted cones of light represents a possible limitation of heavily iron doped lithium niobate for data storage applications

because optical power is lost into the scattering induced diffraction cones that could otherwise be used to increase the diffraction efficiency and thus the total bit capacity of the two beam grating hologram. However, it has already been shown by Phillips, Amodei, and Staebler [12] that the "scattered" light may be erased 1) by illumination with uniform incoherent light or 2) by writing additional superposed holograms at new angles. In the latter case, "scattered" light from the previous holograms tends to be erased.

Our Ref. 13 is reproduced here for completeness.

Reprinted from APPLIED OPTICS, Vol. 13, page 1545, July 1974

Laser Scattering Induced Holograms in Lithium Niobate

R. Magnusson and T. K. Gaylord

School of Electrical Engineering, Georgia Institute of Technology, Atlanta, Georgia 30332.
Received 6 March 1974.

The presence of cones of diffracted light on illumination of previously laser-exposed crystals of lithium niobate is reported here. These diffraction cones are shown to result from the internally recorded interference pattern (hologram) resulting from the interference of the original incident laser beam with light scattered from material inhomogeneities. Diffraction cones are observed in iron-doped lithium niobate crystals that were exposed to a single laser beam and in crystals that were exposed to two superposed laser beams (i.e., during conventional holographic recording). In the two-beam case, the diffraction cones are present in addition to the first order diffracted beam when the conventional two-beam thick hologram is reconstructed. The diffraction cones produce the impression of scattered light during hologram reconstruction, an effect that has previously been reported in transition metal-doped lithium niobate[1] and photopolymers.[2]

The diffraction cones, which have their apex in the ex-

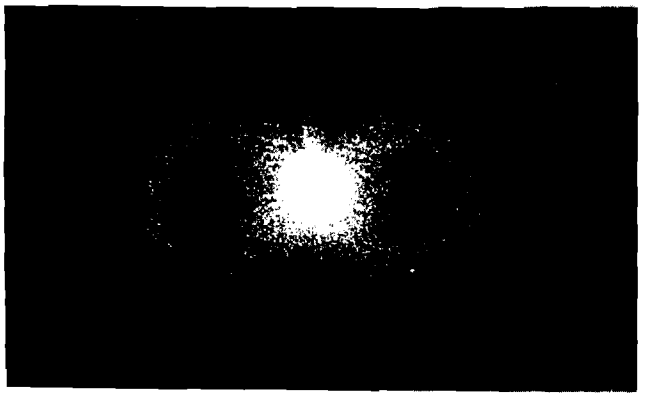

(a)

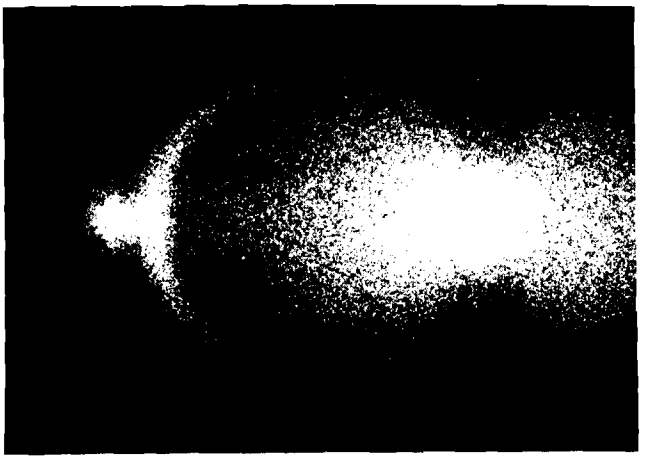

(b)

Fig. 1. Typical observed diffraction rings from a lithium niobate crystal in which a plane holographic grating has been recorded. The original writing beams had a wavelength λ_w = 515 nm, and the subsequent probing beam for the above photographs was λ_r = 633 nm and had an angle of incidence in (a) of $\alpha = 0°$, resulting in cone angles of $\Phi_1 = 5.7°$ and $\Phi_2 = -5.7°$, and an angle of incidence in (b) of $\alpha = 4.5°$, resulting in a cone angle $\Phi_1 = 10.6°$. Note in (b) the first order diffracted beam just to the left of the diffraction ring.

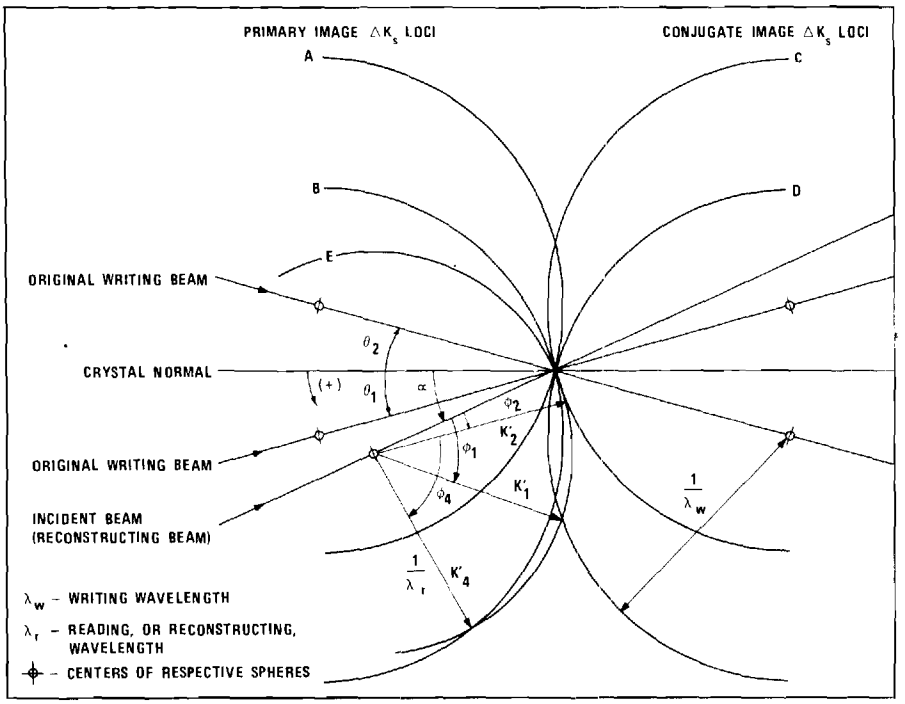

Fig. 2. Ewald sphere construction used in deriving the relationship between the diffraction cone angles, Φ, and the angle of incidence, α.

posed region of the crystal, are observed as rings (referred to as scattering rings, or diffraction rings) when a screen or a piece of film intersects the cone of light. Figure 1 shows two typical diffraction ring patterns. For the single-beam case, the observed results in lithium niobate are effectively the same as the experimental observations of Moran and Kaminow[3] for polymethyl methacrylate (PMMA), which had been exposed to ultraviolet laser light. The cones of diffracted light for this case of a single original exposing beam have been explained by Forshaw[2,4] using the Ewald sphere construction from diffraction theory (see, e.g., Ref. 5). This method is extended here to describe the diffraction cones that result when there are two intersecting exposing beams as in conventional holographic recording.

The Bragg diffraction condition $\Delta\vec{K}_G = \vec{K}' - \vec{K}$, where K' and $\vec{K}$ are the diffracted and incident beam wave vectors, respectively, and $\Delta\vec{K}_G$ is the fundamental holographic grating vector, predicts the direction of the well-defined first order diffracted beam. Another diffraction pattern is also produced that is described by $\Delta\vec{K}_S = \vec{K}_S - \vec{K}_i$, where $\vec{K}_S$ is any one of the wave vectors of the scattered wavelets of the original writing beam, and $\vec{K}_i$ is the wavevector of the original incident writing beam. The scattered light within the crystal interferes with the original beam, and this interference pattern is written into the crystal in the

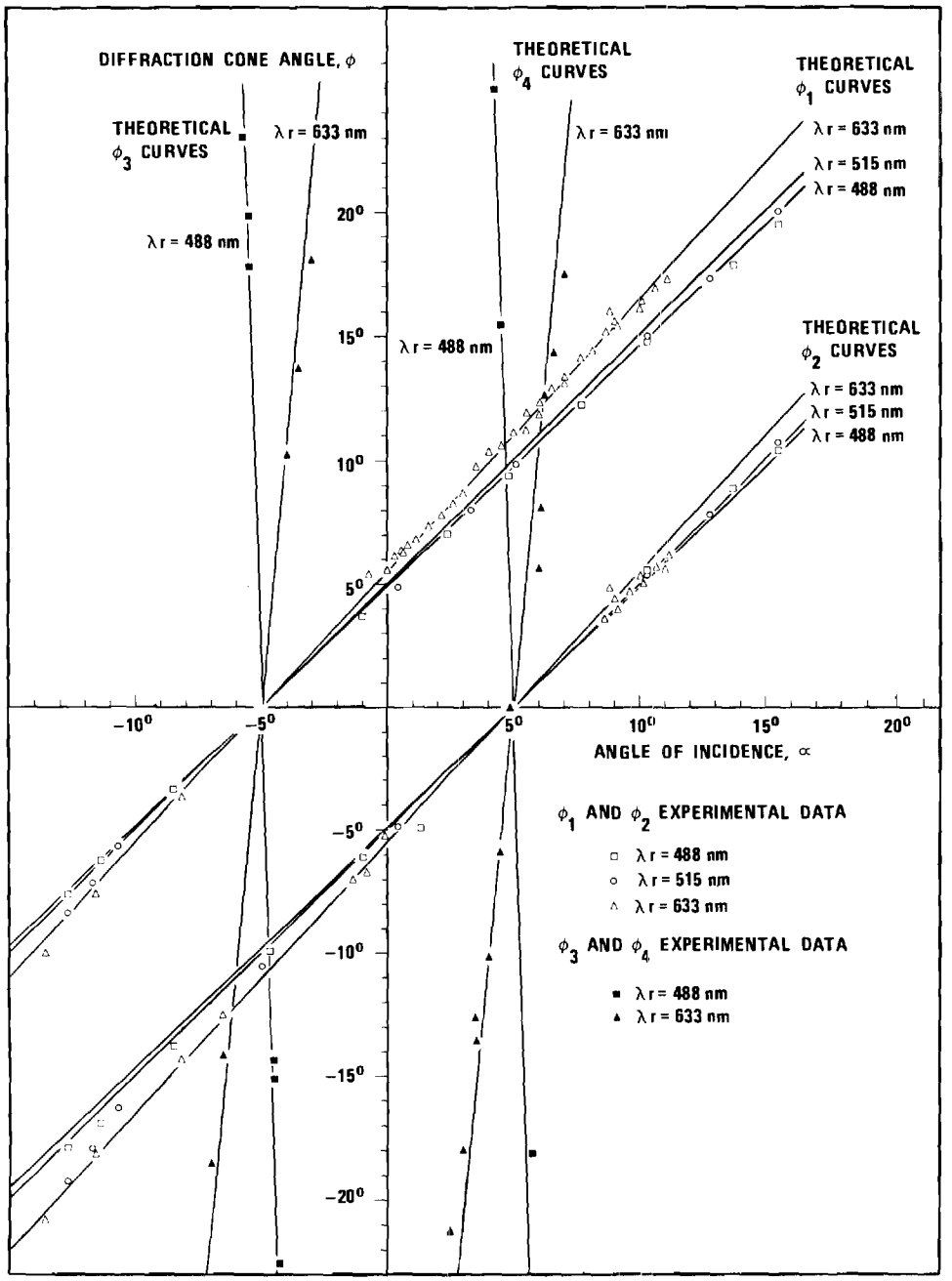

Fig. 3. Comparison of theoretical and experimental results for a $LiNbO_3$ crystal originally exposed to two intersecting laser beams of λ_w = 515 nm having angles of incidence equal to +5° and −5° and subsequently probed with a single low power laser beam of λ_r = 488 nm, 515 nm, and 633 nm. The theoretical curves are the same as those in Fig. 4, the patterns having been displaced by $\Delta\alpha = \pm 5°$.

same manner as the basic holographic grating is recorded in the crystal. Figure 2 illustrates the Ewald sphere construction necessary to analyze the diffraction cones that result for the case of two intersecting exposing beams. The surfaces A and B are the primary image loci for the $\Delta\vec{K}_s$ pattern, and the surfaces C and D are the corresponding conjugate image loci. That is, the vectors $+\Delta\vec{K}_s$ and $-\Delta\vec{K}_s$, if originating at the intersection of the original writing beams, terminate on the primary and conjugate spheres, respectively. All of these spheres have radii $1/\lambda_w$ where λ_w is the writing wavelength. The surface E is the reconstructing sphere with radius $1/\lambda_r$ where λ_r is the reading wavelength. $\vec{K}_1'$, $\vec{K}_2'$, and $\vec{K}_4'$ are the reconstruction wave vectors, and Φ_1, Φ_2, and Φ_4 are the corresponding diffraction cone angles. The intersection of the surface E with each of the other spheres describes a circle.

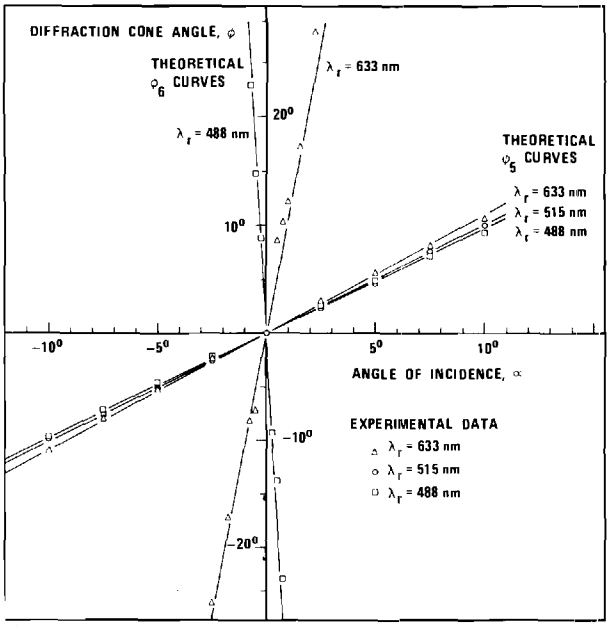

Fig. 4. Comparison of theoretical and experimental results for a $LiNbO_3$ crystal originally exposed to a single laser beam of λ_w = 515 nm at normal incidence and subsequently probed with a laser beam of λ_r = 488 nm, 515 nm, and 633 nm.

Wave vectors drawn from the center of E to these intersection circles represent the diffraction cones. By trigonometry it can be shown that

$$\phi_1,\phi_2 = 2\tan^{-1}\{[\sin(\alpha - \theta_2,\theta_1)]/[\cos(\alpha - \theta_2,\theta_1) + \lambda_w/\lambda_r]\}, \quad (1)$$

$$\phi_3,\phi_4 = 2\tan^{-1}\{[\sin(\alpha - \theta_2,\theta_1)]/[\cos(\alpha - \theta_2,\theta_1) - \lambda_w/\lambda_r]\}, \quad (2)$$

where Φ_1 and Φ_3 are the diffraction cone angles associated with the original writing beam that was at angle Θ_2. Likewise, Φ_2 and Φ_4 are associated with the writing beam that was at Θ_1. Angle Φ_3 is not shown in Fig. 2 because the intersection to which it corresponds (of reconstructing sphere E and primary sphere A) is not pictured. The diffraction cone angles, Φ_5 and Φ_6, for the normal incidence single writing beam case are obtained by setting Θ_1 and Θ_2 equal to zero in the above equations.

$$\phi_5 = \phi_1|_{\theta_2=0} = \phi_2|_{\theta_1=0} = 2\tan^{-1}[(\sin\alpha)/(\cos\alpha + \lambda_w/\lambda_r)], \quad (3)$$

$$\phi_6 = \phi_3|_{\theta_2=0} = \phi_4|_{\theta_1=0} = 2\tan^{-1}[(\sin\alpha)/(\cos\alpha - \lambda_w/\lambda_r)]. \quad (4)$$

These equations can be shown to be mathematically identical to Eqs. (3) and (4) in Ref. 2 on appropriate redefinition of angles.

Equations (1) and (2) are plotted in Fig. 3 as functions of the angle of incidence, α, for $\Theta_1 = +5°$, $\Theta_2 = -5°$, λ_w = 515 nm, and λ_r = 488 nm, 515 nm, and 633 nm. Experimentally measured values of the cone angle Φ are also plotted in Fig. 3. These are found to be in agreement with the theoretical predictions. It is seen from Fig. 3 that two rings are visible at all times. These represent the diffraction cones (of angles Φ_1 and Φ_2) generated by the intersection of the reconstructing surface with the conjugate writing surfaces. The angles Φ_3 and Φ_4 are found to be very sensitive to changes in α. Consequently, the corresponding rings are seen only for a very narrow angular range about $\alpha = \Theta_1, \Theta_2$ at our experimental wavelengths. This may also be seen from Fig. 2. (Imagine α varies and observe Φ_4.)

Equations (3) and (4) for the single exposing beam case at normal incidence ($\Theta_1 = 0$ or $\Theta_2 = 0$) are plotted as functions of the angle of incidence, α, in Fig. 4 for λ_w = 515 nm and λ_r = 488 nm, 515 nm, and 633 nm. Experimental data for the diffraction cone angle Φ are also included in Fig. 4. The data are seen to conform very closely to the theoretically predicted values.

The material used in these experiments was a 3.0-mm thick poled single crystal of lithium niobate doped with 0.1 mole% iron (in the melt). This heavily doped material, which was initially reddish, was oxygen annealed to make it transparent (presumably changing Fe^{2+} to Fe^{3+}). Laser scattering induced holograms were written with a single beam and with two intersecting beams of an argon ion laser operating at λ_w = 515 nm. Writing exposures to produce a readily observable diffraction cone pattern were typically 1 J. In the intersecting beam case the plane-wave grating holograms produced had a diffraction efficiency of approximately 20%.

The presence of diffracted cones of light represents a possible limitation of heavily iron-doped lithium niobate for data storage applications because optical power is lost into the scattering induced diffraction cones that could otherwise be used to increase the diffraction efficiency and thus the total bit capacity of the two-beam grating hologram. However, it has already been shown by Phillips, Amodei, and Staebler[1] that the scattered light may be erased (1) by illumination with uniform incoherent light or (2) by writing additional superposed holograms at new angles. In the latter case, scattered light from the previous holograms tends to be erased.

In addition, the reconstruction of laser scattering induced holograms in a material is potentially useful as a diagnostic tool to determine the nature of the scattering centers in the material. The above analysis has shown the *geometrical* relationships that exist for the diffraction cones. An analysis of the *distribution* of diffracted light within these cones is expected to yield detailed information about the scatterers.

This work was supported by the National Science Foundation and by the National Aeronautics and Space Administration.

References

1. W. Phillips, J. J. Amodei, and D. L. Staebler, RCA Rev. 33, 94 (1972).
2. M. R. B. Forshaw, Appl. Opt. 13, 2 (1974).
3. J. M. Moran and I. P. Kaminow, Appl. Opt. 12, 1964 (1973).
4. M. R. B. Forshaw, Opt. Commun. 8, 201 (1973).
5. V. V. Aristov and V. Sh. Shekhtman, Sov. Phys. Usp. 14, 263 (1971).

VIII. MULTIPLE HOLOGRAM STORAGE

In the last four sections, problems associated with multiple hologram storage have been discussed. The experimental results presented have been obtained using the basic experimental configuration shown in Fig. 1. Basic diagnostic experiments were performed by storing both single holograms and by storing multiple holograms [15] at a single location. The theoretical storage density of two dimensional (thin) holograms is 4×10^8 bits/cm^2 (one bit per square area one wavelength on a side) whereas in three dimensional volume (thick) holograms the theoretical storage density is 8×10^{12} bits/cm^3 (one bit per cube volume wavelength on a side) [16]. Obviously for truly high capacity storage, thick holograms (such as in optical crystals) need to be used instead of thin holograms (such as in photographic emulsions or metal films). Holographic memory systems have been described that utilize three-dimensional storage [17]. These systems superpose many holograms at a single location inside the thick recording medium by using a different reference beam angle for each hologram. The superposition of multiple holograms at a single volume location introduces the additional problem of writing new holograms in that volume without affecting those already there. When lithium niobate is used as the three dimensional storage material, this problem may be solved by the application of an external electric field [18], [19]. This greatly increases the sensitivity for writing while the sensitivity for erasure remains unchanged at a much lower value. Thus, as a new hologram is written, the other holograms at that location are only slightly erased. Work is presently underway in our laboratory to duplicate these electric field effects.

IX. RECORDED HOLOGRAM ANALYSIS

A method for analyzing the diffraction efficiency of thick, lossless transmission holograms in lithium niobate was developed. In lithium niobate and similar ferroelectrics, the literature assumes the induced changes in index of refraction are sinusoidal in nature, like the two beam plane wave interference pattern. The diffraction efficiency can be predicted for the sinusoidal case [3]. In actual fact, the index of refraction variation is probably not sinusoidal due to the obviously nonlinear writing characteristic (diffraction efficiency versus exposure), which is experimentally observed.

We have developed [5] a method for calculating arbitrary-order diffraction efficiencies of thick, lossless transmission gratings with arbitrary periodic grating shapes. For illustration, numerical values of the diffraction efficiencies at the first three Bragg angles were calculated for sinusoidal, square wave, triangular, and sawtooth gratings. The complete details of this method are expounded in Ref. 5, which is duplicated in this report. Also a comparison of our method to an extension of the Burckhardt matrix method [20] is presented in Fig. 7. Our method was determined to be 20 times faster on the computer!

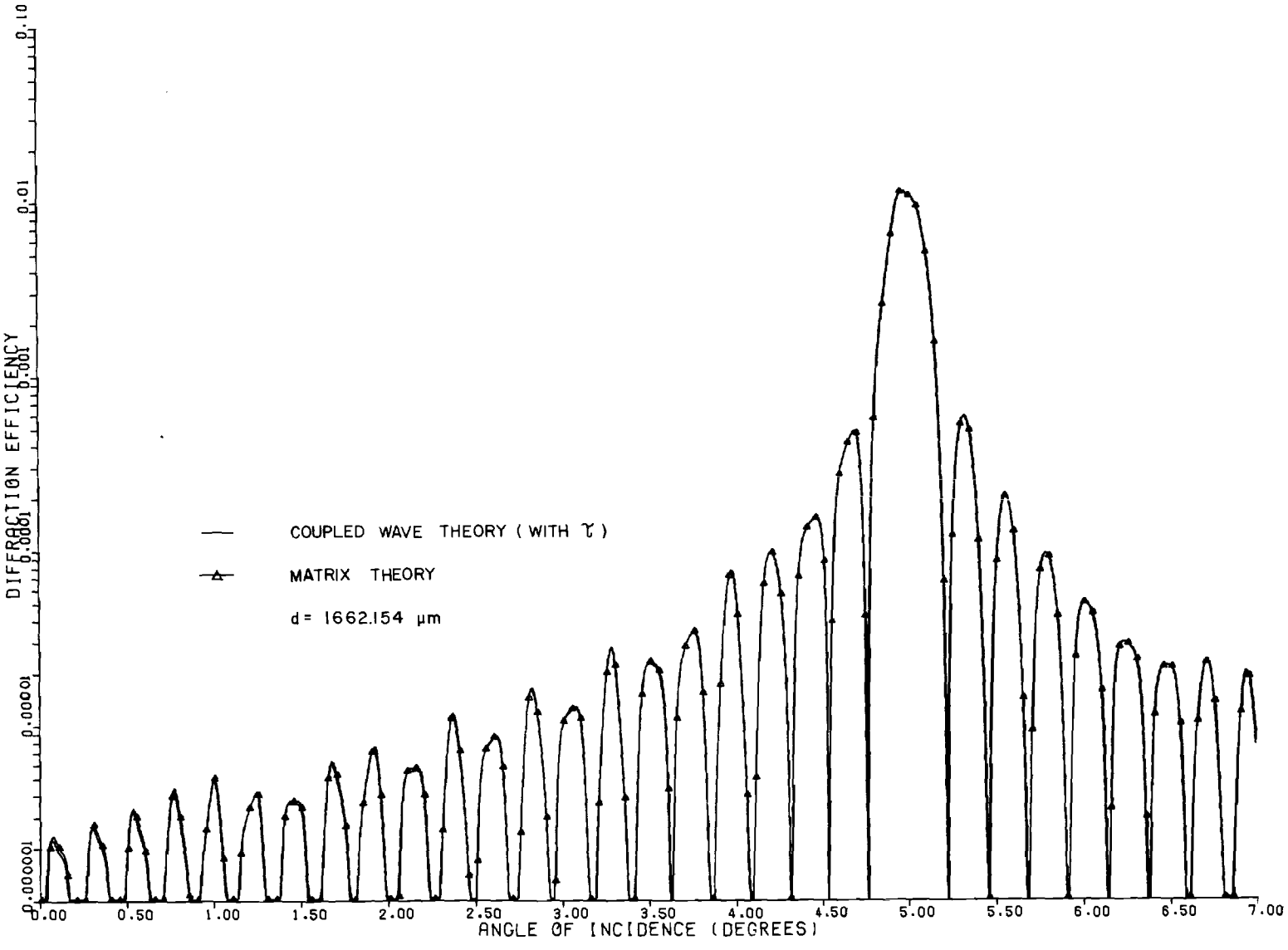

FIGURE 7. COMPARISON OF COUPLED-WAVE AND MATRIX THEORIES. The plot actually consists of two curves, but the difference is not discernible.

Calculation of arbitrary-order diffraction efficiencies of thick gratings with arbitrary grating shape*

S. F. Su and T. K. Gaylord

School of Electrical Engineering, Georgia Institute of Technology, Atlanta, Georgia 30332
(Received 18 July 1974)

A method for calculating arbitrary-order diffraction efficiencies of thick, lossless transmission gratings with arbitrary periodic grating shapes has been developed. This represents an extension of previous work to nonsinusoidal gratings and to higher-order Bragg angles. A Fourier-series representation of the grating is employed, along with a coupled-mode theory of diffraction. For illustration, numerical values of the diffraction efficiencies at the first three Bragg angles are calculated for sinusoidal, square-wave, triangular, and saw-tooth gratings. Numerical results for the same grating shapes with the same parameters are also calculated for comparison, by extending Burckhardt's numerical method for analyzing thick sinusoidal gratings. The comparison shows that the coupled-mode theory provides results with relative computational ease and results that are in agreement with calculations obtained by extending the more-rigorous Burckhardt theory to nonsinusoidal grating shapes and to higher-order Bragg angles.

Index Headings: Gratings; Diffraction.

It is well known that thick dielectric diffraction gratings differ from thin gratings in a number of important ways. Among these are the capability of high diffraction efficiency,[1] wavelength selectivity,[1] angular selectivity,[1] and reduced noise.[2] These give rise to the use of thick gratings as highly efficient diffraction gratings, narrow-band spectral filters,[3] thick-grating optical components, such as lenses,[4] and imaging systems capable of spectral resolution of extended objects.[2] In the field of integrated optics, thick gratings may be used as diffraction gratings for surface guiding of waves,[5] for thin-film distributed-feedback lasers,[6] for frequency-selective grating reflectors in thin-film lasers,[7] for grating couplers for launching single-mode light waves into thin-film waveguides,[8,9] and for electro-optic grating deflectors and modulators.[10]

In addition, thick (volume) holograms may be regarded as recordings of an infinite number of thick gratings. Thick holograms have attracted a great deal of interest by their use in high-capacity information storage,[11] in color holography,[12] and in white-light reconstruction of holograms.[13]

The diffraction of a plane wave by a thick sinusoidal grating at or near Bragg incidence has been considered by Burckhardt[14] and by Kogelnik.[1] Burckhardt has treated this case by solving the exact electromagnetic boundary-value problem and has obtained numerical results with a digital computer to determine the eigenvalues of a matrix and to solve the resulting set of linear algebraic equations. Kogelnik has obtained a closed-form expression for the diffraction efficiency at the first-order Bragg angle, by employing a coupled-wave theory. Coupled-wave theories also have been used successfully in the treatment of light diffraction by acoustic waves.[15,16] Recently, Chu and Tamir[17] treated this problem by using a guided-wave technique. They assumed sinusoidal modulation of the relative permittivity by the sound wave. Their treatment was based on a rigorous modal approach, utilizing the interrelationships between the characteristic-mode and the coupled-mode representations. With their method, not only the diffraction efficiency at the first order but also that of any higher order can be obtained.

In this paper, Chu and Tamir's approach is extended to examine the first- and higher-order diffraction efficiencies of thick, arbitrary-shape gratings. Because of the periodicity of the grating, a Fourier-series representation of the grating is employed. The gratings are assumed to be lossless. The reflections at surfaces of the gratings are at first neglected in the derivation, because, in practice, these can be eliminated by antireflection coatings. When surface and internal reflections are present, the results are corrected by a multiplicative transmittance factor.[18] For illustration, numerical values of the diffraction efficiencies at the first three Bragg angles are calculated for sinusoidal, square-wave, triangular, and saw-tooth gratings. For comparison, numerical results for the same grating shapes with the same parameters are also calculated by extending Burckhardt's numerical method. The comparison shows that the results from these two methods are in close agreement and that the present method is computationally simpler and more efficient.

THEORETICAL ANALYSIS

The model for a thick periodic grating is represented by Fig. 1. The x axis is chosen in the plane of incidence and parallel to the surfaces of the medium, the z axis is perpendicular to the surfaces of the medium, and the y axis is perpendicular to the page. For convenience, the fringe planes of the grating are assumed to be perpendicular to the surfaces of the medium and to the plane of incidence. The grating vector $\vec{K}$ is, therefore, parallel to the x axis. Thus, for lossless periodic gratings, the fringes of the grating can be represented by a spatial modulation of the relative dielectric constant

$$\epsilon_r(x)=\frac{\epsilon(x)}{\epsilon_0}=\epsilon_{r0}+\sum_{h=1}^{\infty}[\epsilon_{ch}\cos(hKx)+\epsilon_{sh}\sin(hKx)], \quad (1)$$

where $K=2\pi/L$, L is the period of the grating, ϵ_{r0} is the average value of ϵ_r, and ϵ_{ch} and ϵ_{sh} are the spatial modulations of ϵ_r, the subscripts c, s, and h denoting the

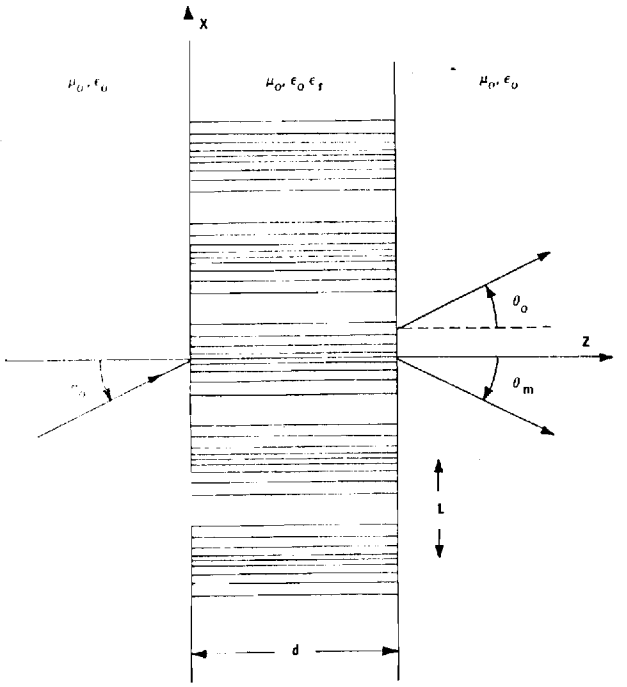

FIG. 1. Geometry of a thick grating with unslated fringes. The spatial modulation of ϵ is indicated by the line pattern.

quantities connected with the cosine gratings, the sine gratings and the hth-harmonic grating, respectively. Corresponding to the distribution of the relative dielectric constant, the distribution of the refractive index of the medium is

$$n(x) = n_0 + \sum_{h=1}^{\infty} [n_{ch} \cos(hKx) + n_{sh} \sin(hKx)], \tag{2}$$

where n_0 is the average refractive index of the medium, and n_{ch} and n_{sh} are the spatial modulations of n.

The electric field of the incident wave is assumed to be polarized perpendicular to the plane of incidence (H mode) and is of the form $\exp[j(\eta_0 x + \xi_0 z - \omega_0 t)]$. The wave propagation in the grating can be described by the scalar wave equation

$$[\nabla^2 + k^2 \epsilon_r(x)] E(x, z) = 0, \tag{3}$$

where $k = 2\pi/\lambda$, λ is the free-space wavelength of the incident plane wave, and $E(x, z)$ is the complex amplitude of the y component of the electric field, which is independent of y.

Equation (3) has been solved by Burckhardt,[14] using separation of variables, an infinite-series solution for the x-dependent equation, and a matrix method to solve the eigenvalue problem associated with a truncated set of the resulting infinite system of equations. This approach has been used to obtain numerical results for sinusoidal gratings. Kaspar[19] has extended Burckhardt's method to find the diffraction efficiency for nonsinusoidal absorption gratings. He has pointed out that when the absorption is strong, the phase-grating contribution to the diffraction efficiency is very small.

Chu and Tamir[17] have shown that the field inside the grating can be described in terms of coupled modes if the modulations of the relative dielectric constant are very small. In general, in addition to the zeroth mode, many higher-order modes are excited, because of the presence of the grating. For an incident wave (zero-order mode) of wavelength λ, and at an angle θ_0, the fundamental grating will diffract this wave if the Bragg condition, $m\lambda = 2L \sin\theta_0$, is satisfied or nearly satisfied. For this particular wavelength and angle, the harmonic gratings may or may not produce diffraction, depending on whether or not their corresponding Bragg conditions are satisfied or nearly satisfied. These diffracted modes of the fundamental and the harmonic gratings propagate in the same direction.

The dimensionless quantities

$$q_{ch} = 2(L/h\lambda)^2 \epsilon_{ch}, \quad h = 1, 2, 3, \ldots \tag{4}$$

$$q_{sh} = 2(L/h\lambda)^2 \epsilon_{sh}, \quad h = 1, 2, 3, \ldots \tag{5}$$

are called the effective-modulation indices.[17,20] Because ϵ_{ch} and ϵ_{sh} would typically be 10^{-4} or smaller, q_{ch} and q_{sh} are small even if L is many times as large as λ. For example, if $\theta_0 = 5°$ and $\epsilon_{c1} = 10^{-4}$, then $q_{c1} = 0.0066$. When q is very small compared to unity, it can be shown[17,21] that two coupled-wave equations and therefore two modes are sufficient to describe the coupling effects when the incident angle is equal to or near the Bragg angle. Therefore, for an incident wave of wavelength λ and at an angle θ_0, the electric field inside the grating can be written as the sum of the fundamental mode and an arbitrary mode

$$\tilde{E}(x, z) = \tilde{S}_0(z) \exp(j\tilde{\eta}_0 x) + \tilde{S}_m(z) \exp(j\tilde{\eta}_m x), \tag{6}$$

where $\tilde{\eta}_0$ and $\tilde{\eta}_m$ are the zeroth-mode and the mth-mode (with respect to the fundamental grating) transverse wave numbers, respectively. The continuity of the electric field at $z = 0$ and the Floquet theorem require that $\tilde{\eta}_0 = \eta_0 = k \sin\theta_0$ and $\tilde{\eta}_m = \eta_m = \eta_0 - 2m\pi/L$. The tilde will henceforth be used to denote the quantities in the dielectric medium when the gratings are present. The integer subscript m represents the mth-order diffraction. The integer h represents the hth-harmonic grating. Diffraction occurs when the hth-harmonic grating satisfies or nearly satisfies the Bragg condition $m_h \lambda = 2(L/h) \sin\theta_0$, where m_h represents the m_hth mode (with respect to the hth-harmonic grating) excited due to the hth-harmonic grating. Exact Bragg conditions occur when m_h is equal to m/h, where h divides evenly into m. Near-Bragg conditions occur for the wavelength λ when (i) the angle of incidence is near, but not equal to θ_0, and/or (ii) when the value of m is large, and h divides nearly evenly into m, so that m/h is almost an integer. Thus $\tilde{S}_m(z)$ in Eq. (6) represents the total amplitude, together with the propagation factor in the z direction, of the diffracted mode due to all of the gratings that satisfy or nearly satisfy the foregoing Bragg condition. At the boundary $z = d$, $\tilde{S}_0$ propagates at the angle θ_0, whereas $\tilde{S}_m$ propagates at an angle θ_m, which is determined by

$$\theta_m = -\sin^{-1}(\eta_m/k) = -\sin^{-1}(\sin\theta_0 - m\lambda/L). \tag{7}$$

The diffracted modes due to the gratings that are far from obeying the Bragg condition are assumed to be

negligibly small compared with $\bar{S}_0$ and $\bar{S}_m$. Therefore, the interaction between $\bar{S}_0$ and $\bar{S}_m$ can be characterized by the coupled-mode equations[22]

$$\frac{d\bar{S}_0}{dz} - j\bar{\xi}_0\bar{S}_0 - j\left(\sum_h^m (C_{chm_h} + jC_{shm_h})\right)\bar{S}_m = 0, \tag{8}$$

$$\frac{d\bar{S}_m}{dz} - j\bar{\xi}_m\bar{S}_m - j\left(\sum_h^m (C_{chm_h} - jC_{shm_h})\right)\bar{S}_0 = 0, \tag{9}$$

where $\bar{\xi}_0$ and $\bar{\xi}_m$ are the longitudinal wave numbers inside the medium when the gratings are absent. They are given by $\bar{\xi}_0 = k(\epsilon_{r0})^{1/2}\cos\varphi$ and

$$\bar{\xi}_m = \{k^2\epsilon_{r0} - [k(\epsilon_{r0})^{1/2}\sin\varphi - (2m\pi/L)]^2\}^{1/2},$$

where φ, the refraction angle in the medium, is given by $\varphi = \sin^{-1}[(\sin\theta_0)/(\epsilon_{r0})^{1/2}]$. The bar notation will henceforth be used to denote the quantities inside the medium when the gratings are absent. For a given value of the integer m, the subscript h may be any integer that divides evenly or nearly evenly into m, provided that the corresponding hth-harmonic grating exists. The symbol $\sum_h^m$ denotes the summation over all of these possible values of h. The coupling coefficients in Eqs. (8) and (9) are given by[17,21]

$$C_{chm_h} \cong \frac{1}{\bar{\xi}_0 + \bar{\xi}_m}\left(\frac{1}{(2)^{(m_h-1)}(m_h-1)!}\right)^2\left(\frac{\pi}{L/h}\right)^2\{[(q_{ch})^2 + (q_{sh})^2]^{1/2}\}^{m_h} \times\cos[m_h\tan^{-1}(\epsilon_{sh}/\epsilon_{ch})], \tag{10}$$

$$C_{shm_h} \cong \frac{1}{\bar{\xi}_0 + \bar{\xi}_m}\left(\frac{1}{(2)^{(m_h-1)}(m_h-1)!}\right)^2\left(\frac{\pi}{L/h}\right)^2\{[(q_{ch})^2 + (q_{sh})^2]^{1/2}\}^{m_h} \times\sin[m_h\tan^{-1}(\epsilon_{sh}/\epsilon_{ch})]. \tag{11}$$

If the grating does not exist, $C_{chm_h} = C_{shm_h} = 0$, there is no coupling between $\bar{S}_0$ and $\bar{S}_m$ and therefore no diffraction. Under this condition, only Eq. (8) has physical significance. It represents the propagation of the fundamental mode (incident wave) inside the medium.

The solutions of Eqs. (8) and (9) are of the form

$$\bar{S}_0(z) = A_0\exp(j\tilde{\xi}_0 z) + B_0\exp(j\tilde{\xi}_m z), \tag{12}$$

$$\bar{S}_m(z) = A_m\exp(j\tilde{\xi}_0 z) + B_m\exp(j\tilde{\xi}_m z). \tag{13}$$

The wave numbers $\tilde{\xi}_0$ and $\tilde{\xi}_m$ can be found directly by substituting Eqs. (12) and (13) into Eqs. (8) and (9). They are

$$\tilde{\xi}_{0,m} = \frac{\bar{\xi}_0 + \bar{\xi}_m}{2} \pm \left[\left(\frac{\bar{\xi}_0 - \bar{\xi}_m}{2}\right)^2 + \left(\sum_h^m C_{chm_h}\right)^2 + \left(\sum_h^m C_{shm_h}\right)^2\right]^{1/2}, \tag{14}$$

where the plus sign corresponds to $\tilde{\xi}_0$ and the minus sign to $\tilde{\xi}_m$. The constants A_0, B_0, A_m, and B_m are determined by the boundary conditions and

$$\left(\sum_h^m (C_{chm_h} - jC_{shm_h})\right)A_0 - (\tilde{\xi}_0 - \bar{\xi}_m)A_m = 0, \tag{15}$$

$$\left(\sum_h^m (C_{chm_h} - jC_{shm_h})\right)B_0 - (\tilde{\xi}_m - \bar{\xi}_m)B_m = 0, \tag{16}$$

which are obtained from Eqs. (9), (12), and (13). To specify the boundary conditions, the amplitude of the incident wave is assumed to be unity at $z = 0$ so that, from Eq. (12),

$$\bar{S}_0(0) = A_0 + B_0 = 1. \tag{17}$$

Initially, the amplitude of the diffracted wave is zero. Therefore, evaluating Eq. (13) at $z = 0$ gives

$$\bar{S}_m(0) = A_m + B_m = 0. \tag{18}$$

Solving Eqs. (15), (16), (17), and (18) for A_0, B_0, A_m, and B_m gives

$$A_0 = \frac{\tilde{\xi}_0 - \bar{\xi}_m}{\tilde{\xi}_0 - \tilde{\xi}_m} = \frac{1}{2}\left(\left(\bar{\xi}_0 - \bar{\xi}_m\right) + \left\{(\bar{\xi}_0 - \bar{\xi}_m)^2 + 4\left[\left(\sum_h^m C_{chm_h}\right)^2 + \left(\sum_h^m C_{shm_h}\right)^2\right]\right\}^{1/2}\right) \Bigg/ \left(\left\{(\bar{\xi}_0 - \bar{\xi}_m)^2 + 4\left[\left(\sum_h^m C_{chm_h}\right)^2 + \left(\sum_h^m C_{shm_h}\right)^2\right]\right\}^{1/2}\right), \tag{19}$$

$$B_0 = \frac{\bar{\xi}_m - \tilde{\xi}_m}{\tilde{\xi}_0 - \tilde{\xi}_m} = \frac{1}{2}\left(\left(\bar{\xi}_m - \bar{\xi}_0\right) + \left\{(\bar{\xi}_0 - \bar{\xi}_m)^2 + 4\left[\left(\sum_h^m C_{chm_h}\right)^2 + \left(\sum_h^m C_{shm_h}\right)^2\right]\right\}^{1/2}\right) \Bigg/ \left(\left\{(\bar{\xi}_0 - \bar{\xi}_m)^2 + 4\left[\left(\sum_h^m C_{chm_h}\right)^2 + \left(\sum_h^m C_{shm_h}\right)^2\right]\right\}^{1/2}\right), \tag{20}$$

$$A_m = -B_m = \left[\left(\sum_h^m C_{chm_h}\right) - j\left(\sum_h^m C_{shm_h}\right)\right] \Bigg/ \left(\left\{(\bar{\xi}_0 - \bar{\xi}_m)^2 + 4\left[\left(\sum_h^m C_{chm_h}\right)^2 + \left(\sum_h^m C_{shm_h}\right)^2\right]\right\}^{1/2}\right). \tag{21}$$

For the exact Bragg condition, $\bar{\xi}_m = \bar{\xi}_0$ and $\theta_m = \theta_0$. Hence, Eqs. (14), (19), (20), and (21) become

$$\tilde{\xi}_{0,m} = \bar{\xi}_0 \pm \left[\left(\sum_h^m C_{chm_h}\right)^2 + \left(\sum_h^m C_{shm_h}\right)^2\right]^{1/2}, \tag{22}$$

$$A_0 = \tfrac{1}{2} = B_0, \tag{23}$$

$$A_m = -B_m = \frac{1}{2}\left[\left(\sum_h^m C_{chm_h}\right) - j\left(\sum_h^m C_{shm_h}\right)\right] \Bigg/ \left\{\left[\left(\sum_h^m C_{chm_h}\right)^2 + \left(\sum_h^m C_{shm_h}\right)^2\right]^{1/2}\right\}. \tag{24}$$

Thus, the transmitted and the diffracted modes are

$$\bar{S}_0(z) = \exp(j\bar{\xi}_0 z)\cos\left\{\left[\left(\sum_h^m C_{chm_h}\right)^2 + \left(\sum_h^m C_{shm_h}\right)^2\right]^{1/2} z\right\}, \tag{25}$$

$$\bar{S}_m(z) = j2A_m \exp(j\bar{\xi}_0 z) \times \sin\left\{\left[\left(\sum_h^m C_{chm_h}\right)^2 + \left(\sum_h^m C_{shm_h}\right)^2\right]^{1/2} z\right\}, \tag{26}$$

where C_{chm_h} and C_{shm_h} are given by Eqs. (10) and (11) with $\bar{\xi}_m = \bar{\xi}_0$, and A_m is given by Eq. (24). Equation (26) is the general formula for the mth-diffracted mode due to any periodic grating when the incident angle of the zeroth mode satisfies the Bragg condition $m\lambda = 2L\sin\theta_0$. The diffraction efficiency for the mth order of diffraction is defined as

$$DE_m \equiv \bar{S}_m(d)\bar{S}_m^*(d)/\bar{S}_0(0)\bar{S}_0^*(0), \tag{27}$$

and thus for exact Bragg conditions

$$DE_m = \sin^2\left\{\left[\left(\sum_h^m C_{chm_h}\right)^2 + \left(\sum_h^m C_{shm_h}\right)^2\right]^{1/2} d\right\}, \tag{28}$$

where the asterisk denotes complex conjugate. Upon substituting Eqs. (10) and (11), with $\bar{\xi}_m = \bar{\xi}_0$, into Eq. (28) and performing some algebraic manipulations, we find that

$$DE_m = \sin^2\left(\left\{\left[\sum_h^m \frac{\pi}{(2)^{m_h}}\left(\frac{L^{(m_h-1)}}{(m_h-1)!\,(h)^{(m_h-1)}}\right)^2 \times \frac{\{[(\epsilon_{ch})^2 + (\epsilon_{sh})^2]^{1/2}\}^{m_h}}{\lambda^{(2m_h-1)}} \frac{\cos[m_h \tan^{-1}(\epsilon_{sh}/\epsilon_{ch})]}{(\epsilon_{r0})^{1/2}\cos\varphi}\right]^2 + \left[\sum_h^m \frac{\pi}{(2)^{m_h}}\left(\frac{L^{(m_h-1)}}{(m_h-1)!\,(h)^{(m_h-1)}}\right)^2 \frac{\{[(\epsilon_{ch})^2 + (\epsilon_{sh})^2]^{1/2}\}^{m_h}}{\lambda^{(2m_h-1)}} \times \frac{\sin[m_h \tan^{-1}(\epsilon_{sh}/\epsilon_{ch})]}{(\epsilon_{r0})^{1/2}\cos\varphi}\right]^2\right\}^{1/2} d\right). \tag{29}$$

Equation (29) is the general expression for the diffraction efficiency at the mth-order Bragg angle for a periodic grating of arbitrary grating shape. For example, the first-, second-, and third-order diffraction efficiencies for a grating, whose dielectric constant profile can be expressed as a Fourier sine series, are

$$DE_1 = \sin^2\left(\frac{\epsilon_{s1}\pi d}{2\lambda(\epsilon_{r0})^{1/2}\cos\varphi}\right), \tag{30}$$

$$DE_2 = \sin^2\left[\left(\frac{L^4(\epsilon_{s1})^4}{4\lambda^4} + (\epsilon_{s2})^2\right)^{1/2} \frac{\pi d}{2\lambda(\epsilon_{r0})^{1/2}\cos\varphi}\right], \tag{31}$$

and

$$DE_3 = \sin^2\left[\left(\epsilon_{s3} - \frac{L^4(\epsilon_{s1})^3}{16\lambda^4}\right) \frac{\pi d}{2\lambda(\epsilon_{r0})^{1/2}\cos\varphi}\right]. \tag{32}$$

In Eqs. (30), (31), and (32), only the Fourier grating components ϵ_{s1}, ϵ_{s2}, and ϵ_{s3} are required to evaluate the diffraction efficiencies DE_1, DE_2, and DE_3. Table I gives these Fourier components, normalized to the amplitude of the fundamental grating ϵ_{s1} for gratings having sinusoidal, square-wave, triangular, and saw-tooth dielectric constant profiles. Note that the sinusoidal, square-wave, and triangular grating shapes can each be represented by a Fourier cosine series also. In this case, the resultant diffraction-efficiency expressions contain only ϵ_{c1}, ϵ_{c2}, and ϵ_{c3}. If $n_{ch} \ll n_0$ and $n_{sh} \ll n_0$, which are

TABLE I. First three Fourier components for various relative dielectric constant profiles (grating shapes). Components are normalized to the amplitude of the fundamental grating ϵ_{s1}.

Grating component	Sinusoidal grating	Square-wave grating	Triangular grating	Saw-tooth grating
$\epsilon_{s1}/\epsilon_{s1}$	1	1	1	1
$\epsilon_{s2}/\epsilon_{s2}$	0	0	0	$-\frac{1}{2}$
$\epsilon_{s3}/\epsilon_{s1}$	0	$\frac{1}{3}$	$-\frac{1}{9}$	$\frac{1}{3}$

true in most cases,[1] it can be shown that $\epsilon_{ch} = 2n_0 n_{ch}$ and $\epsilon_{sh} = 2n_0 n_{sh}$. Therefore, with $(\epsilon_{r0})^{1/2} = n_0$, Eq. (29) becomes

$$DE_m = \sin^2\left(\left\{\left[\sum_h^m \left(\frac{L^{(m_h-1)}}{(m_h-1)!\,(h)^{(m_h-1)}}\right)^2 \frac{\pi\{[(n_{ch})^2 + (n_{sh})^2]^{1/2}\}^{m_h}}{\lambda^{(2m_h-1)}} \times \frac{(n_0)^{(m_h-1)}\cos[m_h \tan^{-1}(n_{sh}/n_{ch})]}{\cos\varphi}\right]^2 + \left[\sum_h^m \left(\frac{L^{(m_h-1)}}{(m_h-1)!\,(h)^{(m_h-1)}}\right)^2 \times \frac{\pi\{[(n_{ch})^2 + (n_{sh})^2]^{1/2}\}^{m_h}}{\lambda^{(2m_h-1)}} \frac{(n_0)^{(m_h-1)}\sin[m_h \tan^{-1}(n_{sh}/n_{ch})]}{\cos\varphi}\right]^2\right\}^{1/2} d\right). \tag{33}$$

The results calculated with Eqs. (30)–(32) do not agree with those calculated by use of Burckhardt's matrix method. This is because Burckhardt takes the boundary reflections into account, whereas they are not included in the foregoing derivation. Our results may be corrected to include boundary reflections by multiplying the diffraction efficiency by the transmittance factor,

$$\tau_m = (1-R)^2[1 + 2R\cos(2\beta d) + R^2]/\{(1-R^2)^2 + 4R^2[\cos^2(2\nu_m d) + \cos^2(2\beta d)] - 4R(1+R^2)\cos(2\nu_m d)\cos(2\beta d)\}, \tag{34}$$

where $R = \sin^2(\theta_0 - \varphi)/\sin^2(\theta_0 + \varphi)$, $\beta = 2\pi(\epsilon_{r0})^{1/2}(\cos\varphi)/\lambda$, and $\nu_m = [(\sum_h^m C_{chm_h})^2 + (\sum_h^m C_{shm_h})^2]^{1/2}$ evaluated with $\bar{\xi}_m = \bar{\xi}_0$ for exact Bragg conditions. This factor is the same as the transmittance factor derived by Kogelnik and given as Eq. (8) in Ref. 18, but with νd in that equation replaced by the argument of the sine function in Eq. (28) of this paper. This allows generalization to higher diffraction orders and nonsinusoidal gratings.

RESULTS AND DISCUSSION

The coupled-wave analysis in the preceding section was numerically implemented on a UNIVAC 1108 computer and calculations were performed for gratings having sinusoidal, square-wave, triangular, and saw-tooth distributions of the dielectric constant. Table II gives numerical values for the diffraction efficiencies at the first-, second-, and third-order Bragg angles for these gratings. These results represent $DE_1\tau_1$, $DE_2\tau_2$, and $DE_3\tau_3$ as obtained from Eqs. (30)–(32) and (34) with $\epsilon_{r0} = 2.3225$ (value used in Refs. 14 and 18) and $\epsilon_{s1} = 10^{-4}\epsilon_{r0}$. The fundamental spacing of these gratings is $L = 3.630$ μm (resulting from recording with two beams of $\lambda = 632.8$ nm at $\theta_0 = \pm 5.0°$). For comparison, the results obtained by extending Burckhardt's numerical method (matrix

TABLE II. Comparison of diffraction efficiency in percent at the first-, second-, and third-order Bragg angles for transmission gratings with boundary reflections and with the same average and fundamental Fourier grating components. The grating parameters are $\epsilon_{r0} = 2.3225$ (value used in Refs. 14 and 18), $\epsilon_{s1} = 10^{-4}\,\epsilon_{r0}$, $L = 3.6303$ μm, and the wavelength $\lambda = 0.6328$ μm. Diffraction efficiencies of less than 5×10^{-8}% are listed as 0.00(−5).

Grating thickness (μm)	Diffraction order	Diffraction efficiency (in % with power of 10 in parentheses) Sinusoidal grating Coupled wave	Matrix	Square-wave grating Coupled wave	Matrix	Triangular grating Coupled wave	Matrix	Saw-tooth grating Coupled wave	Matrix
	1	1.61(−3)	1.61(−3)	1.61(−3)	1.61(−3)	1.61(−3)	1.61(−3)	1.61(−3)	1.61(−3)
10	2	0.00(−5)	0.00(−5)	0.00(−5)	0.00(−5)	0.00(−5)	0.00(−5)	3.87(−4)	3.87(−4)
	3	0.00(−5)	0.00(−5)	1.14(−4)	1.14(−4)	1.26(−5)	1.25(−5)	1.14(−4)	1.13(−4)
	1	1.57(−1)	1.57(−1)	1.57(−1)	1.57(−1)	1.57(−1)	1.57(−1)	1.57(−1)	1.57(−1)
100	2	0.15(−5)	0.13(−5)	0.15(−5)	0.14(−5)	0.15(−5)	0.13(−5)	2.53(−2)	2.56(−2)
	3	0.00(−5)	0.00(−5)	1.12(−2)	1.12(−2)	1.25(−3)	1.23(−3)	1.12(−2)	1.12(−2)
	1	1.21(+1)	1.21(+1)	1.21(+1)	1.21(+1)	1.21(+1)	1.21(+1)	1.21(+1)	1.21(+1)
1000	2	2.53(−4)	2.46(−4)	2.53(−4)	2.46(−4)	2.53(−4)	2.46(−4)	4.23(+0)	4.26(+0)
	3	0.00(−5)	0.00(−5)	1.64(+0)	1.64(+0)	1.83(−1)	1.84(−1)	1.64(+0)	1.66(+0)

method) to nonsinusoidal gratings are also shown in Table II. These results were calculated by programming Burckhardt's method on a UNIVAC 1108 computer and using the UNIVAC Math Pack subroutines to solve the eigenvalue problem and the set of linear algebraic equations. Table II shows that the results of these two methods are in close agreement; the deviation between these two methods does not exceed 2.8% for diffraction efficiencies larger than 5×10^{-6}%. Diffraction efficiencies smaller than 5×10^{-6}% are less significant physically because the corresponding low-level diffracted intensities are difficult to measure. Diffraction efficiencies of less than 5×10^{-8}% have been listed as zero in Table II. In addition to the results in Table II, we have performed calculations for other grating thicknesses (15, 50, 1500, and 2000 μm) and other fundamental grating spacings (1.222 and 1.822 μm). We found that the deviation between the coupled-wave analysis and the matrix analysis does not exceed 6.7% for any case with a diffraction efficiency larger than 5×10^{-6}%. Typically, the percentage deviation is a few tenths of 1%.

Although Burckhardt's numerical approach is rigorous, a number of mathematical problems such as truncation of the matrix and discarding of large positive eigenvalues must be overcome. A discussion of these is included in Ref. 14. In addition, another mathematical difficulty associated with the Burckhardt method, encountered in the present work, is a singularity that arises in the process of solving a set of linear algebraic equations. For pure phase gratings, Eq. (9) in Ref. 14 is real and symmetric. When the incident wave is at the Bragg angle, pairs of equal elements are introduced on the principal diagonal of the matrix in that equation. Thus, when the modulation amplitude is small, pairs of equal eigenvalues are usually induced. This results in a singularity in the matrix in Eq. (34) in Ref. 14; therefore, the equation is nonsolvable. For the parameters in the particular examples of Ref. 14, this problem does not occur because the modulation amplitude is large ($0.0035\,\epsilon_{r0}$). However, the modulation amplitude may, in practice, be very small (of the order 10^{-4} or smaller) and the singularity problem must, therefore, be overcome. A way to avoid the singularity is by shifting the incident angle by a negligible amount away from the Bragg angle. Physically, because the shift is negligibly small (10^{-5} degrees was used here), the incident wave can still be regarded as being incident at the Bragg angle. In the present method, a closed-form expression for the diffraction efficiency is obtained, and no mathematical difficulties arise in the process of calculation. The computer time needed in the present method is only about $\frac{1}{20}$ of that needed with the extended Burckhardt method to perform the same calculations.

From the results, we found that boundary reflections produced by the surfaces can considerably change the diffraction efficiency. The change can be an increase or a decrease, depending on whether the transmittance factor is greater or less than unity. This effect has been studied by Cohen and Gordon.[23] For the grating parameters used here, τ is typically in the range 0.70 to 1.20. In practice, the boundary reflections can be eliminated by antireflection coatings on the surfaces of the gratings. We also found that the diffraction efficiency of a given higher order is mainly contributed by the corresponding higher-order Fourier component of the grating. The difference between the diffraction efficiencies for sinusoidal and nonsinusoidal gratings (having the same average and fundamental grating amplitudes) appears only in the higher-order diffractions. The higher-order diffraction efficiencies, however, very strongly depend on the grating shape. Also, for small grating modulations, the diffraction efficiencies at any order are very dependent on grating thickness; they increase with increasing thickness. Marcuse[24] has suggested that, for small-amplitude thick nonsinusoidal phase gratings, the higher-order diffraction efficiencies might be estimated from the relative amplitudes of the spatial harmonics, consistent with the assumption of perturbation theory that only one Fourier component can satisfy the Bragg condition for a given wavelength incident wave. Our calculations show that this is true except when the amplitude of the harmonic grating ($h = m$)

is very small compared to the amplitude of the fundamental and the lower-order contributing harmonic gratings. In this case, the contributions from higher-order diffractions ($h < m$) are significant. In addition, we found that the agreement between the coupled-wave method and the matrix method is better when the $h = m$ term is dominant over $h < m$ terms. Rigrod[25] has shown that for reflection gratings there is no correlation between higher-order diffraction efficiencies and the corresponding harmonics of the index profile. The present results show that this is not true for transmission gratings.

The present method can be used to analyze the diffraction efficiency of any thick periodic grating, regardless of the dielectric-constant profile (grating shape). The examples analyzed here have had even or odd symmetry. However, the method does not require any symmetry to exist, but only that the grating be periodic. From the gratings analyzed, different grating shapes have shown different distributions of higher-order diffraction efficiencies. This indicates the possibility that this type of analysis might be used in reverse to determine the grating shapes of thick hologram gratings such as those recorded in ferroelectric crystals.[26] Due to nonlinearities in these materials a sinusoidal exposure does not necessarily produce a sinusoidal change in index of refraction. Depending on which of the possible physical mechanisms is operative in a given situation (such as drift of charge carriers or diffusion of carriers) different grating shapes are generated.[27]

Further, the derivations in the preceding section have assumed that the grating medium is lossless, that the gratings are unslanted with respect to the grating boundaries (grating vector parallel to surfaces of medium), and that the incident wave is H mode polarized. If the medium is lossy, the results still apply, except that the coupling coefficients are complex; therefore, the attenuation factors are implicitly contained in the expressions for the transmitted wave and the diffracted wave. The method presented here can also be straightforwardly applied to the analysis of slanted gratings and to E-mode polarization of the incident wave.

CONCLUSIONS

A simple method of calculating arbitrary-order diffraction efficiencies of thick transmission gratings with arbitrary periodic grating shapes has been presented. The analysis uses a coupled-mode theory to obtain a closed-form expression for the diffraction efficiency of an arbitrary order. This method provides results with relative computational ease and results that are in close agreement with those obtained by extending Burckhardt's numerical method.

ACKNOWLEDGMENT

The authors are indebted to Frank G. Kaspar for his helpful comments on this work.

*Work supported by the National Science Foundation under Grant No. GK-37453 and by the National Aeronautics and Space Administration under Contract No. NAS8-30246.

[1]H. Kogelnik, Bell Syst. Tech. J. 48, 2909 (1969).
[2]M. R. B. Forshaw, Opt. Laser Technol. 6, 28 (1974).
[3]B. H. Crawford, J. Sci. Instrum. 31, 333 (1954).
[4]J. N. Latta and R. C. Fairchild, J. Opt. Soc. Am. 63, 487 (1973).
[5]R. Shubert and J. H. Harris, J. Opt. Soc. Am. 61, 154 (1971).
[6]H. Kogelnik and C. V. Shank, Appl. Phys. Lett. 18, 152 (1971).
[7]I. P. Kaminow, H. P. Weber, and E. A. Chandross, Appl. Phys. Lett. 18, 497 (1971).
[8]H. Kogelnik and T. P. Sosnowski, Bell Syst. Tech. J. 49, 1602 (1970).
[9]M. L. Dakss, L. Kuhn, P. F. Heidrich, and B. A. Scott, Appl. Phys. Lett. 16, 523 (1970).
[10]J. M. Hammer, Appl. Phys. Lett. 18, 147 (1971).
[11]P. J. Van Heerden, Appl. Opt. 2, 393 (1963).
[12]K. S. Pennington and L. H. Lin, Appl. Phys. Lett. 7, 56 (1965).
[13]G. W. Stroke and A. E. Labeyrie, Phys. Lett. 20, 368 (1966).
[14]C. B. Burckhardt, J. Opt. Soc. Am. 56, 1502 (1966).
[15]P. Phariseau, Proc. Indian Acad. Sci. A 44, 165 (1956).
[16]C. F. Quate, C. D. W. Wilkinson, and D. K. Winslow, Proc. IEEE 53, 1604 (1965).
[17]R. S. Chu and T. Tamir, IEEE Tran. Micro. Thry. Tech. 18, 486 (1970).
[18]H. Kogelnik, J. Opt. Soc. Am. 57, 431 (1967).
[19]F. G. Kaspar, J. Opt. Soc. Am. 63, 37 (1973).
[20]T. Tamir and H. C. Wang, Can. J. Phys. 44, 2073 (1966).
[21]T. Tamir, Can. J. Phys. 44, 2461 (1966).
[22]D. A. Watkins, *Topics in Electromagnetic Theory* (Wiley, New York, 1958).
[23]M. G. Cohen and E. I. Gordon, Bell Syst. Tech. J. 45, 945 (1966).
[24]D. Marcuse, *Light Transmission Optics* (Van Nostrand Reinhold, New York, 1972), p. 71.
[25]W. W. Rigrod, J. Opt. Soc. Am. 64, 97 (1974); 64, 895E (1974).
[26]F. S. Chen, J. T. LaMacchia, and D. B. Fraser, Appl. Phys. Lett. 13, 223 (1968).
[27]J. J. Amodei, RCA Rev. 32, 185 (1971).

X. SYSTEMS CONSIDERATIONS

A three-dimensional lithium niobate recording and storage system is shown schematically in Fig. 8. The systems aspects of such an optical recording scheme were thoroughly reviewed in this study. One of the results of this review was the publication of a state-of-the-art review [8]. This article is reproduced in this report and is a self-contained review. Another result of this review was a change in our experimental reading system. An angular accessing system was developed and it is illustrated in Fig. 9. This system allows accurate and simple angular beam positioning without the need to rotate the crystal.

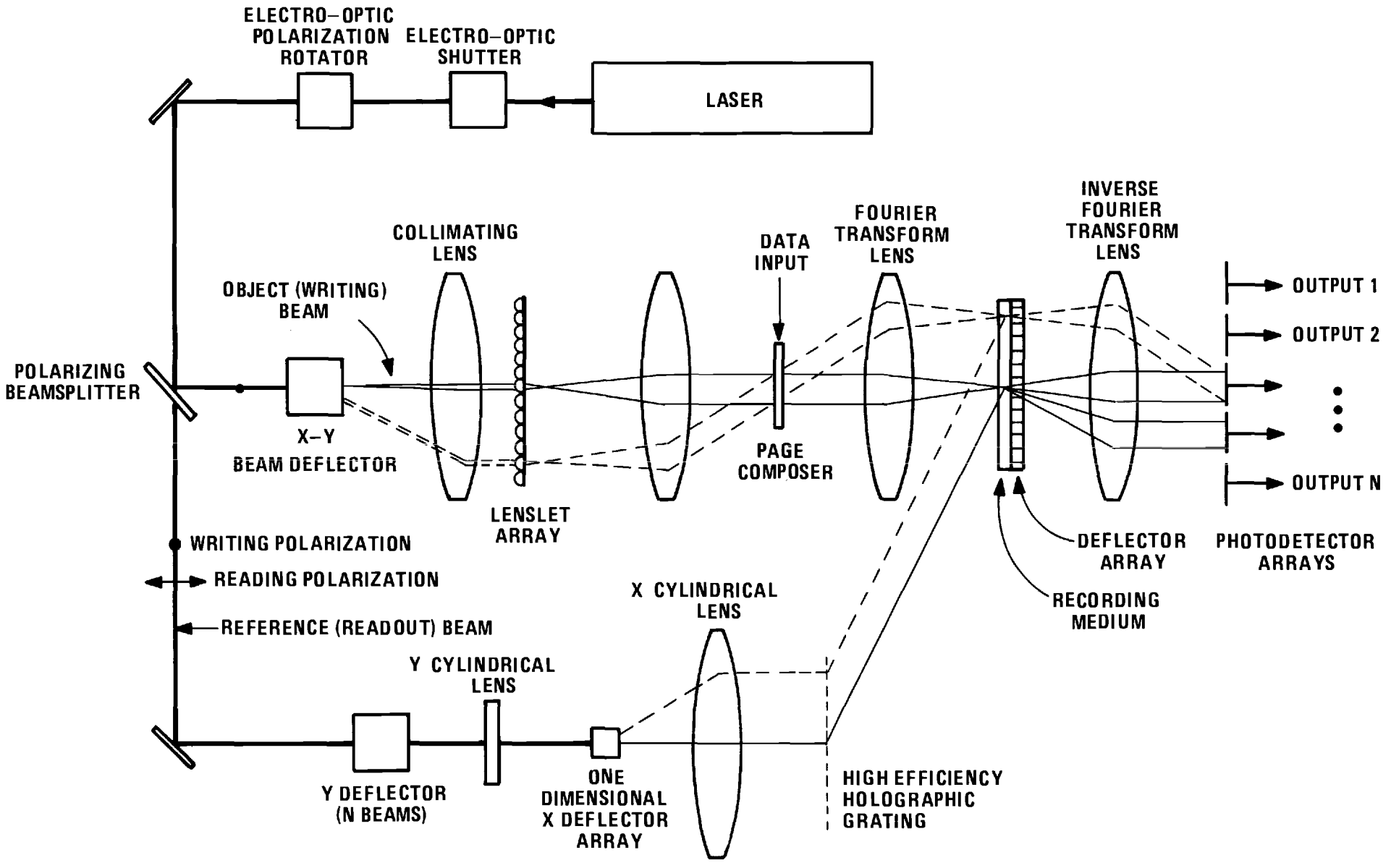

FIGURE 8. SCHEMATIC OF A READ-WRITE-ERASE OPTICAL HOLOGRAPHIC COMPUTER MEMORY.

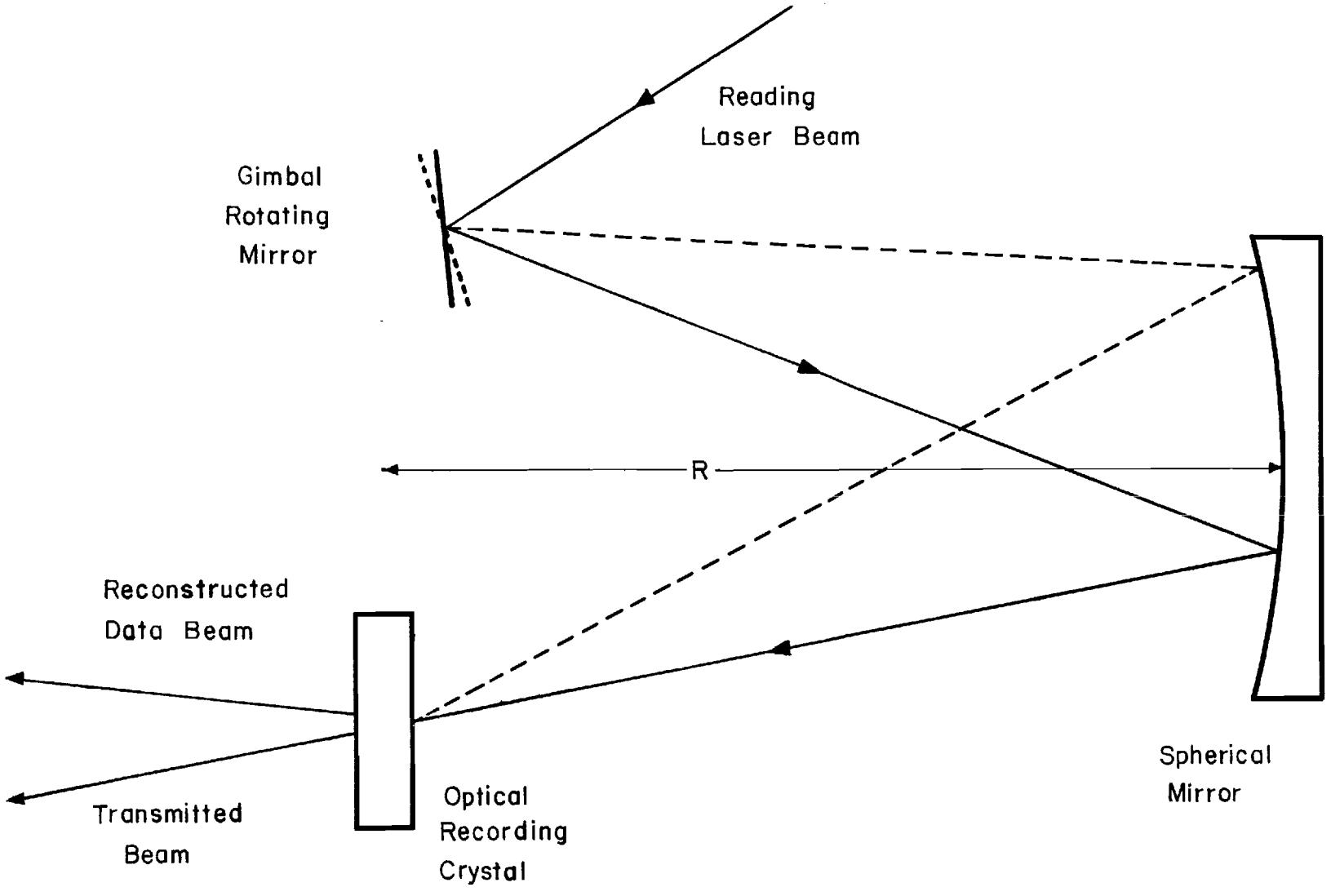

FIGURE 9. ANGULAR ACCESS SCANNER FOR READING MULTIPLE HOLOGRAMS STORED AT A SINGLE LOCATION.

OPTICAL MEMORIES:

Filling the storage gap

by Thomas K. Gaylord

THAT GAP BETWEEN THE MEMORY system needed and existing memories has only increased. Already the need for large-capacity rapid-access storage has raced ahead of existing technology. And the need is steadily growing.

Have your cake . . .

There has been what seems to be an inherent tradeoff between memory capacity and access time. Rapidly developing optical memory technology, however, promises to avoid the tradeoff and fill the gap. Figure 1 graphically represents the state of existing memories, and the expected performance of optical memories.

From slow and steady

The need for mass storage may be divided into several categories. Perhaps the least demanding of these categories is archival storage or record access. In this category large amounts of data need to be stored in a central memory and occasionally accessed. Examples include libraries, insurance data, medical data, seismic data, criminal data, tax information, patent records, national defense data, telephone numbers, stock market information, computer software packages, etc. Numerous governmental and private organizations currently have magnetic tape libraries containing over 200,000 reels of magnetic tape. Information stored in this manner is both expensive and very slowly accessible. This category of storage primarily requires a read-only memory, as changing the data occurs infrequently by computer standards.

To a burst of data

A second category requires high data rate recording and temporary storage. An example would be high bit rate optical communications systems. In optical communications efficient use of turbulent channels will require very high capacity, very fast, reusable mass storage for recording during temporary interruptions of these channels. Another example is data recording during a space probe fly-by. Here a very large amount of data is gathered during a brief period of time. If this information could be stored, it could later be transmitted at a low bit rate to minimize transmission errors in the data.

And replacing the hierarchy

A third category for high capacity storage is in computer memories. Present day computing systems utilize a complex hierarchy of storage devices. Some of the more important of these memories are magnetic tape, disks, drums, cores, and semiconductors. The access times and storage capacities of these devices are given in Fig. 1. Modern computers use a combination of the large and slow along with small and fast memories in a hierarchical structure to realize efficient computing. The optical memory, due to its very high capacity and fast random access, offers the potential of replacing a large portion of the existing memory hierarchy. This is probably the most obvious application of high capacity, rapid access optical memories.

Or changing it

The development of new computer architectures is another area where optical memories will prove useful. This represents a new area based largely on the multi-port capability of optical memories [2] and will be discussed in more detail in a later section.

A long way to go

Today several high capacity memories using nonoptical technology are available [3]. These include the Ampex Terabit System (TBM) and the Grumman Masstape System. These memory systems are shown in Fig. 1 to have access times of about 10 seconds. The maximum storage capacities, for these memories are 8.8×10^{11} bits for the Grumman Mosstape and 2.9×10^{12} bits for the Ampex Terabit System. While this amount of storage is certainly adequate, the long access times make these systems unusable as rapid random access memories.

Down to basics

Design of an optical memory system has received much analysis (see e.g. refs. 1, 4-8). Among the fundamental design decisions are:

INFORMATION SHOULD BE STORED IN HOLOGRAPHIC FORM AS OPPOSED TO DIRECT IMAGE STORAGE. In the typical configuration, the hologram will be the recording of the interference pattern between the Fourier transform of the bit pattern and a plane wave reference beam. Due to the distributed nature of the information, the storage of data in holographic form provides protection from localized loss of data due to material imperfections or dust.

INFORMATION SHOULD BE STORED IN A PAGE ORGANIZED FORMAT AS OPPOSED TO A THREE DIMENSIONAL ISOMETRIC VIEW. The ability of holography to provide three dimensional views of objects is of no particular value in mass data storage. The reconstructed data will simply be in the form of two dimensional pages.

INFORMATION SHOULD BE STORED IN A BINARY CODE AS OPPOSED TO A PICTORIAL REPRESENTATION. A page of binary data would appear as a series of bright and dark spots representing the 1's and 0's of the digital data. Pictoral representations, such as a printed page, a drawing, a map or a photograph, are also usable. However, for very high information densities, constraints on the page composer and the detector matrix favor the use of binary code.

INFORMATION SHOULD BE STORED IN THICK HOLOGRAMS AS OPPOSED TO THIN HOLOGRAMS. The theoretical storage density of two dimensional (thin) holograms is 4×10^8 bits/cm^2 (one bit per square area one wavelength on a side) whereas in three dimensional volume (thick) holograms the theoretical storage density is 8×10^{12} bits/cm^3 (one bit per cube volume wavelength on a side) [9]. Obviously for truly high capacity storage, thick holograms (such as in optical crystals) need to be used instead of thin holograms (such as in photographic

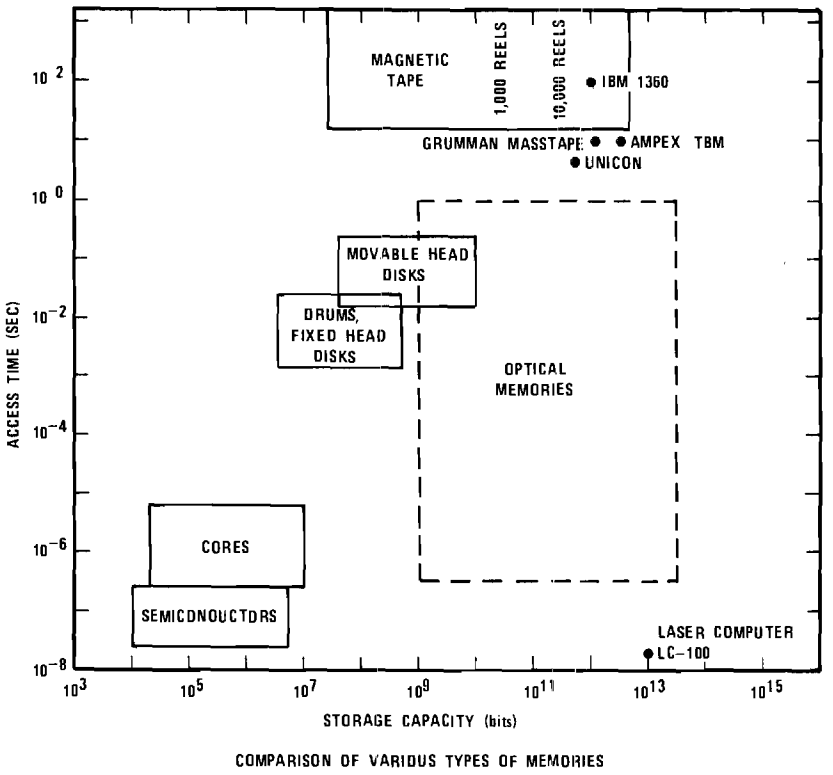

Figure 1. A graphic view of present and future memory performance.

emulsions or metal films). Holographic memory systems have been described which utilize three-dimensional storage [10, 11]. These systems superpose many holograms at a single location inside the thick recording medium by using a different reference beam angle for each hologram. Because of their volume nature, these holograms exhibit very strong angular selectivity [12, 13]. That is, in order to read a hologram, the reference beam must illuminate the hologram within a narrow angular corridor about the Bragg angle for that hologram. Illumination outside of this angular corridor produces a rapidly decreasing intensity of reconstructed data. In addition, the thicker the hologram is, the narrower the angular corridor for reconstruction becomes. The superposition of multiple holograms at a single volume location introduces the additional problem of writing new holograms in that volume without affecting those already there. When lithium niobate is used as the three dimensional storage material, this problem may be solved by the application of an external electric field [14, 15]. This greatly increases the sensitivity for writing while the sensitivity for erasure remains unchanged at a much lower value. Thus as a new hologram is written, the other holograms at that location are only slightly erased.

THE OPTICAL MEMORY SYSTEM SHOULD CONTAIN NO MOVING PARTS. This is necessary to achieve realistic operating speeds that are consistent with computer requirements. In addition, mechanical movements in a complex memory system may well reduce the reliability to an unacceptable level.

Memory building blocks

To construct an optical memory five basic components are needed: an optical source, beam defelectors, a page composer, the recording material, and a detector matrix. These components are then interfaced with each other using conventional optics and electronics. The technologies associated with page composers, beam deflectors, and recording materials, overlap each other to a large extent. Specifically, it is conceivable that lithium niobate may be used in all three components.

OPTICAL SOURCE A laser is needed to produce the coherent, collimated light required in an optical memory system. The laser must be gated or pulsed so as to operate at about 10^6 pulses per second. Additionally, an average optical power of about one watt will be needed. These requirements as well as requirements on the reliability, amplitude stability, and frequency stability can all be met with existing lasers. Completely satisfactory, argon ion lasers are available. The drawbacks of this laser are its high cost (about $20,000) and its low efficiency of conversion of electrical power to optical power (about 0.1%).

BEAM DEFLECTORS An optical memory system must utilize a number of beam deflectors to accurately position the laser beams for the reading, writing, and erasing operations. This positioning process must be both quick and accurate.

As shown in Table 1, there are three basic types of deflectors: galvonometers, acousto-optic deflectors, and electro-optic deflectors. A number of examples in each of these categories are also listed in the Table. The performance of a deflector may be quantified by the resolution and the random access time. Resolution may be defined as the maximum deflection angle divided by the diffraction limited angle. This ratio gives the total number of resolvable spots or total number of resolvable angular positions. Random access time is the time required to deflect the laser beam to a new angular position.

An extensive comparison of light beam deflectors has been performed by Zook [16]. Mechanical galvonometer deflectors are too slow for fast access memory applications (which require an access time of approximately one microsecond). Acousto-optic and electro-optic deflectors, on the other hand, can be constructed to achieve the necessary access times. These devices, however, lack the resolution attainable in galvonometers and must frequently be cascaded to achieve the number of resolvable locations needed. For example, an electro-optic deflector has been built capable of resolving a two dimensional array of 1024 × 1024 spots using twenty stages of deflection with an access time of 0.8 microseconds [17].

PAGE COMPOSER The input device for the optical memory is a page composer (block data composer), which converts digital electrical signals directly into a two dimensional optical array of bits. The page composer will be located in the object beam of the two beam holographic configuration. Reconstruction of the recorded data will duplicate the array of 1's and 0's (bright and dark spots) generated by the page composer.

There are a number of characteristics that the page composer must possess. These requirements include: 1. High frame speed — It must be possible to rapidly change the data page in the page composer. The change time ideally must be in the microsecond range. 2. High resolution — The size of each bit in the page composer needs to be small. Sizes in the range 10 to 100 microns would be suitable. 3. Large aperture — The total area of the page composer transverse to the laser beam needs to be large enough to accommodate the number of bits per page desired. For many applications the bit array size should be in the range 64 × 64 elements to 1024 × 1024 elements. 4. High contrast ratio — The achievement of a high contrast ratio relaxes the subsequent requirements on the recording material and the detector matrix. A contrast ratio of 100 to 1 or greater is desirable and this has been achieved in a number of page composer type devices. 5. Stability — The characteristics of page composer materials must not be degraded by exposure to high intensity light (the object beam). 6. Uniformity — Material nonuniformities in the block data composer must be below the minimum level associated with the onset of readout errors in the memory system.

A wide variety of approaches exist for the construction of page composers. A number of these approaches are listed in Table 2. Obviously, a large number of physical effects and a large number of materials are potentially usable in page composers. Liquid crystal block data composers (see Ref. 18 and Ref. 19) appear to be very useful. RCA has constructed a 1024 bit liquid crystal page composer [8]. A major problem with liquid crystal page composers has been their relatively slow frame speed (on the order of 100 ms). Lead lanthanum zirconate titanate (PLZT) block data composers [20] also appear to be very promising. These page composers, which do not suffer from a slow frame rate, have four basic modes of operation: strain biased mode, scattering mode, edge effect mode, and differential phase mode [21]. This last mode of operation eliminates the detrimental effects of background nonuniformities in the PLZT, but requires a double hologram exposure through the data mask. Two recently developed approaches to block data composers utilize a thin, deformable, membrane mirror array [22] and the thermally induced shift in the optical absorption band edge in CdS [23].

Table 1
Types of Beam Deflectors

Galvonometers
Moving iron galvonometer
Moving coil galvonometer

Acousto-Optic
Alpha-iodic acid (α - HIO_3)
Lead molybdate ($PbMoO_4$)
Tellurite glass
Tl_3AsS_4
H_2O
As_2S_3 glass
TeO_2

Electro-Optic
Lithium niobate ($LiNbO_3$)
Strontium barium niobate ($Sr_{0.75}Ba_{0.25}Nb_2O_6$)
Nitrobenzene
Potassium tantalum niobate (KTN)

RECORDING MATERIAL The central element of the optical memory is the recording material. This piece of material, often rather small in size, provides the entire storage capacity of the optical memory system. Recording materials must possess a number of important characteristics to achieve the high storage capacities that have been predicted for optical memories. These requirements on the optical recording material include: 1. High sensitivity — It is desirable that only a small amount of optical energy per unit area be needed to record the hologram of a data page. Table 3 lists the necessary writing energy densities for a number of recording materials. For a practical system an energy density of about 1 millijoule/cm² or less will be needed. 2. Large diffraction efficiency — Diffraction efficiency is the fraction of the reading light (reference beam) that is diffracted into the reconstructed data beam. It must be possible to record a single hologram with a large diffraction efficiency, so that in practice many holograms may be recorded at a single location, each with an equal share of the total maximum diffraction efficiency. Therefore it is desirable to have the maximum diffraction efficiency as close to 100% as possible. 3. Erasable and rewritable — For a rapid cycle read-write-erase memory system, it must be possible to continuously alter the stored data in the memory without encountering any degradation in the material characteristics. 4. Long lifetime of stored information — Stored data should persist for long periods of time before having to be refreshed. Ideally, storage should be permanent. 5. Nonvolatile storage — Data should remain recorded in the memory in the absence of system power. 6. Nondestructive readout — It should be possible to perform an essentially unlimited number of read operations without degrading or altering the stored data. 7. Three dimensional storage — To achieve very high capacity storage, the information should be stored in thick (volume) holograms. Together with the requirement of high diffraction efficiency, this means that the hologram should be a thick phase (nonabsorbing) hologram. 8. High resolution — The storage material obviously must be capable of recording the very fine (wavelength size) variations of the interference pattern produced by the intersection of the object and reference beams.

Research and development on optical recording materials for optical memories has produced remarkable advances in the past few years. Many different types of materials, as indicated in Table 2, are contenders for recording applications. Considering all of the above material requirements, the photorefractive materials (optically induced changes in index of refraction) appear to be especially promising. These materials, often ferroelectric crystals such as lithium niobate and strontium barium niobate (SBN), have been considerably developed and improved. For example, in the first use of lithium niobate as a recording material in 1968 a writing energy density of approximately 100 joules/cm² was required [24]. Less than six years later, doped versions of lithium niobate were shown to exhibit writing energy densities of 2 millijoules/cm² [25]. This is an improvement in sensitivity of almost 5 orders of magnitude. Similar sensitivity improvements have been reported for SBN [26]. The other needed material characteristics have all been reported in the photorefractive ferroelectrics — large diffraction efficiency [24, 27], optical erasing and rewriting [14, 15, 28], long lifetime of stored data [29], three dimensional storage [13, 24], etc. At the present time these very favorable material characteristics have not been simultaneously observed in a single sample. Further, it is still not clear that all of the desired characteristics can coexist in a single doped ferroelectric material. Trade-offs that have not been discovered may exist between the various desired properties. Clearly,

Table 2
Types of Page Composers*

Page Composer Concept	Materials	Addressing Techniques
Polarization rotation by induced birefringence (electrooptic effects)	PLZT (ceramic), $Bi_4Ti_3O_{12}$ KDP, KD*P, ADP	Electrode matrix, Electron beam, Light beam (with photoconductor)
Phase changes by formation of surface relief pattern	Thermoplastics, Photoplastics, Thin metalized membranes	Electron beam, Electrode matrix plus charge
Phase disturbances by piezoelectric excitation of reflecting surfaces	Mirrored piezoelectric crystals	Individual switches to an rf driver
Optical density change by induced absorption	Photochromics, Cathodochromics	Light beam (uv) plus flood illumination for erase, Electron beam plus flood illumination for erase
Optical scattering change by electrical agitation	Liquid crystals	Electrode matrix, Light beam (with photoconductor)
Polarization rotation by magnetooptic effects	MnBi, EuO_3Fe, Ni-Fe $FeBO_3$, FeF_3	Light beam (absorption), Conductor matrix
Traveling phase changes by acoustooptic interaction (Debye-Sears and Bragg effects)	Water (and other liquids), Fused quartz (and other amorphous solids), $PbMoO_4$ (and other crystals)	Transverse interaction of coherent light and traveling acoustic waves
Thermally induced shift in absorption band edge	CdS, CdSe, As_2S_3	Electrode matrix for heating and heat sink substrate for cooling
Optical scattering by poled and unpaled regions of a ferroelectric	PLZT (ceramic)	Electrode matrix
Phase changes by variation of optical path length	Electrastrictive materials, PLZT (ceramic)	Electrode matrix, Double hologram recording method
Reflection changes from thin, deformable membrane mirror elements	Metal films over a substrate support structure	Electrode feedthrough from transistor on back of substrate

*adapted from H. N. Roberts, Applied Optics, vol. 11, pp. 397-404, February 1972.

more basic research on optical recording materials is required to resolve the many remaining questions. If a single material can reliably and reproducibly be made with all of the above required properties, it is certain that read-write-erase optical memories will become commercially available.

DETECTOR MATRIX An array of photodetectors is needed to convert the optical holographically reconstructed data into an electrical signal. This photosensitive readout array would have one photodiode or phototransistor for each bit of data in the reconstructed page. Each sensor in the array would function as a threshold detector indicating the presence or absence of light (a binary 1 or 0). All stored holograms would be read out with the same detector matrix (for a single port memory).

The photodetectors ideally must exhibit a low threshold detection power. Noise associated with the operation of the photodetector determines the lower limit of optical power needed for threshold detection. For a signal-to-noise ratio of about 10, an optical power in the range of 0.1 to 1.0 microwatts per bit will be required. Already readout arrays operating at 0.3 microwatts per bit have been constructed [30].

The second basic requirement on the detector matrix is that a large defect free array be constructable with existing technology. Modern semiconductor technology has fulfilled this requirement. Bell Laboratories has constructed a silicon-diode-array camera tube that consists of 525,000 individual photodiodes on a single silicon slice [31]. An LSI phototransistor array with 51,200 silicon phototransistors has been built [32] using multilayer interconnection techniques so that any bit can be read out in about a microsecond. Continuing advances in semiconductor technology assure the availability of high quality photodetector arrays.

Where we are now

Optical mass memories currently in existence include the IBM 1360 memory, introduced in 1966 but no longer in production. This Photo Digital Mass Storage System uses electron beams for recording and is read out optically. As shown in Fig. 1 its trillion bits are only very slowly accessible. Precision Instrument's Unicon laser mass memory system is an optical mass memory that now is commercially available. It uses an argon laser to perform bit-by-bit recording by vaporizing small holes in a metallized polyester belt. This read-only nonholographic memory has a storage capacity of 7×10^{11} bits and an average access time of somewhat less than 10 seconds.

The Laser Computer Corporation has aroused a great deal of discussion by its

announcement of a 10^{13} bit memory having a 20 nanosecond access time. As shown in Fig. 1 this would place their memory beyond the predicted future limits associated with optical memories. Unfortunately, very few details are available about this system.

Table 3
Required Writing Energy Density for Various Optical Recording Materials

Material	Type of Material	Writing Energy Density (joules/cm²)
$Bi_{12}SiO_{20}$	Ferroelectric-Photoconductive	1×10^{-6}
Malachite Green:		
Sucrose Benzoate	Thermoplastic	2×10^{-6}
Agfa 8E70	Photographic	2×10^{-5}
Kodak 649F	Photographic	7×10^{-5}
$Bi_4Ti_3O_{12}$-ZnSe	Ferroelectric-Photoconductive	1×10^{-3}
$LiNbO_3$:Fe	Photorefractive	2×10^{-3}
$Sr_{0.75}Ba_{0.25}Nb_2O_6$	Photorefractive	6×10^{-3}
Dichromated Geletin	Photochemical	1×10^{-2}
CaF_2:Ce	Photochromic	1×10^{-2}
PLZT	Ferroelectric-Photoconductive	1×10^{-2}
KCL:Na	Photochromic	1×10^{-2}
MnBi	Magnetooptic	3×10^{-2}
$Te_{86}Ge_7As_6$	Amorphous Semiconductor	5×10^{-2}
GdIG	Magnetooptic	9×10^{-2}
EuO	Magnetooptic	9×10^{-2}
NaF	Photochromic	9×10^{-2}
CoPniFe	Magnetooptic	1×10^{-1}
$SrTiO_3$:Ni:Mo	Photochromic	2×10^{-1}
$BaTiO_3$	Photorefractive	2×10^{-1}
MnAlGe	Magnetooptic	3×10^{-1}
$Te_{81}Ge_{15}Sb_2S_2$	Amorphous Semiconductor	5×10^{-1}
PMMA (Q-doped)	Photopolymer	1
KBr	Photochromic	1
Cu_2HgI_4	Thermoplastic	3
$BaNaNb_5O_{15}$	Photorefractive	5
$As_{15}S_{85}$	Amorphous Semiconductor	5
$Bi_4Ti_3O_{12}$	Photorefractive	10
$LiNbO_3$ (undoped)	Photorefractive	100
PMMA (undoped)	Photopolymer	100

A design revolution

Optical memories, in addition to increasing the capabilities of existing computers, promise to spur the development of new computer architectures [2]. It is conceptually simple to construct an optical memory in which any of the data pages may be accessed by multiple users simultaneously. This feature, not available in conventional memories, allows access to the memory through any of its multiple ports.

Speed, capacity, and cost relationships have determined a basic computer architecture that utilizes a hierarchical memory structure. A common way of inplementing this structure has been to provide for page swaps between a local memory and the mass store, and for word (or character) swaps between the local store and the central processing unit. Such a structure has inevitably led to problems of addressing, replacing pages, multiple contention for pages and memory allocation. The contention problem can be relieved by building a mass memory with multiple access ports. If such a memory has simultaneous read/write capability, then each user demanding use of mass memory appears to have complete control. Problems of write protection, memory allocation and paging still remain, but the speed of the mass memory has been effectively increased by having multi-port capability.

Speed can be further enhanced by utilizing a mass memory which accesses a single page in one access cycle. This differs from mass memory devices such as a disk where the page is accessed sequentially making the access time proportional to page size. A parallel transfer of a single page between the mass memory and an individual memory port coupled with the idea of multi-port simultaneous page access can provide a distinctly new storage device for parallel computation. Current methods in parallel computation utilize multiple processors and multiple memories and require many memory to memory swaps to perform array type computations. A mass memory with multi-port access capability would reduce the word exchanges and could enhance parallel computation.

Three typical applications for a multi-port memory as shown in Fig. 2 are: 1. Record access — As previously discussed, many applications exist that require the storage and retrieval of large blocks of information. This can be realized very efficiently with a multi-port memory. In these systems, data would be stored in page format in the multi-port memory. In these systems, data would be stored in page format in the multi-port memory. Access to any page would be via a terminal through one of the memory access ports. The data requirement of each terminal is, in some applications, low enough to have one memory port support several terminals through a multiplexer. Normally these terminals are used in a read access mode and would not be allowed to perform write operations to the memory. 2. Simultaneously shared memory computing — In this application the user performs transformations on the data accessed. This adds arithmetic logic units to the architecture as shown. 3. Parallel processing — There are many scientific problems requiring enormous numbers of computations. One approach to this problem has been a multiprocessor parallel computation technique. Essentially all processors are dedicated to solving one step and then after a transfer to the appropriate processor, repeating the step-wise computation. Problems arise from synchronization and system reliability when the parallelism is carried as far as that in Illiac IV. A possible structure for parallel processing is also shown in Fig. 2. Each processor is connected to the multi-port memory through a port. Transfers between processors can be made on an outer bus connecting each processor.

Summary

There has been a great deal of activity in recent years related to optical memories. Research and development has produced advances in optical memory components and the materials used in these components. In the area

of recording materials, more basic research clearly is required. The other components for the optical memory are either available or can be with additional engineering effort.

In the realm of system configurations for optical memories, there has been a sizeable effort to develop prototype memory systems. Holographic optical memories have been built by RCA Labs, Harris-Intertype, Bell Labs, Thomson-CSF, Nippon Corp., and others. For the most part these are limited versions of the full scale high capacity read-write-erase memory system of the future. In additon, new computer architectures are being identified to take advantage of and efficiently use the unique capabilities that are possible in optical memories. □

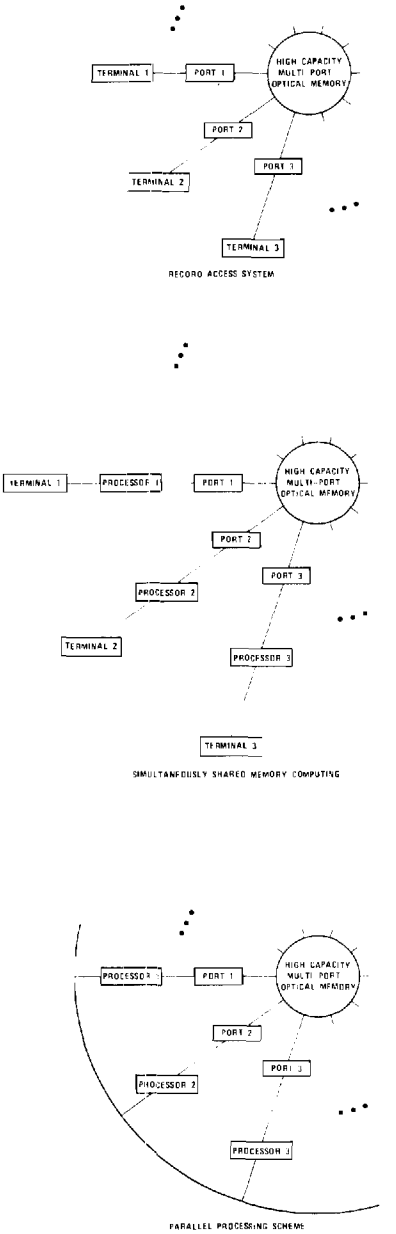

Figure 2. Possible schemes for new computer architectures using optical memories.

References

1. Rajchman, J. A., "Promise of optical memories," J. Appl. Phys., vol. 41, pp. 1376-1383, March 1, 1970.
2. Alford, C. O. and Gaylord, T. K., "Applications and implementation of a multi-port laser optical memory," NSF Proposal, April 1974.
3. Houston, G. B., "Trillion bit memories," Datamation, vol. 19, pp. 52-58, October 1973.
4. Vander Lugt, A., "Design relationships for holographic memories," Appl. Optics, vol. 12, pp. 1675-1685, July 1973.
5. Anderson, L. K., "Application of holographic optical techniques to bulk memory," IEEE Trans. Magnetics, vol. MAG-7, pp. 601-605, Sept. 1971.
6. Graf, P. and Lang, M., "Geometrical aspects of consistent holographic memory design," Appl. Optics, vol. 11, pp. 1382-1388, June 1972.
7. Hill, B., "Some aspects of a large capacity holographic memory," Appl. Optics, vol. 11, pp. 182-191, January 1972.
8. Stewart, W. C., Mezrich, R. S., Cosentino, L. S., Nagle, E. M., Wendt, F. S., and Lohman, R. D., "An experimental read-write holographic memory," RCA Review, vol. 34, pp. 3-44, March 1973.
9. van Heerden, P. J., "Theory of optical information storage in solids," Appl Optics, vol. 2, pp. 393-400, April 1963.
10. Gaylord, T. K., "The high capacity storage problem: Is optical holography the answer?" Optical Spectra, vol. 6, 25-37, November 1972.
11. d'Auria, L., Huignard, J. P., Slezak, C., and Spitz, E., "Experimental holographic read-write memory using 3-D storage," Appl. Optics, vol. 13, no. 4, pp. 808-818, April 1974.
12. Kogelnik, H., "Coupled wave theory for thick hologram gratings," Bell Sys. Tech. J., vol. 48, pp. 2909-2947, November 1969.
13. Gaylord, T. K. and Tittel, F. K., "Angular selectivity of lithium niobate volume holograms," J. Appl. Phys., vol. 44, pp. 4771-4773, October 1973.
14. Amodei, J. J. and Staebler, D. L., "Holographic recording in lithium niobate," RCA Review, vol. 33, pp. 71-93, March 1972.
15. Staebler, D. L., and Phillips, W., "Fe-doped $LiNbO_3$ for read-write applications," Appl. Optics, vol. 13, pp. 788-794, April 1974.
16. Zook, J. D., "Light beam deflector performance: a comparative analysis," Applied Optics, vol. 13, pp. 875-887, April 1974.
17. Meyer, H., Riekmann, D., Schmidt, K.P., Schmidt, U.J., Rahlff, M., Schröeder, E., and Thust, W., "Design and performance of a 20-stage digital light beam deflector," Applied Optics, vol. 11, pp. 1732-1736, August 1972.
18. White, D. L. and Feldman, M., "Liquid crystal light valves," Electronics Letters, vol. 6, pp. 837-840, December 1970.
19. Special Issue of Display Devices, IEEE Trans. on Electron Devices, vol. ED-20, November 1973.
20. Roberts, H. N., "Strain-biased PLZT input devices (page composers) for holographic memories and optical data processing," Appl. Optics, vol. 11, pp. 397-404, February 1972.
21. Drake, M. D., "PLZT matrix-type block data composers," Applied Optics, vol. 13, pp. 45-79, March 1973.
23. Hill, B. and Schmidt, K. P., "New page composer for holographic data storage," Applied Optics, vol. 12, pp. 1193-1198, June 1973.
24. Chen, F. S., LaMacchia, J. T., and Fraser, D. B., "Holographic storage in lithium niobate," Appl. Phys. Letters, vol. 13, pp. 223-225, October 1, 1968.
25. Shah, P., Rabson, T. A., Tittel, F. K., and Gaylord, T. K., "Volume holographic recording and storage in Fe-doped $LiNbO_3$ using optical pulses," Appl. Phys. Letters, vol. 24, pp. 130-131, February 1974.
26. Thaxter, J. B., and Kestigian, M., "Unique properties of SBN and their use in a layered optical memory," Appl. Optics, vol. 13, pp. 913-924, April 1974.
27. Amodei, J. J., Phillips, W., and Staebler, D. L., "Improved electro optic materials and fixing techniques for holographic recording," Appl. Optics, vol. 11, pp. 390-396, February 1972.
28. Gaylord, T. K., Rabson, T. A., and Tittel, F. K., "Optically erasable and rewritable solid-state holograms," Appl. Phys. Letters, vol. 20, pp. 47-49, January 1, 1972.
29. Amodei, J. J. and Staebler, D. L., "Holographic pattern fixing in electro-optic crystals," Appl. Phys. Letters, vol. 18, pp. 540-542, June 15, 1971.
30. Assour, J. M. and Lohman, R. D., "A photodector array for holographic optical memories," RCA Review, vol. 30, pp. 557-566, December 1969.
31. Crowell, M. H. and Labuda, E. F., "The silicon diode array camera tube," Bell Sys. Tech. J., vol. 48, pp. 1481-1528, May-June 1969.
32. Mend, W. G., McCoy, E. E., and Anders, R. A., "Microminiature solid-state imaging system utilizing hybrid LSI techniques," IEEE J. Solid-State Circuits, vol. SC-5, pp. 254-260, October 1970.

Meet the author

Thomas K. Gaylord received his B.S. degree in physics and his M.S. degree in electrical engineering from the University of Missouri-Rolla. He earned his Ph.D. degree in electrical engineering from Rice University in 1970. He is currently on the faculty of the School of Electrical Engineering of Georgia Institute of Technology. Dr. Gaylord was recently named to the Editorial Advisory Board of The Optical Publishing Company.

XI. REFERENCES

[1] J. A. Rajchman, "Promise of optical memories," J. Appl. Phys., Vol. 41, pp. 1376-1383, March 1, 1970.

[2] C. O. Alford and T. K. Gaylord, "The potential of multi-port optical memories in digital computing," International Optical Computing Conference, Washington, D.C., April 1975.

[3] H. Kogelnik, "Coupled wave theory for thick hologram gratings," Bell System Tech. J., Vol. 48, No. 4, pp. 2902-2947, November 1969.

[4] T. K. Gaylord and F. K. Tittel, "Angular selectivity of lithium niobate holograms," J. Appl. Phys., Vol. 44, No. 9, pp. 4771-4773, September 1973.

[5] S. F. Su and T. K. Gaylord, "Calculation of arbitrary-order diffraction efficiencies of thick gratings with arbitrary grating shape," J. Optical Soc. of Am., Vol. 65, No. 1, January 1975.

[6] H. Kogelnik, "Bragg diffraction in hologram gratings with multiple internal reflections," J. Optical Soc. of Am., Vol. 57, pp. 431-433, March 1967.

[7] M. G. Cohen and E. I. Gordon, "Acoustic scattering of light in Fabry-Perot resonator," Bell System Tech. J., Vol. 45, pp. 945-966, July-August 1966.

[8] T. K. Gaylord, "Optical memories," Optical Spectra, Vol. 8, No. 6, pp. 29-34, June 1974.

[9] F. S. Chen, J. T. LaMacchia, and D. B. Fraser, "Holographic storage in lithium niobate," Appl. Phys. Letters, Vol. 13, pp. 223-225, October 1, 1968.

[10] P. Shah, T. A. Rabson, F. K. Tittel, and T. K. Gaylord, "Volume holographic recording and storage in Fe-doped $LiNbO_3$," Appl. Phys. Letters, Vol. 24, No. 3, pp. 130-131, February 1974.

[11] D. von der Linde, A. M. Glass, and K. F. Rogers, "Multiphoton photo-refractive processes for optical storage in $LiNbO_3$," Appl. Phys. Letters, Vol. 25, No. 3, pp. 155-157, August 1, 1974.

[12] W. Phillips, J. J. Amodei, and D. L. Staebler, "Optical and holographic storage properties of transition metal doped lithium niobate," RCA Review, Vol. 33, No. 1, pp. 94-109, March 1972.

[13] R. Magnusson and T. K. Gaylord, "Laser scattering induced holograms in lithium niobate," Appl. Optics, Vol. 13, No. 7, pp. 1545-1548, July 1974.

[14] J. M. Moran and I. P. Kaminow, "Properties of holographic gratings photo-induced in polymethyl methacrylate," Applied Optics, Vol. 12, pp. 1964-1970, August 1973.

[15] D. L. Staebler, J. J. Amodei, and W. Phillips, "Multiple storage of thick phase holograms in $LiNbO_3$," Digest of Technical Papers, 1972 International Quantum Electronics Conference, p. 93, May 8-17, 1972.

[16] P. J. van Heerden, "Theory of optical information storage in solids," Appl. Optics, Vol. 2, No. 4, pp. 393-400, April 1963.

[17] L. d'Auria, J. P. Huignard, C. Siezak, and E. Spitz, "Experimental holographic read-write memory using 3-D storage," Appl. Optics, Vol. 13, No. 4, pp. 808-818, April 1974.

[18] J. J. Amodei and D. L. Staebler, "Holographic recording in lithium niobate," RCA Review, Vol. 33, No. 1, pp. 71-93, March 1972.

[19] D. L. Staebler and W. Phillips, "Fe-doped $LiNbO_3$ for read-write applications," Appl. Optics, Vol. 13, No. 4, pp. 788-794, April 1974.

[20] C. B. Burckhardt, "Diffraction of a plane wave at a sinusoidally stratified dielectric grating," J. Optical Soc. Am., Vol. 56, pp. 1502-1509, November 1966.

XII. OPTICAL MEMORY BIBLIOGRAPHIES

REFERENCES ON OPTICAL HOLOGRAPHIC MEMORY SYSTEMS

[1] Aagard, R. L., Lee, T. C., and Chen, D., "Advanced Optical Storage Techniques for Computers," Appl. Optics, vol. 11, no. 10, pp. 2133-2139, October 1972.

[2] Akahori, H., and Sakurai, K., "Information Search using Holography," Appl. Optics, vol. 11, no. 2, pp. 413-415, February 1972.

[3] Amodei, J. J. and Bosomworth, D. R., "Hologram Storage and Retrieval in Photochromic Strontium Titanate Crystals," Appl. Optics, vol. 8, no. 12, pp. 2473-2477, December 1969.

[4] Amodei, J. J. and Staebler, D. L., "Holographic Pattern Fixing in Electro-Optic Crystals," Appl. Phys. Letters, vol. 18, pp. 540-542, June 15, 1971.

[5] Amodei, J. J., Phillips, W., and Staebler, D. L., "Improved Electro-Optic Materials and Fixing Techniques for Holographic Recording," Appl. Optics, vol. 11, pp. 390-396, February 1972.

[6] Amodei, J. J. and Staebler, D. L., "Holographic Recording in Lithium Niobate," RCA Review, vol. 33, pp. 71-93, March 1972.

[7] Anderson, L. K., "Holographic Optical Memory for Bulk Data Storage," Bell Labs Record, vol. 6, pp. 318-325, November 1968.

[8] Anderson, L. K., "Optical Memories-1971," Electro-Optical Systems Design, vol. 3, pp. 26-28, January 1971.

[9] Anderson, L. K., "Application of Holographic Optical Techniques to Bulk Memory," IEEE Trans. Magnetics, vol. MAG-7, pp. 601-605, September 1971.

[10] Assour, J. M. and Lohman, R. D., "A Photodetector Array for Holographic Optical Memories," RCA Review, vol. 30, pp. 557-566, December 1969.

[11] Bardos, A., "Wideband Holographic Recorder," Appl. Optics, vol. 13, no. 4, pp. 832-840, April 1974.

[12] Barrekette, E. S., "Trends in Storage of Digital Data," Appl. Optics, vol. 13, no. 4, pp. 749-754, April 1974.

[13] Baugh, R. A., "High-Efficiency Volume Holography," Ph.D. Thesis, Stanford University, 1969.

[14] Bergstein, L., and Kermisch, D., "Image Storage and Reconstruction in Volume Holography," Proc. Symp. on Modern Optics, MRI ser., vol. 17. Brooklyn, N.Y.: Polytechnic Press, 1967, pp. 655-680.

[15] Bousky, S. and Diermann, J., "Characteristics of Scanning Laser and Electron Beams in Bulk Data Storage," IEEE Trans. Magnetics, vol. MAG-7, pp. 594-598, September 1971.

[16] Brown, B. R., "Optical Data Storage Potential of Six Materials," Appl. Optics, vol. 13, no. 4, pp. 761-766, April 1974.

[17] Carlson, W. J., "Holographic Page Synthesis for Sequential Input of Data," Appl. Optics, vol. 13, no. 4, pp. 896-903, April 1974.

[18] Chen, F. S., Denton, R. T., Nassau, K., and Ballman, A. A., "Optical Memory Planes using $LiNbO_3$ and $LiTaO_3$," Proc. IEEE, vol. 56, no. 4, pp. 782-783, April 1968.

[19] Chen, F. S., LaMacchia, J. T., and Fraser, D. B., "Holographic Storage in Lithium Niobate," Appl. Physics Letters, vol. 13, pp. 223-225, October 1, 1968.

[20] Chen, D., "Magnetic Materials for Optical Recording," Appl. Optics, vol. 13, no. 4, pp. 767-778, April 1974.

[21] Cosentino, L. S. and Stewart, W. C., "A Membrane Page Composer," RCA Review, vol. 34, pp. 45-79, March 1973.

[22] Crowell, M. H. and Labuda, E. F., "The Silicon Diode Array Camera Tube," Bell Sys. Tech. J., vol. 48, pp. 1481-1528, May-June 1969.

[23] Damon, R. W., McMahon, D. H., and Thaxter, J. B., "Materials for Optical Memories," Electro-Optical Systems Design, vol. 2, pp. 68-77, August 1970.

[24] d'Auria, L., Huignard, J. P., Siezak, C., and Spitz, E., "Experimental Holographic Read-Write Memory using 3-D Storage," Appl. Optics, vol. 13, no. 4, pp. 808-818, April 1974.

[25] Drake, M. D., "PLZT Matrix-Type Block Data Composers," Appl. Optics, vol. 13, no. 2, pp. 347-352, February 1974.

[26] Esho, S., Noguchi, S., Ono, Y., and Nagao, M., "Optimum Thickness of MnBi Films for Magnetic Memory," Appl. Optics, vol. 13, no. 4, pp. 779-783, April 1974.

[27] Fan, G. J., "Magnetooptic Storage," IEEE Trans. Magnetics, vol. MAG-7, pp. 590-594, September 1971.

[28] Firester, A. H., and Heller, M. E., "Use of Diode Lasers to Recover Holographically Stored Information," IEEE J. Quan. Electronics, vol. QE-6, no. 9, pg. 572, September 1970.

[29] Friedrich, O. M. and Dougal, A. A., "Optical Data Systems," Instrumentation Technology, pp. 43-47, May 1971.

[30] Friedrich, O. M. and Dougal, A. A., "Optical Data Systems, Part II: Processing Techniques," Instrumentation Technology, pp. 53-59, June 1971.

[31] Friesem, A. A., "Three-Dimensional Recording Media in Holography," Ph.D. Thesis, The University of Michigan, 1968.

[32] Gaylord, T. K., "The High Capacity Storage Problem: Is Optical Holography the Answer?" Optical Spectra, vol. 6, no. 11, pp. 25-37, November 1972.

[33] Gaylord, T. K., "Optical Memories," Optical Spectra, vol. 8, no. 6, pp. 29-34, June 1974.

[34] Gentile, R. B. and Lucas Jr., J. R., "The TABLON Mass Storage Network," Spring Joint Computer Conference, pp. 345-356, 1971.

[35] Graf, P. and Lang, M., "Geometrical Aspects of Consistent Holographic Memory Design," Appl. Optics, vol. 11, no. 6, pp. 1382-1388, June 1972.

[36] Hammond, A. L., "Optical Data Storage: Mass Memories for Future Computers?" Science, vol. 180, pp. 287-288, April 20, 1973.

[37] Haskal, H., Bernal, G., and Chen, D., "Subnanosecond Laser Recording on MnBi Thin Films," Appl. Optics, vol. 13, no. 4, pp. 866-868, April 1974.

[38] Heilmeier, G. H. and Goldmacher, J. E., "A New Electric Field Controlled Reflective Optical Storage Effect in Liquid Crystal Systems," Proc. IEEE, vol. 57, no. 1, pp. 34-38, January 1969.

[39] Heilmeier, G. H., "Liquid Crystal Display Devices," Scientific American, vol. 222, pp. 100-106, March 1970.

[40] Hill, B., "Some Aspects of a Large Capacity Holographic Memory," Appl. Optics, vol. 11, no. 1, pp. 182-189, January 1972.

[41] Hill, B. and Schmidt, K. P., "New Page Composer for Holographic Data Storage," Appl. Optics, vol. 12, no. 6, pp. 1193-1198, June 1973.

[42] Hodges, D. A., "Computer Memories," IEEE Student J., vol. 8, pp. 15-20, September 1970.

[43] Houston, G. B., "Trillion Bit Memories," Datamation, vol. 19, pp. 52-58, October 1973.

[44] Inagaki, T., Furukawa, Y., Goto, Y., Akimura, T., and Nishimura, Y., "Hologram Writer using a Plasma Display Panel," Appl. Optics, vol. 13, no. 4, pp. 819-824, April 1974.

[45] Keneman, S. A., Miller, A., and Taylor, G. W., "Phase Holograms in a Ferroelectric-Photoconductor Device," Appl. Otpics, vol. 9, no. 10, pp. 2279-2282, October 1970.

[46] Keneman, S. A., Taylor, G. W., and Miller, A., "Ferroelectric-Photoconductor Optical Storage Medium Utilizing Bismuth Titanate," Ferroelectrics, vol. 1, pp. 227-241, October 1970.

[47] Kermisch, D., "Image Storage and Reconstruction in Volume Holography," Ph.D. Thesis, Polytechnic Institute of Brooklyn, 1968.

[48] Kiemle, H., "Holographic Memories in the Gigabit Region," Appl. Otpics, vol. 13, no. 4, pp. 803-807, April 1974.

[49] Kogelnik, H., "Coupled Wave Theory for Thick Hologram Gratings," Bell Sys. Tech. J., vol. 48, no. 4, pp. 2909-2947, November 1969.

[50] Kozma, A. and Barrekette, E. S., "Topical Meeting on Optical Storage of Digital Data," Appl. Optics, vol. 13, no. 4, pp. 747-748, April 1974.

[51] Knight, G. R., "Page-Oriented Associative Holographic Memory," Appl. Optics, vol. 13, no. 4, pp. 904-912, April 1974.

[52] Labrunie, G., Robert, J., and Borel, J., "Nematic Liquid Crystal 1024 Bits Page Composer," Appl. Optics, vol. 13, no. 6, pp. 1355-1358, June 1974.

[53] LaMacchia, J. T., "Optical Memories: A Progress Report," Laser Focus, vol. 6, pp. 35-39, February 1970.

[54] Lee, T. C., "Holographic Recording on Thermoplastic Films," Appl. Optics, vol. 13, no. 4, pp. 888-895, April 1974.

[55] Lin, L. H. and Beauchamp, "Write-Read-Erase in Situ Optical Memory Using Thermoplastic Holograms," Appl. Optics, vol. 9, no. 9, pp. 2088-2092, September 1970.

[56] Lo, D. S., "Photochromic Salicylideneaniline as Storage Medium for Interferometry and High Speed Recording," Appl. Optics, vol. 13, no. 4, pp. 861-865, April 1974.

[57] Macovski, A., "Hologram Information Capacity," J. Optical Soc. America, vol. 60, no. 1, pp. 21-29, January 1970.

[58] Maslowski, A., "High Density Data Storage on Ultraviolet Sensitive Tape," Appl. Optics, vol. 13, no. 4, pp. 857-860, April 1974.

[59] Mattson, R. L., "Role of Optical Memories in Computer Storage," Appl. Optics, vol. 13, no. 4, pp. 755-760, April 1974.

[60] Mend, W. G., McCoy, E. E., and Anders, R. A., "Micro-Miniature Solid-State Imaging System Utilizing Hybrid LSI Techniques," IEEE J. Solid-State Circuits, vol. SC-5, pp. 254-260, October 1970.

[61] Meyer, H., Riekmann, D., Schmidt, K. P., Schmidt, U. J., Rahlff, M., Schröder, E., and Thust, W., "Design and Performance of a 20-Stage Digital Light Beam Deflector," Appl. Optics, vol. 11, no. 8, pp. 1732-1736, August 1972.

[62] Mezrich, R. S., "Magnetic Holography," Appl Optics, vol. 9, no. 10, pp. 2275-2278, October 1970.

[63] Mezrich, R. S. and Stewart, W. C., "Heterodyne Readout for Read-Write Holographic Memories," Appl. Optics, vol. 12, no. 11, pp. 2677-2682, November 1973.

[64] Micheron, F., Mayeux, C. and Trotier, J. C., "Electrical Control in Photoferroelectric Materials for Optical Storage," Appl. Optics, vol. 13, no. 4, pp. 784-787, April 1974.

[65] Norman, S. L., "Holography in Unconventional Materials," Optical Spectra, vol. 4, pp. 26-30, November 1970.

[66] Okuda, M., Matsushita, T., Yamagami, T., and Yamamoto, K., "Highly Sensitive Light-Induced Memory Effect with Amorphous Se-SnO_2 Heterojunction," Appl. Optics, vol. 13, no. 4, pp. 799-802, April 1974.

[67] Patlach, A. M., "Design Considerations for a Magnetic-Optic Cryogenic Film Memory," IBM J. Res. Develop., vol. 16, pp. 313-319, May 1972.

[68] Pohl, D., "Stacked Optical Memories," Appl. Optics, vol. 13, no. 2, pp. 341-346, February 1974.

[69] Rajchman, J. A., "Promise of Optical Memories," J. Appl. Phys., vol. 41, no. 3, pp. 1376-1383, March 1, 1970.

[70] Rajchman, J. A., "An Optical Read-Write Mass Memory," Appl. Optics, vol. 9, no. 10, pp. 2269-2271, October 1970.

[71] Ramberg, E. G., "Holographic Information Storage," RCA Review, vol. 33, no. 1, pp. 5-53, March 1972.

[72] Roberts, H. N., "Strain-Biased PLZT Input Devices (page composers) for Holographic Memories and Optical Data Processing," Appl. Optics, vol. 11, no. 2, pp. 397-404, February 1972.

[73] Roberts, H. N., Watkins, J. W., and Johnson, R. H., "High Speed Holographic Digital Recorder," Appl. Optics, vol. 13, no. 4, pp. 841-856, April 1974.

[74] Shankoff, T. A., "Phase Holograms in Dichromated Gelatin," Appl. Optics, vol. 7, no. 10, pp. 2101-2105, October 1968.

[75] Shore, B., "Electro-Optic Crystals: A New Development in Information Storage," New Engineer, vol. 1, pp. 17-18, October 1971.

[76] Smith, A. W., "Injection Laser Writing on Chalcogenide Films," Appl. Optics, vol. 13, no. 4, pp. 795-798, April 1974.

[77] Smits, F. M. and Gallaher, L. E., "Design Considerations for a Semipermanent Optical Memory," Bell Sys. Tech. J., vol. 46, pp. 1267-1278, July-August 1967.

[78] Snaper, A. A., "The Ultimate Computer Memory," Optical Spectra, vol. 6, pp. 25-27, March 1972.

[79] Special Issue of Display Devices, IEEE Trans. on Electron Devices, vol. ED-20, no. 11, November 1973.

[80] Staebler, D. L., and Phillips, W., "Fe-Doped $LiNbO_3$ for Read-Write Applications," Appl. Optics, vol. 13, no. 4, pp. 788-794, April 1974.

[81] Stepke, E. T., "Optical Mass Memories: The Impossible Dream?", Electro-Optical Systems Design, vol. 4, pp. 12-20, October 1972.

[82] Stewart, W. C. and Cosentino, L. S., "Optics for a Read-Write Holographic Memory," Appl. Optics, vol. 9, no. 10, pp. 2271-2275, October 1970.

[83] Stewart, W. C., Mezrich, R. S., Cosentino, L. S., Nagle, E. M., Wendt, F. S., and Lohman, R. D., "An Experimental Read-Write Holographic Memory," RCA Review, vol. 34, pp. 3-44, March 1973.

[84] Sussman, A., "Electrooptic Liquid Crystals Devices: Principles and Applications," IEEE Trans. Parts. Hybrids, and Packaging, vol. PHP-8, no. 4, pp. 24-37, December 1972.

[85] Sutherlin, K. K., Lauer, J. P., and Olenick, R. W., "Holoscan: A Commercial Holographic ROM." Appl. Optics, vol. 13, no. 6, pp. 1345-1354, June 1974.

[86] Szentesi, O. I., "An Acoustooptic Page Composer Based on Bragg Imaging," Proc. IEEE, vol. 60, pp. 1461-1462, November 1972.

[87] Takeda, Y., Oshida, Y., and Miyamura, Y., "Random Phase Shifters for Fourier Transformed Holograms," Appl. Optics, vol. 11, no. 4, pp. 818-822, April 1972.

[88] Takeda, Y., "Digital Spatial Modulators," Appl. Optics, vol. 13, no. 4, pp. 825-831, April 1974.

[89] Taylor, G. W., "A Method of Matrix Addressing Polarization Rotating or Retarding Light Valve Arrays," Proc. IEEE, vol. 58, no. 11, pp. 1812-1818, November 1970.

[90] Thaxter, J. B., and Kestigian, M., "Unique Properties of SBN and Their use in a Layered Optical Memory," Appl. Optics, vol. 13, no. 4, pp. 913-924, April 1974.

[91] Tomlinson, W. J., "Phase Holograms in Photochromic Materials," Appl. Optics, vol. 11, no. 4, pp. 823-831, April 1972.

[92] Tsukamoto, K., Ishil, A., Ishida, A., Sumi, M., and Uchida, N., "Holographic Information Retrieval System," Appl. Optics, vol. 13, no. 4, pp. 869-874, April 1974.

[93] Tufte, O. N. and Chen, D., "Optical Techniques for Data Storage," IEEE Spectrum, vol. 10, pp. 26-32, February 1973.

[94] Tufte, O. N. and Chen, D., "Optical Memories: Controlling the Beam," IEEE Spectrum, vol. 10, pp. 48-53, March 1973.

[95] Vander Lugt, A., "Design Relationships for Holographic Memories," Appl. Optics, vol. 12, no. 7, pp. 1675-1685, July 1973.

[96] van Heerden, P. J., "Theory of Optical Information Storage in Solids," Appl. Optics, vol. 2, no. 4, pp. 393-400, April 1963.

[97] White, D. L. and Feldman, M., "Liquid Crystal Light Valves," Electronics Letters, vol. 6, no. 26, pp. 837-840, December 1970.

[98] Wieder, H., "Superresolution in Optical Data Storage," Appl. Phys. Lett., vol. 22, no. 10, pp. 487-489, May 15, 1973.

[99] Zech, R. G., "Data Storage in Volume Holograms," Ph.D. Thesis, University of Michigan, 1974.

[100] Zook, J. D., "Light Beam Deflector Performance A Comparative Analysis," Appl. Optics, vol. 13, no. 4, pp. 875-887, April 1974.

REFERENCES ON VOLUME HOLOGRAPHY

[1] Baugh, R. A., "High-Efficiency Volume Holography," Ph.D. Thesis, Stanford University, 1969.

[2] Bergstein, L. and Kermisch, D., "Image Storage and Reconstruction in Volume Holography," Proc. Symp. on Modern Optics, MRI ser., vol. 17, Brooklyn, N.Y.: Polytechnic Press, 1967, pp. 655-680.

[3] Biedermann, K., Ragnarsson, S., and Komlos, P., "Volume Holograms in Photographic Emulsions of Extended Thickness," Optics Comm., vol. 6, no. 2, pp. 205-209, October 1972.

[4] Bosomworth, D. R., and Gerritsen, H. J., "Thick Holograms in Photochromic Materials," Appl. Optics, vol. 7, no. 1, pp. 95-98, January 1968.

[5] Collier, R. J., Burckhardt, C. B., and Lin, L. H., Optical Holography, Academic Press, New York, 1971, Chapter 9.

[6] Friesem, A. A., "Three-Dimensional Recording Media in Holography," Ph.D. Thesis, The University of Michigan, 1968.

[7] Hsiao, S. S., "Resolution Distribution and Information Capacity of a Hologram," J. Optical Soc. Am., vol. 63, no. 9, pp. 1108-1119, September 1973.

[8] Kasper, F. G., "Diffraction by Thick, Periodically Stratified Gratings with Complex Dielectric Constant," J. Optical Soc. Am., vol. 63, no. 1, pp. 37-45, January 1973.

[9] Kermisch, D., "Image Storage and Reconstruction in Volume Holography," Ph.D. Thesis, Polytechnic Institute of Brooklyn, 1968.

[10] Kermisch, D., "Nonuniform Sinusoidally Modulated Dielectric Gratings," J. Optical Soc. Am., vol. 59, no. 11, pp. 1409-1414, November 1969.

[11] Kermisch, D., "Efficiency of Photochromic Gratings," J. Optical Soc. Am., vol. 61, no. 9, pp. 1202-1206, September 1971.

[12] Kogelnik, H., "Coupled Wave Theory for Thick Hologram Gratings," Bell Sys. Tech. J., vol. 48, no. 4, pp. 2909-2947, November 1969.

[13] Ludwig, U. W., "Generalized Grating Ray-Tracing Equations," J. Optical Soc. Am., vol. 63, no. 9, pp. 1105-1107, September 1973.

[14] Ninomiya, Y., "Recording Characteristics of Volume Holograms," J. Optical Soc. Am., vol. 63, no. 9, pp. 1124-1130, September 1973.

[15] Shankoff, T. A., "Phase Holograms in Dichromated Gelatin," Appl. Optics, vol. 7, no. 10, pp. 2101-2105, October 1968.

[16] Singh, K., Rattan, R., and Jain, N. K., "Diffraction Images of Truncated Sine and Square Wave Periodic Objects in the Presence of Linear Image Motion," Appl. Optics, vol. 12, no. 8, pp. 1846-1850, August 1973.

[17] Uchida, N., "Calculation of Diffraction Efficiency in Hologram Gratings Attenuated Along the Direction Perpendicular to the Grating Vector," J. Optical Soc. Am., vol. 63, no. 3, pp. 280-287, March, 1973.

[18] Zech, R. G., "Data Storage in Volume Holograms," Ph.D. Thesis, University of Michigan, 1974.

REFERENCES ON OPTICALLY-INDUCED REFRACTIVE INDEX CHANGES IN SOLIDS

[1] Amodei, J. J., and Bosomworth, D. R., "Hologram Storage and Retrieval in Photochromic Strontium Titanate Crystals," Appl. Optics, vol. 8, no. 2, pp. 2473-2477, December 1969.

[2] Amodei, J. J., "Electron Diffusion Effects During Hologram Recording in Crystals," Appl. Phys. Letters, vol. 18, pp. 22-24, January 1, 1970.

[3] Amodei, J. J., "Electron Diffusion Effects During Hologram Recording in Crystals," Appl. Phys. Letters, vol. 18, no. 1, pp. 22-24, January 1, 1971.

[4] Amodei, J. J., "Analysis of Transport Processes During Holographic Recording in Insulators," RCA Review, vol. 32, pp. 185-198, June 1971.

[5] Amodei, J. J., and Staebler, D. L., "Holographic Pattern Fixing in Electro-Optic Crystals," Appl. Phys. Letters, vol. 18, pp. 540-542, June 15, 1971.

[6] Amodei, J. J., Phillips, W. and Staebler, D. L., "Improved Electrooptic Materials for Holographic Storage," IEEE J. Quantum Electronics, vol. QE-7, pg. 321, June 1971.

[7] Amodei, J. J., Staebler, D. L., and Stephens, A. W., "Holographic Storage in Doped Barium Sodium Niobate ($Ba_2NaNb_5O_{15}$)," Appl. Phys. Letters, vol. 18, pp. 507-509, June 1, 1971.

[8] Amodei, J., Phillips, W., and Staebler, D. L., "Holographic Storage Performance of Iron-Doped $LiNbO_3$," IEEE International Electron Device Meeting, pp. 112-114, October 1971.

[9] Amodei, J. J., Phillips, W. and Staebler, D. L., "Improved Electrooptic Materials and Fixing Techniques for Holographic Recording," Appl. Optics, vol. 11, no. 2, pp. 390-396, February 1972.

[10] Amodei, J. J., and Staebler, D. L., "Holographic Recording in Lithium Niobate," RCA Review, vol. 33, no. 1, pp. 71-93, March 1972.

[11] Amodei, J. J., and Staebler, D. L., "Holographic Storage in Electrooptic Crystals," IEEE J. of Quantum Electronics, vol. QE-9, no. 6, pp. 708-709, June 1973.

[12] Ashkin, A., Boyd, G. D., Dziedzic, J. M., Smith, R. G., Ballman, A. A., Levinstein, J. J., and Nassau, K., "Optically-Induced Refractive Index Inhomogeneities in $LiNbO_3$ and $LiTaO_3$," Appl. Phys. Letters, vol. 9, no. 1, pp. 72-74, July 1, 1966.

[13] Ashkin, A., Tell, B., and Dziedzic, M., "Laser Induced Refractive Index Inhomogeneities and Absorption Saturation Effects in CdS," IEEE J. Quantum Electron., vol. QE-3, no. 10, pp. 400-406, October 1967.

[14] Bass, M., "Nd:YAG Laser Irradiation-Induced Damage to $LiNbO_3$ and KDP," IEEE J. Quantum Electronics, vol. QE-7, pp. 350-359, July 1971.

[15] Chen, F. S., "A Laser Induced Inhomogeneity of Refractive Indices in KTN," J. Appl. Phys., vol. 38, pp. 3418-3420, July 1967.

[16] Chen, F. S., LaMacchia, J. T., and Fraser, D. B., "Holographic Storage in Lithium Niobate," Appl. Phys. Letters, vol. 13, pp. 223-225, October 1, 1968.

[17] Chen, F. S., "Optically Induced Change of Refractive Indices in $LiNbO_3$ and $LiTaO_3$," J. Appl. Phys., vol. 40, no. 8, pp. 3389-3396, July 1969.

[18] Gaylord, T. K., Rabson, T. A., and Tittel, F. K., "Optically Erasable and Rewritable Solid-State Holograms," Appl. Phys. Letters, vol. 20, pp. 47-48, January 1, 1972.

[19] Gaylord, T. K., Rabson, T. A., Tittel, F. K., and Quick, C. R., "Pulsed Writing of Solid State Holograms," Appl. Optics, vol. 12, no. 2, pp. 414-415, February 1973.

[20] Gaylord, T. K., Rabson, T. A., Tittel, F. K., and Quick, C. R., "Self-Enhancement of $LiNbO_3$ Holograms," J. Appl. Phys., vol. 44, no. 2, pp. 896-897, February 1973.

[21] Gaylord, T. K., and Tittel, F. K., "Angular Selectivity of Lithium Niobate Holograms," J. Appl. Phys., vol. 44, no. 9, September 1973.

[22] Glass, A. M., von der Linde, D., and Negran, T. J., "High-Voltage Bulk Photovoltaic Effect and the Photorefractive Process in $LiNbO_3$," Appl. Phys. Letters, vol. 25, no. 4, pp. 233-235, August 15, 1974.

[23] Ishida, A., Mikami, O., Miyazawa, S., and Sumi, M., "Rh-Doped $LiNbO_3$ as an Improved New Material for Reversible Holographic Storage," Appl. Phys. Lett., vol. 21, no. 5, pp. 192-193, September 1972.

[24] Jarzebski, Z. M., "Review of Proposed Defect Structures in $LiNbO_3$," Mat. Res. Bull., vol. 9, pp. 233-240, 1974.

[25] Johnston, Jr., W. D., "Optical Damage in $LiNbO_3$ and Other Pyroelectric Insulators," J. Appl. Phys., vol. 41, pp. 3279-3285, July 1970.

[26] King, S. R., Hartwick, T. S., and Chase, A. B., "Optical Damage in KTN," Appl. Phys. Letts., vol. 21, no. 7, pp. 312-314, October 1972.

[27] Kogelnik, H., "Coupled Wave Theory for Thick Hologram Gratings," Bell Sys. Tech. J., vol. 48, no. 4, pp. 2909-2947, November 1969.

[28] Kurtz, S. K., Perry, T. T., and Bergman, J. G., "Alphaiodic Acid: A Solution-Grown Crystal for Nonlinear Optical Studies and Applications," Appl. Phys. Letts., vol. 12, no. 5, pp. 186-188, March 1, 1968.

[29] Levinstein, H. J., Ballmann, A. A., Denton, R. T., Ashkin, A., Dziedzic, J. M., "Reduction of the Susceptibility to Optically Induced Index Inhomogeneities in $LiTaO_3$ and $LiNbO_3$," J. Appl. Phys., vol. 38, pp. 3101-3102, July 1967.

[30] Lin, L. H., "Holographic Measurements of Optically Induced Refractive Index Inhomogeneities in Bismuth Titanate," Proc. IEEE, vol. 57, pp. 252-253, February 1969.

[31] Magnusson, R. and Gaylord, T. K., "Laser Scattering Induced Holograms in Lithium Niobate," Appl. Optics, vol. 13, no. 7, pp. 1545-1548, July 1974.

[32] Micheron, F., and Bismuth, G., "Variation de Birefringence Induite Dans un Cristal de $LiNbO_3$," Optics Communications, vol. 3, pp. 390-394, August 1971.

[33] Micheron, F., and Bismuth, G., "Electrical Control of Fixation and Erasure of Holographic Patterns in Ferroelectric Materials," Appl. Phys. Letters, vol. 20, pp. 79-81, January 15, 1972.

[34] Micheron, F. and Bismuth, G., "Holographic Optical Storage Using Electrical Control of Fixation and Erasure in Ferroelectrics," Digest of Technical Papers, 1972 IEEE International Solid-State Circuits Conference, pp. 104-105, February 27, 1972.

[35] Micheron, F., and Bismuth, G., "Electrical Control in Photo Ferroelectrics for Optical Storage," Digest of Technical Papers, Topical Meeting on Optical Storage of Digital Data, pp. MB3-1--MB3-4, March 19-21, 1973.

[36] Micheron, F., and Bismuth, G., "Field and Time Thresholds for the Electrical Fixation of Holograms Recorded in $(Sr_{0.75}Ba_{0.25})Nb_2O_6$ Crystals," Appl. Phys. Lett., vol. 23, no. 2, pp. 71-72, June 15, 1973.

[37] Micheron, F., and Mayeux, C., and Trotier, J. C., "Electrical Control in Photoferroelectric Materials for Optical Storage," Appl. Optics, vol. 13, no. 4, pp. 784-787, April 1974.

[38] Miller, R. C. and Nordland, W. A., "Relative Signs of Nonlinear Optical Coefficients of Polar Crystals," Appl. Phys. Letters, vol. 16, no. 4, pp. 174-176, February 15, 1970.

[39] Nath, G., and Haussuhl, S., "Large Nonlinear Optical Coefficient and Phase Matched Second Harmonic Generation in $LiIO_3$," Appl. Phys. Letters, vol. 14, no. 5, pp. 154-156, March 1, 1969.

[40] Norman, S. L., "Holography in Unconventional Materials," Optical Spectra, vol. 4, pp. 26-30, November 1970.

[41] Peterson, G. E., Glass, A. M., and Negran, T. J., "Control of the Susceptibility of Lithium Niobate to Laser-Induced Refractive Index Changes," Appl. Phys. Letters, vol. 19, pp. 130-132, September 1, 1971.

[42] Phillips, W., Amodei, J. J., and Staebler, D. L., "Optical and Holographic Storage Properties of Transition Metal Doped Lithium Niobate," RCA Review, vol. 33, no. 1, pp. 94-109, March 1972.

[43] Phillips, W. and Staebler, D. L., "Control of the Fe^{2+} Concentration in Iron-Doped Lithium Niobate," J. Electronic Materials, vol. 3, no. 2, pp. 601-617, 1974.

[44] Shah, P., Rabson, T. A., Tittel, F. K., and Gaylord, T. K., "Volume Holographic Recording and Storage in Fe-Doped $LiNbO_3$ using Optical Pulses," Appl. Phys. Letters, vol. 24, no. 3, pp. 130-131, February 1974.

[45] Smakula, P. H., and Claspy, P. C., "The Electrooptic Effect in $LiNbO_3$ and KTN," Transactions of the Metallurgical Society of AIME, vol. 239, pp. 421-424, March 1967.

[46] Spencer, E. G., Lenzo, P. V., and Ballman, A. A., "Dielectric Materials for Electrooptic and Ultrasonic Device Applications," Proc. IEEE, vol. 55, no. 12, pp. 2074-2108, December 1967.

[47] Spinhirne, J. M., and Estle, T. L., "Sensitivity and Fatigue of $LiTaO_3$ for Holographic Recording," Appl. Phys. Lett., vol. 23, no. 1, pp. 38-39, July 1974.

[48] Smith, R. G., Fraser, D. B., Denton, R. T., and Rich, T. C., "Correlation of Reduction in Optically Induced Refractive-Index Inhomogeneity with OH Content in $LiTaO_3$ and $LiNbO_3$," J. Appl. Phys., vol. 39, pp. 4600-4602, September 1968.

[49] Staebler, D. L., and Amodei, J. J., "Coupled-Wave Analysis of Holographic Storage in $LiNbO_3$," J. Appl. Phys., vol. 43, pp. 1042-1049, March 1972.

[50] Staebler, D. L., Amodei, J. J., and Phillips, W., "Multiple Storage of Thick Phase Holograms in $LiNbO_3$," Digest of Technical Papers, 1972 International Quantum Electronics Conference, p. 93, May 8-17, 1972, and IEEE J. Quantum Electron., vol. QE-8, no. 6, pg. 611, June 1972.

[51] Staebler, D. L. and Amodei, J. J., "Thermally Fixed Holograms in $LiNbO_3$," Ferroelectrics, vol. 3, pp. 107-113, 1972 and IEEE Trans. Sonics & Ultrasonics, vol. SU-10, pp. 107-113, 1972.

[52] Staebler, D. L. and Phillips, W., "Fe-Doped $LiNbO_3$ for Read-Write Applications," Appl. Optics, vol. 13, no. 4, pp. 788-794, April 1974.

[53] Thaxter, J. B., "Electrical Control of Holographic Storage in Strontium-Barium Niobate," Appl. Phys. Letters, vol. 15, no. 7, pp. 210-212, October 1, 1969.

[54] Tomlinson, W. J., Kaminow, I. P., Chandross, E. A., Fork, R. L., and Silfvast, W. T., "Photo Induced Refractive Index Increase in Poly(methylmethacrylate) and its Applications," Appl. Phys. Letters, vol. 16, no. 12, pp. 486-489, June 15, 1970.

[55] Townsend, R. L. and LaMacchia, J. T., "Optically Induced Refractive Index Changes in $BaTiO_3$," J. Appl. Phys., vol. 41, no. 13, pp. 5188-5192, December 1970.

[56] von der Linde, D., Glass, A. M., and Rodgers, K. F., "Multiphoton Photorefractive Processes for Optical Storage in $LiNbO_3$," Appl. Phys. Letters, vol. 25, no. 3, pp. 155-157, August 1, 1974.

[57] Wax, S. I., Chodorow, M., and Puthoff, H. E., "Optical Damage in KDP," Appl. Phys. Letters, vol. 16, no. 4, pp. 157-159, February 15, 1970.

[58] Wemple, S. H., "Polarization Fluctuations and the Optical Absorption Edge in $BaTiO_3$," Phys. Rev., vol. 2B, October 1970.

[59] Young, L., Wong, W. K. Y., Thewalt, M. L. W., and Cornish, W. D., "Theory of Formation of Phase Holograms in Lithium Niobate," Appl. Phys. Lett., vol. 24, no. 6, pp. 264-265, March 15, 1974.

REFERENCES ON OPTICAL PROPERTIES OF
MATERIALS RELATED TO OPTICAL STORAGE

[1] Abrahams, S. C., Reddy, J. M., and Bernstein, J. L., "Ferroelectric Lithium Niobate. No. 3. Single Crystal X-Ray Diffraction Study at 24°C," J. Phys. Chem. Solids, vol. 27, pp. 997-1012, 1966.

[2] Abrahams, S. C., Hamilton, W. C., and Reddy, J. M., "Ferroelectric Lithium Niobate. No. 4. Single Crystal Neutron Diffraction Study at 24°C," J. Phys. Chem. Solids, vol. 27, pp. 1013-1018, 1966.

[3] Abrahams, S. C., Levinstein, H. J., and Reddy, J. M., "Ferroelectric Lithium Niobate. No. 5. Polycrystal X-Ray Diffraction Study Between 24°C and 1200°C," J. Phys. Chem. Solids, vol. 27, pp. 1019-1026, 1966.

[4] Boyd, G. D., Miller, R. C., Nassau, K., Bond, W. L., and Savage, A., "$LiNbO_3$: An Efficient Phase Matchable Nonlinear Optical Material," Appl. Phys. Letters, vol. 5, no. 11, pp. 234-236, December 1, 1964.

[5] Bridenbaugh, P. M., Carruthers, J. R., Dziedzic, J. M., and Nash, F. R., "Spatially Uniform and Alternate SHG Phase-Matching Temperatures in Lithium Niobate," Appl. Phys. Letters, vol. 17, no. 3, pp. 104-106, August 1, 1970.

[6] Campillo, A. J., and Tang, C. L., "Spontaneous Parametric Scattering of Light in $LiIO_3$," Appl. Phys. Letters, vol. 16, no. 6, pp. 242-244, March 15, 1970.

[7] Chen, F. S., Geusic, J. E., Kurtz, S. K., Skinner, J. G., and Wemple, S. H., "Light Modulation and Beam Deflection with Potassium Tantalate-Niobate Crystals," J. Appl. Phys., vol. 37, no. 1. pp. 388-398, January 1966.

[8] Damon, R. W., McMahon, D. H., and Thaxter, J. B., "Materials for Optical Memories," Electro-Optical Systems Design, vol. 2, no. 8, pp. 68-77, August 1970.

[9] Daniel, M. R., "Acoustic Radiation from a High Coupling Cut of Lithium Niobate," J. Appl. Physics, vol. 44, no. 7, pp. 2942-2945, July 1973.

[10] Faughnan, B. W. and Kiss, Z. J., "Photoinduced Reversible Charge-Transfer Processes in Transition Metal-Doped Single-Crystal $SrTiO_3$ and TiO_2," Phys. Rev. Letters, vol. 21, no. 18, pp. 1331-1334, October 28, 1968.

[11] Glass, A. M., "Comment on 'Luminescence for $LiNbO_3$'," J. Appl. Phys., vol. 44, no. 1, p. 508, January 1973.

[12] Hordvik, A., and Schlossberg, H., "Luminescence from $LiNbO_3$," International Quantum Electronics Conference, May 8-17, Digest of Technical Papers, pp. 75, 1972.

[13] Hordvik, A., and Schlossberg, H., "Reply to "Comment on 'Luminescence for $LiNbO_3$'"," J. Appl. Phys., vol. 44, no. 1, p. 509, January 1973.

[14] Jarzebski, Z. M., "Review of Proposed Defect Structures in $LiNbO_3$," Mat. Res. Bull., vol. 9, pp. 233-240, 1974.

[15] Jerphagnon, J., "Invariants of the Third-Rank Cartesian Tensor: Optical Nonlinear Susceptibilities," Phys. Rev., vol. 2B, no. 4, pp. 1091-1098, August 15, 1970.

[16] Jerphagnon, J., "Optical Nonlinear Susceptibilities of Lithium Iodate," Appl. Phys. Letters, vol. 16, no. 8, pp. 298-299, April 15, 1970.

[17] Kurtz, S. K., Perry, T. T., and Bergman, J. G., "Alpha-iodic Acid: A Solution-Grown Crystal for Nonlinear Optical Studies and Applications," Appl. Phys. Letters, vol. 12, no. 5, pp. 186-188, March 1, 1968.

[18] Lenzo, P. V., Spencer, E. G., Nassau, K., "Electro-Optic Coefficients in Single-Domain Ferroelectric Lithium Niobate," J. Opt. Soc. Am., vol. 56, no. 5, pp. 633-635, May 1966.

[19] Lenzo, P. V., Turner, E. H., Spencer, E. G., and Ballman, A. A., "Electrooptic Coefficients and Elastic Wave Propagation in Single-Domain Ferroelectric Lithium Tantalate," Appl. Phys. Letters, vol. 8, no. 4, pp. 81-82, February 15, 1966.

[20] Miller, R. C. and Savage, A., "Temperature Dependence of the Optical Properties of Ferroelectric $LiNbO_3$ and $LiTaO_3$," Appl. Phys. Letters, vol. 9, no. 4, pp. 169-171, August 15, 1966.

[21] Miller, R. C. and Nordland, W. A., "Relative Signs of Nonlinear Optical Coefficients of Polar Crystals," Appl. Phys. Letters, vol. 16, no. 4, pp. 174-176, February 15, 1970.

[22] Nassau, K. and Levinstein, H. J., "Ferroelectric Behavior of Lithium Niobate," Appl. Phys. Letters, vol. 7, no. 3, pp. 69-70, August 1, 1965.

[23] Nassau, K., Levinstein, J. J., and Loiacono, G. M., "Ferroelectric Lithium Niobate. No. 1. Growth, Domain Structure, Dislocations and Etching," J. Phys. Chem. Solids, vol. 27, pp. 983-988, 1966.

[24] Nassau, K., Levinstein, J. J., and Loiacono, G. M., "Ferroelectric Lithium Niobate. No. 2. Preparation of Single Domain Crystals," J. Phys. Chem. Solids, vol. 27, pp. 989-996, 1966.

[25] Nath, G., and Haussuhl, S., "Large Nonlinear Optical Coefficient and Phase Matched Second Harmonic Generation in $LiIO_3$," Appl. Phys. Letters, vol. 14, no. 5, pp. 154-156, March 1, 1969.

[26] Ng, W. K., and Woodbury, E. J., "Observation of the Simultaneous Generation of the Second, Third, and Fourth Harmonics of 1.06 - μ Radiation in $Ba_2NaNb_5O_{15}$, $LiNbO_3$ and $LiIO_3$ Crystals," Appl. Phys. Letters, vol. 18, no. 12, pp. 550-552, June 15, 1971.

[27] Otaguro, W. S., Wiener-Avnear, W., and Porto, S. P. S., "Determination of the Second-Harmonic-Generation Coefficient and the Linear Electro-Optic Coefficient in $LiIO_3$ through Oblique Raman Phonon Measurements," Appl. Phys. Letters, vol. 18, no. 11, pp. 499-501, June 1, 1971.

[28] Phillips, W. and Staebler, D. L., "Control of the Fe^{2+} Concentration in Iron-Doped Lithium Niobate," J. Electronic Materials, vol. 3, no. 2, pp. 601-617, 1974.

[29] Plourde, J. K., "Temperature Stable Microwave Dielectric Resonators Utilizing Ferroelectrics," Digest of Technical Papers, 1973 IEEE G-MTT International Microwave Symposium, pp. 202-204, June 1973.

[30] Rez, I. S., "Crystals with Non-Linear Polarizability," Sov. Phys. Uspekhi, vol. 10, no. 6, pp. 759-782, May-June 1968.

[31] Singh, S., Draegert, D. A., and Geusic, J. E., "Optical and Ferroelectric Properties of Barium Sodium Niobate," Phys. Rev., vol. 2B, October 1, 1970.

[32] Spencer, E. G., Lenzo, P. V., and Nassau, K., "Elastic Wave Propagation in Lithium Niobate," Appl. Phys. Letters, vol. 7, no. 3, pp. 67-69, August 1, 1965.

[33] Spencer, E. G., Lenzo, P. V., and Ballman, A. A., "Dielectric Materials for Electrooptic, and Ultrasonic Device Applications," Proc. IEEE, vol. 55, no. 12, pp. 2074-2108, December 1967.

[34] Toyoda, K., "Bibliography of Ferroelectrics," Ferroelectrics, vol. 3, pp. 59-66, 1971.

[35] Tsuya, H., Fujino, Y., and Sugibuchi, K., "Dependence of Second Harmonic Generation on Crystal Inhomogeneity," J. Appl. Phys., vol. 41, no. 6, pp. 2557-2563, May 1970.

[36] Turner, E. H., "High Frequency Electro-Optic Coefficients of Lithium Niobate," Appl. Phys. Letters, vol. 8, pp. 303-304, June 1, 1966.

[37] Van Uitert, L. G., Singh, S., Levinstein, H. J., Geusic, J. E., and Bonner, W. A., "A New and Stable Nonlinear Optical Material," Appl. Phys. Letters, vol. 11, no. 5, pp. 161- , September 1, 1967.

[38] Vedam, K. and Davis, T. A., "Piezo- and Thermo-Optic Behavior of $LiNbO_3$," Appl. Phys. Letters, vol. 12, no. 4, pp. 138-140, February 15, 1968.

[39] Venturini, E. L., Spencer, E. G., Lenzo, P. V. and Ballman, A. A., "Refractive Indices of Strontium Barium Niobate," J. Appl. Phys., vol. 38, pp. 343-344, 1967.

[40] Warner, A. W., Onoe, M., and Coquin, G. A., "Determination of Elastic and Piezoelectric Constants for Crystals in Class (3m)," J. Acoustical Soc. of America, vol. 42, pp. 1223-1231, 1967.

[41] Wemple, S. H., DiDomenico, Jr., M., and Camlibel, I., "Relationship Between Linear and Quadratic Electrooptic Coefficients in $LiNbO_3$, $LiTaO_3$, and Other Oxygen-Octahedra Ferroelectrics Based on Direct Measurement of Spontaneous Polarization," Appl. Phys. Letters, vol. 12, no. 6, pp. 209-211, March 15, 1968.

[42] Wemple, S. H., "Polarization Fluctuations and the Optical Absorption Edge in $BaTiO_3$," Phys. Rev., vol. 2B, pp. October 1970.

[43] Wiesendanger, E., "Optical Properties of $KNbO_3$," Ferroelectrics, vol. 1, pp. 141-148, July 1970.

[44] Zook, J. D., Chen, D., and Otto, G. N., "Temperature Dependence and Model of the Electrooptic Effect in $LiNbO_3$," Appl. Phys. Letters, vol. 11, no. 5, pp. 159-161, September 1, 1967.

XIII. PERSONNEL

Gaylord, Thomas K.

Education

B.S.	in Physics, University of Missouri-Rolla	1965
M.S.	in E.E., University of Missouri-Rolla	1967
Ph.D.	in E.E., Rice University	1970

Employment History

Western Electric Co. (Kansas City, Missouri)	
Special Technical Assistant	1964-1965
Rice University	
Post Doctoral Fellow	1970
Research Associate	1971
Adjunct Assistant Professor of Electrical Engineering	1972
Georgia Institute of Technology	
Assistant Professor of Electrical Engineering	1972-Present

Experience Summary

The research and development work at Western Electric Co. was in the area of solid state devices and materials. At Rice University research was conducted on high electric field effects in semiconductors, microelectronics, switching phenomena in semiconductor devices, optical recording of information in crystals, and development of new instrumentation techniques. At Georgia Tech research has been in optical memory implementation, optical holographic recording in crystals, semiconductor devices, microelectronics, and instrumentation. Dr. Gaylord has been Principal Investigator on a number of NSF and NASA research grants. Teaching activities have been in the areas of solid state, optics, electromagnetics, and circuit analysis.

Current Fields of Interest

optical holographic information storage, optical properties of solids, optical memory implementation, semiconductor materials and devices microelectronics and instrumentation techniques.

Engineering Consulting

Rice University (optics instrumentation)
Vector Cable Company (electromagnetics)
Engineering and Scientific Consultants (solid state device modeling)
Western Electric Company (microelectronics instrumentation)
Modern Optics (optics instrumentation)
Spectra Physics (optics instrumentation)
Hewlett-Packard (electronics instrumentation)
Optical Publishing Company (optics technology)
East Tennessee State University ("Optical Engineering" and "Optical Memories for Digital Data" short courses)

Technical Societies

Sigma Pi Sigma, Tau Beta Pi, Kappa Mu Epsilon, Phi Kappa Phi, Sigma Xi (full member), Eta Kappa Nu, AAAS, AAUP, AIP, ASEE, IEEE, and OSA.

Professional Engineer Registration

Missouri (EIT-12866-E)
Texas (PE-33921)

Publications

1. Lyon, D. H., and Gaylord, T. K., "An electro-mechanical effect in the silicon alloy diode," American Physical Society meeting, Kansas City, Mo., March 1965, Bulletin American Physical Society, vol. 10, no. 5, pg. 599, June 1965.

2. Gaylord, T. K., Shah, P. L., and Rabson, T. A., "Gunn effect bibliography," IEEE Transactions on Electron Devices, vol. ED-15, no. 10, pp. 777-778, October 1968.

3. Gaylord, T. K., "An engineer's obligation to society," The Rice Engineer, vol. 17, no. 2, pp. 13-21, Winter 1968.

4. Gaylord, T. K., Shah, P. L., and Rabson, T. A., "Gunn effect bibliography supplement," IEEE Transactions on Electron Devices, vol. ED-16, no. 5, pp. 490-494, May 1969.

5. Gaylord, T. K., and Rabson, T. A., "A method for estimating the location of energy minima near the Brillouin zone boundary and its application to gallium arsenide," Physics Letters, vol. 29A, no. 11, pp. 716-717, August 25, 1969.

6. Gaylord, T. K., "High electric field conduction anisotropies in semiconductors," (Ph.D. thesis, Rice University, 1970), Dissertation Abstracts International, vol. 31, no. 6, pg. 3393-B, December 1970.

7. Gaylord, T. K., and Rabson, T. A., "Anisotropy in the conductivity of gallium arsenide," Physics Letters, vol. 33A, no. 2, pp. 95-96, October 5, 1970.

8. Gaylord, T. K., and Rabson T. A., and Tittel, F. K., "Optically erasable and rewritable solid state holograms," Applied Physics Letters, vol. 20, no. 1, pp. 47-49, January 1, 1972.

9. Gaylord, T. K., and Rabson, T. A., "On the possibility of transverse negative differential conductivity in semiconductors," Physics Letters, vol. 38A, no. 7, pp. 493-494, March 27, 1972.

10. Gaylord, T. K., "Microelectronics," Rice University Review, vol. 7, no. 2, pp. 10-13, Summer 1972.

11. Gaylord, T. K., and Rabson, T. A., "Determination of conduction anisotropies in semiconductors," Solid State Electronics, vol. 15, no. 9, pp. 953-960, September 1972.

12. Gaylord, T. K., "A laboratory photomask production facility," Review of Scientific Instruments, vol. 43, no. 9, pp. 1268-1271, September 1972.

13. Gaylord, T. K., "The high capacity storage problem: Is optical holography the answer?" Optical Spectra, vol. 6, no. 11, pp. 25-37, November 1972.

14. Gaylord, T. K., Rabson, T. A., Tittel, F. K. and Quick, C. R., "Self-enhancement of $LiNbO_3$ holograms," Journal of Applied Physics, vol. 44, no. 2, pp. 896-897, February 1973.

15. Gaylord, T. K., Rabson, T. A., Tittel, F. K. and Quick, C. R., "Pulsed writing of solid state holograms," Applied Optics, vol. 12, no. 2, pp. 414-415, February 1973.

16. Gaylord, T. K., "An economical microelectronics laboratory," Microelectronics, vol. 5, no. 1, pp. 3-11, Autumn 1973.

17. Gaylord, T. K. and Tittel, F. K., "Angular selectivity of lithium niobate volume holograms," Journal of Applied Physics, vol. 44, no. 9, pp. 4771-4773, September 1973.

18. Harman, T. L., Gaylord, T. K., and Rabson, T. A., "Effects of intrinsic region width in Si(Li) p-i-n diodes," Solid State Electronics, vol. 17, no. 4, pp. 408-411, April 1974.

19. Gaylord, T. K. (editor), 1974 IEEE S-MTT International Microwave Symposium Digest of Technical Papers, Atlanta: IEEE, 1974.

20. Shah, P., Rabson, T. A., Tittel, F. K., and Gaylord, T. K., "Volume holographic recording and storage in Fe-doped $LiNbO_3$ using optical pulses," Applied Physics Letters, vol. 24, no. 3, pp. 130-131, February 1974.

21. Magnusson, R., and Gaylord, T. K., "Laser scattering induced holograms in lithium niobate," Applied Optics, vol. 13, no. 7, pp. 1545-1548, July 1974.

22. Gaylord, T. K., "Optical memories," Optical Spectra, vol. 8, no. 6, pp. 29-34, June 1974.

23. Su, S. F., and Gaylord, T. K., "Calculation of arbitrary-order diffraction efficiences of thick gratings with arbitrary grating shape," Journal of the Optical Society of America, vol. 65, no. 1, January 1975 (to appear).

24. Gaylord, T. K., "Optical memory systems," Optical Industry and Systems Directory Encyclopedia. Pittsfield, Mass., Optical Publishing Co., pp. 132-136, 1975.

25. Gaylord, T. K., "An undergraduate optical engineering course," IEEE Trans. on Education, vol. E-18, no. 2, May 1975 (to appear).

Conference Papers

1. Gaylord, T. K., "Research project selection by university engineering faculty," IEEE Southeastern Conference, Charlotte, N.C., April 1975.

2. Alford, C. O. and Gaylord, T. K., "The potential of multi-port optical memories in digital computing," International Optical Computing Conference, Washington, D.C., April 1975.

Invited Presentations

1. Gaylord, T. K., "Research in optical storage of information," Physics Department, University of Missouri-Rolla, March 1975.

2. Gaylord, T. K., "Dielectrics for hologram storage," Electrochemcial Society Symposium, May 1976.